

Chiral MHD description of a perfect magnetized QGP using the effective NJL model in a strong magnetic field

Néda Sadooghi*

Department of Physics, Sharif University of Technology, P.O. Box 11155-9161, Tehran-Iran

To study the effect of a strong magnetic field B on the sound velocity v_s of plane waves propagating in a strongly magnetized quark-gluon plasma (QGP), a chiral magnetohydrodynamical (MHD) description of a perfect (non-dissipative) QGP exhibiting dynamical chiral symmetry breaking (D χ SB) is developed using the effective action of the Nambu-Jona-Lasinio (NJL) model of QCD at finite temperature, finite baryon chemical potential and in the presence of a strong magnetic field. Here, the D χ SB arises due to the phenomenon of magnetic catalysis. Apart from an interesting frequency dependence, for plane waves propagating in the transverse or longitudinal direction with respect to the B field, the sound velocity is anisotropic and depends on the angle between the corresponding wave vectors and the direction of the B field. Moreover, for plane waves propagating in the transverse (longitudinal) direction to the external B field, the sound velocity has a maximum (minimum) at $T < T_c$, reaches a local minimum (maximum) at $T \sim T_c$ and remains constant at $T \gtrsim T_c$. Here, T_c is the critical temperature of the chiral phase transition. Thus, the constant value $v_s \sim 1.5c_s$ at $T \gtrsim T_c$ turns out to be a lower (upper) bound for waves propagating in the transverse (longitudinal) direction with respect to the external B field. Here, $c_s = 1/\sqrt{3}$ is the sound velocity in an ideal gas.

PACS numbers: 11.10.Wx, 12.38.Mh, 11.30.Rd

I. INTRODUCTION

Hydrodynamics is a framework to describe the time evolution of a system under local thermal equilibrium (LTE). Its relativistic version is used extensively in the past years to describe the phenomena observed in the heavy ion experiments at BNL-RHIC, where excited nuclear matter has been already created in the Au-Au collisions with the collision energy of ~ 100 GeV per nucleon [1, 2, 3]. As it is known from lattice QCD simulations, for temperatures larger than $T_c \sim 170$ MeV, confined nuclear matter shall build a phase of deconfined plasma of quarks and gluons - the QGP phase [4]. Although the collision energies at RHIC are sufficient to build this phase, the main goals of the physics of heavy ion collision (HIC) are far more than only to create the QGP. One would like to discover the deconfined QGP under thermal and chemical equilibrium in order to study its static properties such as equation of state, temperature, transport coefficients, etc. But, since it is known that the system at RHIC evolves within time duration of the order of $10 - 100$ fm/c, it is necessary to study at the same time its dynamical properties. Filling the large gap between the static and the dynamical aspects of HIC, relativistic hydrodynamics is one of the most effective methods able to describe the time evolution of the expanding QGP [5], and to explore the behavior of nuclear matter in the vicinity of phase transition point [6]. In order for hydrodynamics to be applicable, the duration of a heavy ion event, τ , has to be large compared to the equilibration time. It is widely believed that the QGP produced at RHIC behaves as a nearly perfect fluid: The transverse radius of an Au nucleus is approximately 6 fm and on the order of 7000 particles are produced overall [3]. The motion of particles is relativistic and the nuclei are Lorentz contracted by a factor of $\gamma \sim 100$. The duration of a heavy ion event $\tau \sim 6$ fm. As it is shown in [5], there is indeed a fascinating agreement between predictions from ideal relativistic hydrodynamic models with the experimental data. Whereas plasma instabilities, such as electromagnetic Weibel instabilities in relativistic shocks can be made responsible for the possible short time thermalization of the QGP at RHIC [7], methods based on gauge-string duality starting from collisions of gravitational shock waves [8] can describe the enormous entropy production in the heavy ion

*Electronic address: sadooghi@physics.sharif.ir

experiments [9].

Apart from the confinement-deconfinement phase transition, the chiral symmetry restoration plays an important role in the QCD phase transition. Recent lattice QCD results [10] predict a critical temperature $\sim 180 - 200$ MeV for the transition from a chirally broken to a chirally symmetric phase, the chiral phase transition. At this critical temperature, following a first order phase transition, the energy density as a function of temperature is shown to increase suddenly by ~ 1 GeV/fm³. The same phenomenon is believed to occur during the QCD phase transition in the Early Universe [11]. Here, the phase transition, being of first order, is usually followed by a mechanism of supercooling [11]. Depending on the degree of supercooling the kinetics of domain formation and growth can be described by the mechanism of nucleation or spinodal decomposition. In contrast to the Early Universe, where the QCD phase transition was driven by nucleation of bubbles of true vacuum inside the metastable phase, the QGP created in RHIC expands several orders of magnitude faster than the primordial Universe, and, bypassing the nucleation process enters the domain of spinodal decomposition [12]. The phenomenon of *sudden hadronization* is also suggested by several results from CERN-SPS and BNL-RHIC [13].

The mechanism responsible for the onset of instabilities in an expanding QGP at nonzero temperature and baryon chemical potential is studied in [12]. Using the effective potential of the linear σ -model as the thermodynamic (effective) potential, a *chiral hydrodynamic* description of the expanding QGP near the chiral phase transition is derived (see also [14]). The effective potential is determined by integrating out the quark degrees of freedom that play the role of a heat bath for the chiral fields σ and π with temperature T and baryon chemical potential μ . Instead of using the thermodynamic potential to calculate the total pressure and energy density and to obtain the conserved energy-momentum tensor for the expanding perfect fluid, the authors in [12] adopt the variational formulation to obtain the hydrodynamic equations for their system [15]. This approach provides a natural way to merge chiral and fluid dynamics. Performing a stability analysis up to first order, the dispersion relation for a plane wave propagating in the above QGP coupled to chiral fields is derived. Solving the dispersion relation, the pressure (sound) modes and chiral modes are further determined.

In the present paper, we will use the same variational method to study the effect of large magnetic fields on the sound propagation of a plane wave propagating in an expanding *magnetized* QGP coupled to chiral fields at finite (T, μ) and in a strong magnetic field. For a magnetic field aligned in the third direction, we will, in particular, determine the *anisotropy in the velocity* of a plane wave propagating at angles (φ, θ) of spherical coordinates from the external magnetic field. Similar frequency dependent anisotropy was previously observed in magnetic fluids in condensed matter physics [16].¹ To mimic the hot and dense QGP in a strong magnetic field, we will use the one-loop effective action of the Nambu-Jona Lasinio (NJL) model of QCD [17, 18] at finite (T, μ) and in a strong magnetic field \mathbf{B} . As it is shown in [19], the one-loop effective action of the NJL model exhibits a dynamical chiral symmetry breaking due to the well-known phenomenon of magnetic catalysis. According to this phenomenon, in the limit of strong magnetic fields, NJL dynamics is dominated by the lowest Landau level (LLL), where even at the weakest attractive interaction between fermions the chiral symmetry of the theory is broken by a dynamically generated fermion mass. This mass is shown to depend on (T, μ) and the strength of the applied magnetic field.

The magnetic catalysis has applications in both cosmology [20] and condensed matter physics [21], and seems to be also relevant in the physics of heavy ion collision: As it is reported in [22, 23, 24], in off-central collisions, heavy ions possess a very large relative angular momentum and create very strong magnetic fields. In this situation, the presence of topological charge was predicted to induce the charge separation with respect to the reaction plane. Large magnetic fields play therefore an important role in the physics of non-central heavy ion collisions and provide a possible signature of the presence of CP-odd domains in the presumably formed QGP phase [22, 23, 24]. The detailed theory of this *chiral magnetic effect* describing the interplay between the chiral charge and the background magnetic field has been developed in [23].² Relativistic shock waves, that are

¹ Magnetic fluid is a colloid of tiny (100 Å) magnetic particles or grains suspended in a carrier fluid such as water. The magnetization of the fluid varies with the applied magnetic field, typically reaching a saturation of $10^2 - 10^3$ Gauß [16].

² In [25] an experimental observable sensitive to the chiral magnetic effect has been proposed and the first preliminary results have been reported by STAR Collaborations [26]. As it is suggested in [24], the generation of chirality in the QGP, responsible for the charge separation, is the QCD counterpart of the generation of baryon asymmetry in the electroweak phase transition in the Early Universe [27, 28].

believed to be build in the heavy ion collisions, can be viewed as a possible origin of the magnetic field generation in the heavy ion collision. The mechanism is well-known from astrophysics, where the generation of large magnetic fields in relativistic shocks plays an important role in the fire-ball model for Gamma-ray Bursts [29]. This model proposes that the non-thermal radiation observed in the prompt and afterglow emission from the Gamma-ray Bursts is synchrotron radiation from collisionless relativistic shocks. In collisionless shocks, plasma instabilities can generate magnetic fields. Within the shock transition layer the relative motion of the mixing pre- and post-shock plasma produces *very anisotropic velocity distributions* for all particle species concerned. Fluctuating electromagnetic fields deflect the incoming charged particles and act as the effective collisional process needed to complete the shock transition. These fluctuating fields occur naturally because anisotropic velocity distributions are unstable against several plasma instabilities, such as electromagnetic Weibel instability [30]. The latter is an instability of the currents that result from charge bunching in the beams, and leads to spontaneously growing transverse waves with $|\mathbf{B}| \geq |\mathbf{E}|$. In a relativistic shock, where the velocity of the pre- and post-shock plasma approaches the velocity of light, the Weibel instability dominates, because it has the largest growth rate. In heavy ion collisions, Weibel instabilities are made responsible for the short equilibration time of the system from the initial colliding stage [31].³

The effect of a strong magnetic field to modify the nature of the chiral phase transition in QCD is recently studied in [33, 34, 35]. In [33], using the one-loop effective potential of the linear σ -model, the hot and dense QGP is simulated and it is shown that for high enough magnetic fields, comparable to the ones expected to be created in non-central high energy heavy ion collisions at RHIC, the original crossover is turned into a first order transition. In [34], the finite-temperature effective potential of linear σ -model in the presence of constant and weak magnetic field, including the contribution of the pion ring diagrams in the background of constant classical σ -fields is calculated. It is shown that there is a region of the parameter space where the effect of ring diagrams is to preclude the phase transition from happening. Inclusion of magnetic field has small effects and becomes more important as the system evolves to the lowest temperatures.⁴ In [35], the response of the QCD vacuum to an external Abelian chromomagnetic field in the framework of a nonlocal NJL model with Polyakov loop is studied and a linear relationship between the deconfinement temperature and the squared root of the applied magnetic field is found.

The next question is how the magnetic field would affect the hydrodynamical quantities of an expanding *magnetized* QGP. One of these quantities is the velocity of sound modes of a propagating plane wave in this medium. We investigate this question in the present paper. Further, we are interested on the hydrodynamical signatures of a chiral phase transition once the temperature reaches the critical temperature T_c . Previous studies on the temperature dependence of sound velocity v_s shows that at $T = T_c$ the sound waves has minimum velocity [37]. As it will be shown in Sect. VI, at finite (T, μ) , apart from an anisotropy in the sound velocity with respect to the direction of the magnetic field, the same behavior occurs for a plane wave propagating in the transverse direction to the external magnetic field. In contrast, for the waves propagating in the longitudinal direction to the magnetic field, the sound velocity has a minimum for $T < T_c$, reaches its maximum at $T \sim T_c$ and remains constant after the temperature passes the chiral critical point, i.e. for $T \gtrsim T_c$. On the other hand, at nonzero baryon density, the sound waves seems to die out, as v_s has a real and an imaginary part. Whereas $\Re(v_s)$ has the same behavior as v_s for $\mu = 0$, the $\Im(v_s)$ is several orders of magnitude smaller than $\Re(v_s)$ and oscillates. This behavior which can be interpreted as the onset of the aforementioned spinodal effects is also observed recently in [38], where the dynamical density fluctuations are studied around the QCD critical point using dissipative relativistic fluid dynamics with no chiral fields included. This is interpreted experimentally as a possible fate of Mach cone at the chiral critical point. The disappearance or suppression of the Mach cone would be a signal that the created matter has passed through the critical region, showing the existence of the QCD critical point [38].

The paper is organized as follows: In the first part of the paper (Sects. II and III), we will derive the effective Lagrangian density of the NJL model, consisting of the effective kinetic and the one-loop effective potential of the theory at finite (T, μ) and in the presence of strong magnetic field \mathbf{B} . This part can be viewed

³ Recently, an alternative scenario based on Nielsen-Olesen instability [32] which is characteristic for the configuration of a uniform magnetic field is introduced in [7].

⁴ The effect of ring diagrams on the dynamical chiral phase transition of QED in the presence of strong magnetic field is studied in [36].

as a generalization of the results presented in [19, 39] and the methods introduced in [40] and [41] to the case of nonzero chemical potential. The effective potential and effective kinetic terms are determined in Sects. II A and II C, respectively. The effective kinetic term is in particular determined using a derivative expansion following the standard effective field theory methods presented in [42]. Solving the corresponding gap equation that arises from one-loop effective potential of Sect. II A, the dynamical mass of the NJL model generated in the presence of strong magnetic fields at finite (T, μ) is calculated in Sect. II B. Note that the dynamical mass, being the configuration that minimizes the effective potential, can be viewed as the equilibrium configuration, once the instabilities in the magnetized QGP are set on. Comparing to the effective action of the linear σ -model used in [12], both the effective kinetic term and the minimum of the effective potential of the NJL model in a strong magnetic field depend on (T, μ) and the constant magnetic field. To have a link to hydrodynamics, we will determine in Sect. III the energy-momentum tensor $T^{\mu\nu}$ of the effective NJL model in the presence of a strong magnetic field using the effective Lagrangian density from Sect. II. Here, we will introduce a polarization tensor $M^{\mu\nu}$ containing the magnetization M of the medium. The same tensor appears also in [43, 44], where a MHD description of an expanding dissipative fluid is introduced to study the Nernst effect in the vicinity of superfluid-insulator transition of condensed matter physics.⁵

In the second part of the paper (Sects. IV-VI), we will use the method introduced in [12] and the results from the first part of the paper to present a *chiral magnetohydrodynamic* description of a magnetized perfect (non-dissipative) QGP coupled to chiral fields of the effective NJL model. This is in contrast to the work done in [44] and [45] where in the presence of a weak magnetic field, the magnetized fluid does not involve any chiral fields. In Sect. IV A, we will first generalize the thermodynamic relations to the case of nonzero magnetic field. In Sect. IV B, we describe the variational method used in [12] by comparing first the polarization tensor $M^{\mu\nu}$ of the NJL model with the expected magnetization of the magnetized medium (Sect. IV B 1), and then the energy-momentum tensor of the effective NJL model with the corresponding $T^{\mu\nu}$ of an expanding QGP coupled to chiral fields (Sect. IV B 2). In Sect. V, using the hydrodynamical equations, the energy-momentum conservation relation and the conservation relations for the number and entropy densities, we will perform a first order stability analysis and derive the corresponding dispersion relation of the magnetized QGP coupled to chiral fields σ and π . The sound velocity is then derived in Sect. V B. We will use the method in [16] to determine the anisotropy in the sound velocity. In our specific model studied in this paper, a wave propagating in a plane transverse to the external magnetic field, the anisotropy is independent of the angle φ of the spherical coordinate system. On the other hand, a θ -dependence arises in the anisotropy function, when the propagating wave is in the longitudinal plane with respect to the direction of the magnetic field. In Sect. VI, performing a numerical analysis, we will visualize our results in several figures. Our results are summarized in Sect. VII. In Appendix A, we will generalize the Bessel-function identities appearing in the high temperature expansion of Matsubara sums of finite temperature field theory presented in [40] to the case of finite chemical potential. In Appendix B a generalization of the Mellin transformation [41] for the case of nonzero chemical potential is presented. A detailed derivation of thermodynamic relations used in Sect. V is presented in Appendix C.

II. NJL MODEL AT FINITE T, μ AND IN A STRONG MAGNETIC FIELD

We start with the action of the NJL model in $3 + 1$ dimensions at zero temperature and zero baryonic density

$$\mathcal{L} = \frac{1}{2}[\bar{\psi}, (i\gamma^\mu D_\mu)\psi] + \frac{G}{2}[(\bar{\psi}\psi)^2 + (\bar{\psi}i\gamma^5\psi)^2] - \mathcal{F}, \quad (\text{II.1})$$

where $\mathcal{F} \equiv \frac{1}{4}(F_{\mu\nu})^2$ is the gauge kinetic term. Defining the covariant derivative by $D_\mu \equiv \partial_\mu - ieA_\mu^{ext}$, with the gauge field in the symmetric gauge $A_\mu^{ext} = \frac{1}{2}(0, -Bx_2, Bx_1, 0)$, a constant magnetic field aligned in the x_3 -direction is generated. In the above symmetric gauge, the only non-vanishing elements of the field-strength tensor $F_{\mu\nu}$ are $F_{12} = -F_{21} = B$ and $F_{\mu\nu} = F^{\mu\nu}$. We have therefore $\mathcal{F} = \frac{B^2}{2}$. Note, that (II.1) is chirally invariant under $U_L(1) \times U_R(1)$ group transformation. As it is described in [19], the above theory is equivalent

⁵ In condensed matter physics, the Nernst coefficient measures the transverse voltage arising in response to an applied thermal gradient in the presence of a magnetic field [44].

to the bosonized Lagrangian density

$$\mathcal{L} = \frac{1}{2} [\bar{\psi}, (i\gamma^\mu D_\mu) \psi] - \bar{\psi} (\sigma + i\gamma^5 \pi) \psi - \frac{1}{2G} (\sigma^2 + \pi^2) - \mathcal{F}, \quad (\text{II.2})$$

where the Euler-Lagrange equations for the auxiliary fields σ and π take the form of constraint equations

$$\sigma = -G (\bar{\psi} \psi), \quad \text{and} \quad \pi = -G (\bar{\psi} i\gamma^5 \psi). \quad (\text{II.3})$$

Integrating out the fermion degrees of freedom, we obtain the effective action for the composite fields $\vec{\rho} = (\sigma, \pi)$ at finite temperature T and density μ and in the presence of a constant magnetic field eB .⁶ It is given by

$$\Gamma[\vec{\rho}; eB, \mu, T] = \int d^4x \mathcal{L}_{\text{eff}}(\vec{\rho}; eB, T, \mu) = \int d^4x (\mathcal{L}_k - \Omega - \mathcal{F}). \quad (\text{II.4})$$

In the following, we will first introduce the effective potential Ω , and then determine the kinetic term \mathcal{L}_k using the method introduced in [19].

A. The effective potential of the NJL model at finite T, μ in a strong magnetic field

The effective potential of the NJL model consists of a tree level part and a one-loop part. The latter is determined in [19] at zero temperature and density, and in the presence of a constant magnetic field. It is expressed through the path integral over fermions

$$\begin{aligned} \exp(i\tilde{\Gamma}(\vec{\rho}; eB)) &= \int \mathcal{D}\bar{\psi} \mathcal{D}\psi \exp\left(\frac{i}{2} [\bar{\psi}, (i\gamma^\mu D_\mu - \sigma - i\gamma^5 \pi) \psi]\right) \\ &= \exp(\text{Tr} \ln(i\gamma^\mu D_\mu - \sigma - i\gamma^5 \pi)). \end{aligned} \quad (\text{II.5})$$

Using the definition of $\text{Tr}(\dots)$, $\tilde{\Gamma}$ can be given by

$$\tilde{\Gamma} = \int d^4x V^{(1)}(\vec{\rho}; eB, T = \mu = 0), \quad \text{where} \quad V^{(1)} = -i \text{tr} \ln(i\gamma^\mu D_\mu - \sigma - i\gamma^5 \pi). \quad (\text{II.6})$$

Here, $\text{tr}(\dots)$ is to be built only over the internal degrees of freedom. It can be further evaluated using the Schwinger's proper-time formalism [19, 46]. The effective potential of the NJL model at zero T and μ , Ω including the tree level contribution $V^{(0)}$, and one-loop effective potential $V^{(1)}$, is therefore given by

$$\Omega(\vec{\rho}; eB, T = \mu = 0) = V^{(0)}(\vec{\rho}; eB, T = \mu = 0) + V^{(1)}(\vec{\rho}; eB, T = \mu = 0), \quad (\text{II.7})$$

where

$$V^{(0)} = \frac{\rho^2}{2G}, \quad \text{and} \quad V^{(1)} = \frac{eB}{8\pi^2} \int_{\frac{1}{\Lambda^2}}^{\infty} \frac{ds}{s^2} \coth(eBs) e^{-s\rho^2}. \quad (\text{II.8})$$

Here, $\rho^2 = \sigma^2 + \pi^2$. In the limit of very large magnetic field $eB \rightarrow \infty$,⁷ the UV cutoff Λ can be replaced by $\Lambda \rightarrow \Lambda_B \equiv \sqrt{eB}$, and $\coth(eBs) \approx 1$. The integral over s in (II.8) can therefore be performed using

$$\Gamma(n, z) = \int_z^\infty dt t^{n-1} e^{-t}. \quad (\text{II.9})$$

⁶ It can be shown that the presence of a constant magnetic field, defines a natural scale $\ell_B \equiv \frac{1}{\sqrt{eB}}$, where e is the electromagnetic coupling constant.

⁷ The strong magnetic field limit is characterized by a comparison between eB and the momenta of the particles included in the theory. In this limit $|\mathbf{k}_\parallel|, |\mathbf{k}_\perp| \ll \sqrt{eB}$, where, $|\mathbf{k}_\parallel|$ and $|\mathbf{k}_\perp|$ are the longitudinal and transverse momenta with respect to the direction of the constant magnetic field, respectively.

It leads to

$$\begin{aligned}\Omega(\vec{\rho}; eB, T = \mu = 0) &= \frac{\rho^2}{2G} + \frac{\rho^2 eB}{8\pi^2} \Gamma\left(-1, \frac{\rho^2}{\Lambda_B^2}\right) \\ &\stackrel{eB \rightarrow \infty}{\approx} \frac{\rho^2}{2G} + \frac{(eB)^2}{8\pi^2} - \frac{\rho^2 eB}{8\pi^2} \left(1 - \gamma_E - \ln\left(\frac{\rho^2}{eB}\right)\right) + \mathcal{O}\left(\frac{\rho^2}{eB}\right),\end{aligned}\quad (\text{II.10})$$

where the asymptotic expansion of $\Gamma(-1, z) \approx \frac{1}{z} - 1 + \gamma_E + \ln z + \mathcal{O}(z)$ for $z \rightarrow \infty$ is used. Here, $\gamma_E \simeq 0.577$ is the Euler-Mascheroni number.

Similar methods can be used to determine the effective potential of the NJL model at finite temperature and density, and in the presence of a constant magnetic field [47, 48]

$$\Omega(\vec{\rho}; eB, T, \mu) = \frac{\rho^2}{2G} + \frac{2eB}{\beta} \int_0^\infty ds \frac{\Theta_2\left(\frac{2\pi\mu s}{\beta} \middle| \frac{4\pi i s}{\beta^2}\right)}{(4\pi s)^{(D-1)/2}} \coth(seB) e^{-s(\rho^2 - \mu^2)}.\quad (\text{II.11})$$

Here, β is the inverse temperature, $\beta \equiv \frac{1}{T}$, and

$$\Theta_2(u|\tau) \equiv 2 \sum_{n=0}^{\infty} e^{i\pi\tau(n+\frac{1}{2})^2} \cos((2n+1)u),\quad (\text{II.12})$$

is the elliptic Θ -function of second kind. Using the identity [47]

$$\Theta_2(u|\tau) = \left(\frac{i}{\tau}\right)^{1/2} e^{-\frac{i u^2}{\pi\tau}} \Theta_4\left(\frac{u}{\tau} \middle| -\frac{1}{\tau}\right),\quad (\text{II.13})$$

where

$$\Theta_4(u|\tau) = 1 + 2 \sum_{n=1}^{\infty} (-1)^n e^{i\pi n^2 \tau} \cos(2nu),\quad (\text{II.14})$$

is the fourth Jacobian Θ -function, and setting $\coth(eBs) \approx 1$ in the strong magnetic field limit $eB \rightarrow \infty$,⁸ the one-loop effective potential in (II.11) can be separated into two parts,

$$V^{(1)}(\vec{\rho}; eB, T, \mu) = V^{(1)}(\vec{\rho}; eB, T = \mu = 0) + V^{(1)}(\vec{\rho}; eB, T \neq 0, \mu \neq 0).\quad (\text{II.15})$$

The effective potential $\Omega(\vec{\rho}; eB, T, \mu)$ including the tree level $V^{(0)}$, and the one-loop effective potential $V^{(1)}$ is therefore given by

$$\Omega(\vec{\rho}; eB, T, \mu) = \frac{\rho^2}{2G} + \frac{eB}{8\pi^2} \int_0^\infty \frac{ds}{s^2} e^{-s\rho^2} \left[1 + 2 \sum_{n=1}^{\infty} (-1)^n e^{-\frac{\beta^2 n^2}{4s}} \cosh(n\mu\beta)\right].\quad (\text{II.16})$$

To evaluate the integration over s , the integral (II.9) and

$$\int_0^\infty dx x^{\nu-1} \exp\left(-\frac{\beta}{x} - \gamma x\right) = 2 \left(\frac{\beta}{\gamma}\right)^{\frac{\nu}{2}} K_\nu\left(2\sqrt{\beta\gamma}\right),\quad (\text{II.17})$$

can be used. The effective potential (II.16) is therefore given by

$$\Omega(\vec{\rho}; eB, T, \mu) = \frac{\rho^2}{2G} + \frac{\rho^2 eB}{8\pi^2} \Gamma\left(-1, \frac{\rho^2}{\Lambda_B^2}\right) + \frac{\rho eB}{\beta\pi^2} \sum_{\ell=1}^{\infty} \frac{(-1)^\ell}{\ell} K_1(\beta\ell\rho) \coth(\ell\mu\beta),\quad (\text{II.18})$$

⁸ At finite temperature T , the strong magnetic field limit is characterized by $T^2 \ll eB$.

where $\rho \equiv |\vec{\rho}|$. The (T, μ) independent part of (II.18) is exactly the same as (II.10) and can be similarly evaluated in the strong magnetic field limit. As for the (T, μ) dependent part, it can be expanded in the orders of $(\rho\beta)$, using the Bessel function identities from Appendix A. In particular, we will use the identity

$$\begin{aligned} \sum_{\ell=1}^{\infty} \frac{(-1)^\ell}{\ell} K_1(\ell z) \cosh(\ell z') &= \frac{1}{8} z \left[1 - 2\gamma_E - 2 \ln\left(\frac{z}{\pi}\right) \right. \\ &\quad \left. - \sum_{n=1}^{\infty} \frac{(-1)^n (1+n)}{(\Gamma(2+n))^2} \left(\frac{z}{4\pi}\right)^{2n} \left\{ \left| \psi^{(2n)}\left(\frac{1}{2} - \frac{iz'}{2\pi}\right) \right| + \left| \psi^{(2n)}\left(\frac{1}{2} + \frac{iz'}{2\pi}\right) \right| \right\} \right] \\ &\quad - \frac{z^2}{3} \sum_{k=1}^{\infty} \frac{(-1)^k (2^{2k+1} - 1)}{2^{2k+1}} \left(\frac{z'}{\pi}\right)^{2k} \zeta(2k+1) + \frac{1}{2z} \left\{ \text{Li}_2\left(e^{i(\pi+iz')}\right) + \text{Li}_2\left(e^{-i(\pi+iz')}\right) \right\}, \end{aligned} \quad (\text{II.19})$$

with $z = \rho\beta$ and $z' = \mu\beta$ from (A.23) to evaluate the sum over ℓ in (II.18). In (II.19), the polygamma function $\psi(z) \equiv \frac{d}{dz} \ln \Gamma(z)$, and $\psi^{(m)}(z) \equiv \frac{d^m \psi(z)}{dz^m}$ is the $(m+1)^{th}$ logarithmic derivative of the $\Gamma(z)$ -function. Furthermore, the dilogarithm function $\text{Li}_2(z)$ is defined by

$$\text{Li}_2(z) \equiv \sum_{k=1}^{\infty} \frac{z^k}{k^2}, \quad (\text{II.20})$$

and satisfies

$$\text{Li}_2(z) = - \int_0^z \frac{\ln(1-t)}{t} dt. \quad (\text{II.21})$$

The effective potential of the NJL model (II.18) at finite (T, μ) and in the limit of $eB \rightarrow \infty$ is therefore given by

$$\begin{aligned} \Omega(\vec{\rho}; eB, T, \mu) &\stackrel{eB \rightarrow \infty}{\approx} \frac{\rho^2}{2G} + \frac{(eB)^2}{8\pi^2} - \frac{\rho^2 eB}{8\pi^2} \left(\gamma_E + \ln\left(\frac{eB\beta^2}{\pi^2}\right) \right) \\ &\quad - \frac{eB}{8\pi^2 \beta^2} \sum_{n=1}^{\infty} \frac{(-1)^n}{(16\pi^2)^n} \frac{(n+1)(\rho\beta)^{2(n+1)}}{(\Gamma(2+n))^2} \left\{ \left| \psi^{(2n)}\left(\frac{1}{2} - \frac{i\mu\beta}{2\pi}\right) \right| + \left| \psi^{(2n)}\left(\frac{1}{2} + \frac{i\mu\beta}{2\pi}\right) \right| \right\} \\ &\quad - \frac{eB(\rho\beta)^3}{3\pi^2 \beta^2} \sum_{k=1}^{\infty} \frac{(-1)^k (2^{2k+1} - 1)}{2^{2k+1}} \left(\frac{\mu\beta}{\pi}\right)^{2k} \zeta(2k+1) + \frac{eB}{2\pi^2 \beta^2} \left\{ \text{Li}_2\left(e^{i(\pi+i\mu\beta)}\right) + \text{Li}_2\left(e^{-i(\pi+i\mu\beta)}\right) \right\}. \end{aligned} \quad (\text{II.22})$$

It exhibits a spontaneous symmetry breaking, which is mainly due to a dynamical mass generation in the regime of lowest Landau level (LLL) dominance. The type of the phase transition as well as the critical temperature depends on the strength of the magnetic field eB . Fig. 1 shows two examples of Ω for a) $eB = 10 \text{ GeV}^2$ which is equivalent to $B \sim 10^{21} \text{ Gau\ss}$,⁹ and for b) $eB = 10^{-4} \text{ GeV}^2$ which is equivalent to $B \sim 10^{16} \text{ Gau\ss}$. In both cases the potential Ω from (II.22) is calculated up to $\mathcal{O}((\rho\beta)^7)$ and $\mathcal{O}((\mu\beta)^7)$, and $\mu\beta$ is chosen to be $\mu = 10^{-3} \text{ GeV}$. Let us note that the qualitative picture that arises here does not depend too much on μ .

In the next section, the effective potential (II.22) will be used to determine the dynamical mass, that is generated due to the phenomenon of magnetic catalysis in the strong magnetic field limit [19].

B. Dynamical mass of the NJL model at finite T, μ in a strong magnetic field

As it is shown in [19], a constant magnetic field in $3+1$ dimensions is a strong catalyst of dynamical chiral symmetry breaking. This phenomenon leads to the generation of a fermion dynamical mass even at the weakest

⁹ As it is shown in [36], eB in GeV^2 is equivalent to $B = 1.691 \times 10^{20} \text{ Gau\ss}$.

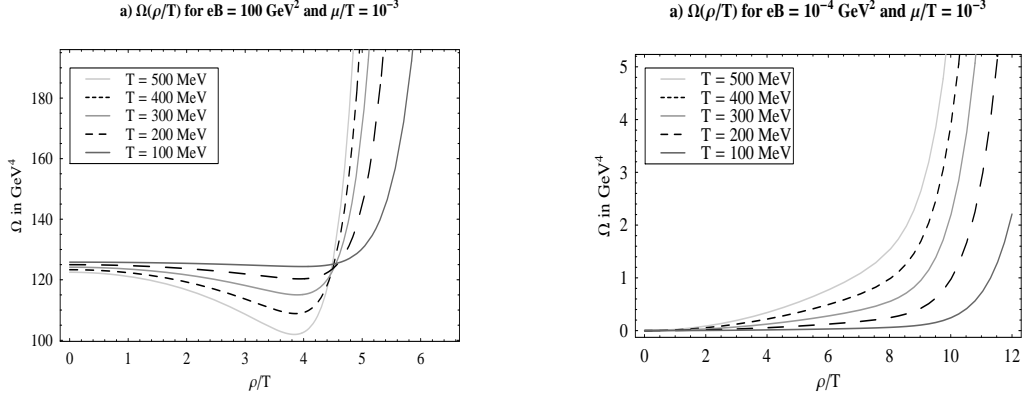


FIG. 1: a) Effective potential Ω of the NJL model as a function of ρ/T for $eB = 10 \text{ GeV}^2$ and $\mu\beta = 10^{-3}$. Here, a second order chiral phase transition occurs at $T_c \simeq 100 \text{ MeV}$ (far right). b) Effective potential Ω of the NJL model as a function of ρ/T for $eB = 10^{-4} \text{ GeV}^2$ and $\mu\beta = 10^{-3}$. Here, a smooth crossover occurs at $T_c \simeq 100 \text{ MeV}$ (far right). Here, the NJL coupling $G = 5.86 \text{ GeV}^{-2}$ and the sum over n in (II.22) is up to $n, k = 7$.

attractive interaction between the fermions. The essence of this effect is a dimensional reduction from $D \rightarrow D-2$ in the dynamics of fermion pairing in a magnetic field. At zero temperature and vanishing chemical potential, the dynamical mass can be determined using the effective potential

$$\Omega(\vec{\rho}; eB, T = \mu = 0) = \frac{\rho^2}{2G} + \frac{\rho^2 eB}{8\pi^2} \left(-1, \frac{\rho^2}{eB} \right),$$

from (II.10) through the gap equation

$$\left. \frac{\partial \Omega(\vec{\rho}; eB, T = \mu = 0)}{\partial \sigma} \right|_{\sigma_0 \neq 0, \pi_0 = 0} = 0. \quad (\text{II.23})$$

Here, the minimum of the potential is assumed to be at unknown but constant σ_0 and vanishing π_0 . The gap equation (II.23) leads to

$$\frac{\sigma_0}{G} = \frac{\sigma_0 eB}{4\pi^2} \Gamma \left(0, \frac{\sigma_0^2}{eB} \right), \quad (\text{II.24})$$

that, after excluding the trivial solution $\sigma_0 = 0$, and using the approximation $\lim_{z \rightarrow 0} \Gamma(0, z) \simeq -\gamma_E - \ln z$, leads to the non-vanishing dynamical mass at zero temperature and chemical potential

$$\sigma_0(eB, T = \mu = 0) = \mathcal{C}_m \sqrt{eB} \exp \left(-\frac{4\pi^2}{GeB} \right), \quad \text{with} \quad \mathcal{C}_m = e^{-\gamma_E/2} \simeq 0.74. \quad (\text{II.25})$$

The same result arises also in [39]. Next, we will determine the mass gap at finite (T, μ) and in the strong magnetic field limit. Using $\Omega(\vec{\rho}; eB, T, \mu)$ from (II.16), we arrive first at the gap equation

$$0 = \left. \frac{\partial \Omega(\vec{\rho}; eB, T, \mu)}{\partial \sigma} \right|_{\sigma_0 \neq 0, \pi_0 = 0} = \frac{\sigma_0}{G} - \frac{\sigma_0 eB}{4\pi^2} \left\{ \Gamma \left(0, \frac{\sigma_0^2}{eB} \right) + 4 \sum_{\ell=1}^{\infty} (-1)^\ell \cosh(\mu\beta\ell) K_0(\beta\ell\sigma_0) \right\}. \quad (\text{II.26})$$

The temperature independent part of (II.26) can be evaluated as in (II.24), leading to the iterative solution

$$\sigma_0(eB, T, \mu) = \mathcal{C}_m \sqrt{eB} \exp \left(-\frac{4\pi^2}{GeB} + 4 \sum_{\ell=1}^{\infty} (-1)^\ell \cosh(\mu\beta\ell) K_0(\beta\ell\sigma_0) \right), \quad (\text{II.27})$$

where the numerical factor $\mathcal{C}_m \simeq 0.74$ is in (II.25). Setting $\mu = 0$, the above result (II.27) coincides with the dynamical mass determined in [39]. At this stage, we would however use the Bessel-function identity (A.16)

from Appendix A that includes a complete expansion in the orders of $(\sigma_0\beta)$ and $(\mu\beta)$,¹⁰

$$\begin{aligned} \sum_{\ell=1}^{\infty} (-1)^\ell \cosh(\mu\beta\ell) K_0(\beta\ell\sigma_0) &= \frac{1}{2} \left(\gamma_E + \ln \frac{\sigma_0\beta}{\pi} \right) + \sum_{k=1}^{\infty} \frac{(-1)^k (2^{2k+1} - 1)}{2^{2k+1}} \left(\frac{\mu\beta}{\pi} \right)^{2k} \zeta(2k+1) \\ &+ \sum_{n=1}^{\infty} \frac{(-1)^n}{4^{2n+1} (n!)^2} \left(\frac{\sigma_0\beta}{\pi} \right)^{2n} \left\{ \left| \psi^{(2n)} \left(\frac{1}{2} - \frac{i\mu\beta}{2} \right) \right| + \left| \psi^{(2n)} \left(\frac{1}{2} + \frac{i\mu\beta}{2} \right) \right| \right\}. \end{aligned} \quad (\text{II.28})$$

We arrive at the dynamical mass of the NJL model at finite temperature and density and in the strong magnetic field limit

$$\begin{aligned} \sigma_0(eB, T, \mu) &= C_m \sqrt{eB} \exp \left[-\frac{4\pi^2}{GeB} + 2 \left(\gamma_E + \ln \frac{\sigma_0\beta}{\pi} \right) + \sum_{k=1}^{\infty} \frac{(-1)^k (2^{2k+1} - 1)}{2^{2k+1}} \left(\frac{\mu\beta}{\pi} \right)^{2k} \zeta(2k+1) \right. \\ &\left. + \sum_{n=1}^{\infty} \frac{(-1)^n}{4^{2n+1} (n!)^2} \left(\frac{\sigma_0\beta}{\pi} \right)^{2n} \left\{ \left| \psi^{(2n)} \left(\frac{1}{2} - \frac{i\mu\beta}{2} \right) \right| + \left| \psi^{(2n)} \left(\frac{1}{2} + \frac{i\mu\beta}{2} \right) \right| \right\} \right]. \end{aligned} \quad (\text{II.29})$$

In (II.28), the polygamma function $\psi(z)$ is defined as in (II.19). The identity (II.28) is a generalization of Bessel-function identities from [40] for $\mu \neq 0$ and will be proved in Appendix A.

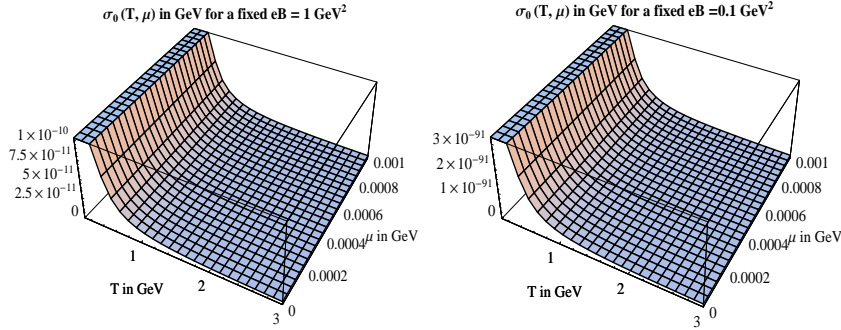


FIG. 2: Qualitative dependence of NJL dynamical mass σ_0 from (II.29) on T and μ in a strong magnetic field $eB = 0.1$ and $eB = 1 \text{ GeV}^2$. The dynamical mass abruptly decreases by a change of the magnetic field of one order of magnitude.

Fig. 2 shows qualitatively the (T, μ) dependence of $\sigma_0(eB, T, \mu)$ from (II.29) for $eB = 0.1, 1 \text{ GeV}^2$, corresponding to $B \simeq 10^{19}, 10^{20} \text{ Gau\ss}$, respectively. Since the solution (II.29) is an iterative one, it is necessary to choose an initial value for σ_0 on the r.h.s. of (II.29). In Fig. 2, this initial value is chosen to be $\sigma_0(eB, T = \mu = 0)$ from (II.25). Further, the sum on the r.h.s. of (II.29) is up to $n = k = 7$. The NJL coupling G is chosen to be $G = 5.86 \text{ GeV}^{-2}$. Fig. 2 shows that the dynamical mass vanishes for a fixed value of eB by increasing the temperature. Its qualitative behavior does not depend too much on the chemical potential μ . In the next section, the kinetic term of the effective action (II.4) will be determined in a high temperature expansion.

C. The kinetic term of the NJL model at finite T, μ and in a strong magnetic field

The kinetic term \mathcal{L}_k of the effective action (II.4) at *zero* temperature and density, and in the presence of a constant magnetic field is previously determined in [19]. In the first part of this section, we will briefly outline the arguments in [19]. We then generalize them for the case of non-vanishing temperature and chemical potential.

Let us start with the general structure of the kinetic term of the effective action in a derivative expansion

$$\mathcal{L}_k = \frac{1}{2} F_1^{\mu\nu} \partial_\mu \rho_j \partial_\nu \rho_j + \frac{1}{\rho^2} F_2^{\mu\nu} (\rho_j \partial_\mu \rho_j) (\rho_i \partial_\nu \rho_i), \quad (\text{II.30})$$

¹⁰ This step turns out to be useful in Sect. V.

that is implied by the $U_L(1) \times U_R(1)$ symmetry of the original Lagrangian density. Here, $\vec{\rho} = (\sigma, \pi)$, and $F_i^{\mu\nu}, i = 1, 2$ are structure constants depending nontrivially on the external magnetic field B . Following the general field theory arguments,¹¹ and the definitions

$$\begin{aligned} \left. \frac{\delta^2 \tilde{\Gamma}}{\delta \sigma(x) \delta \sigma(0)} \right|_{\sigma_0 \neq 0, \pi_0 = 0} &= - (F_1^{\mu\nu} + 2F_2^{\mu\nu}) \Big|_{\sigma_0 \neq 0, \pi_0 = 0} \partial_\mu \partial_\nu \delta^4(x), \\ \left. \frac{\delta^2 \tilde{\Gamma}}{\delta \pi(x) \delta \pi(0)} \right|_{\sigma_0 \neq 0, \pi_0 = 0} &= -F_1^{\mu\nu} \Big|_{\sigma_0 \neq 0, \pi_0 = 0} \partial_\mu \partial_\nu \delta^4(x), \end{aligned} \quad (\text{II.31})$$

the structure functions can be given as

$$\begin{aligned} F_1^{\mu\nu} &= -\frac{1}{2} \int d^4x x^\mu x^\nu \frac{\delta^2 \tilde{\Gamma}}{\delta \pi(x) \delta \pi(0)} \\ F_2^{\mu\nu} &= -\frac{1}{4} \int d^4x x^\mu x^\nu \frac{\delta^2 \tilde{\Gamma}}{\delta \sigma(x) \delta \sigma(0)} - \frac{1}{2} F_1^{\mu\nu}, \end{aligned} \quad (\text{II.32})$$

where $\tilde{\Gamma} = -i \text{Tr} \ln(i\gamma^\mu D_\mu - \sigma - i\gamma_5 \pi)$ is the effective action from (II.5). In (II.31) the minimum of the potential is chosen to be at $\sigma_0 = \text{const.}$ and $\pi_0 = 0$. To calculate $F_i^{\mu\nu}, i = 1, 2$ from (II.32), we use the definition of the fermion propagator $iS^{-1} = i\gamma^\mu D_\mu - \sigma_0$,¹² and arrive therefore at

$$\begin{aligned} \left. \frac{\delta^2 \tilde{\Gamma}}{\delta \sigma(x) \delta \sigma(0)} \right|_{\sigma_0 \neq 0, \pi_0 = 0} &= -i \text{tr} (S(x, 0) S(0, x)) \\ \left. \frac{\delta^2 \tilde{\Gamma}}{\delta \pi(x) \delta \pi(0)} \right|_{\sigma_0 \neq 0, \pi_0 = 0} &= +i \text{tr} (S(x, 0) \gamma_5 S(0, x) \gamma_5). \end{aligned} \quad (\text{II.33})$$

Plugging (II.33) back in (II.32), the structure functions in the momentum space are given by

$$\begin{aligned} F_1^{\mu\nu} &= +\frac{i}{2} \int \frac{d^4k}{(2\pi)^4} \text{tr} \left(\tilde{S}(k) \gamma_5 \frac{\partial^2 \tilde{S}}{\partial k_\mu \partial k_\nu} \gamma_5 \right) \\ F_2^{\mu\nu} &= -\frac{i}{4} \int \frac{d^4k}{(2\pi)^4} \text{tr} \left(\tilde{S}(k) \frac{\partial^2 \tilde{S}}{\partial k_\mu \partial k_\nu} \right) - \frac{1}{2} F_1^{\mu\nu}. \end{aligned} \quad (\text{II.34})$$

As it is shown in [19], the fermion propagator in a constant magnetic field and at zero (T, μ) is given by

$$S(x, y) = \exp \left(\frac{ie}{2} (x - y)^\mu A_\mu^{\text{ext}}(x + y) \right) \tilde{S}(x - y), \quad (\text{II.35})$$

with the Fourier transform of \tilde{S}

$$\tilde{S}(k) = 2i \exp \left(-\frac{\mathbf{k}_\perp^2}{eB} \right) \sum_{n=0}^{\infty} (-1)^n \frac{D_n(eB, k)}{\mathbf{k}_\parallel^2 - \sigma_0^2 - 2eBn}, \quad (\text{II.36})$$

where n labels the Landau levels that arise in the presence of a constant magnetic field, and \mathbf{k}_\parallel as well as \mathbf{k}_\perp are the longitudinal and transverse momenta with respect to the external magnetic field, i.e. for $\mathbf{B} = B\mathbf{e}_3$ we get $\mathbf{k}_\parallel = (k_0, k_3)$, $\mathbf{k}_\perp = (k_1, k_2)$. Further, $D_n(eB, k)$ is given in terms of Laguerre polynomials L_n by

$$D_n(eB, k) = (\mathbf{k}_\parallel \cdot \gamma_\parallel + \sigma_0) \left\{ \mathcal{O}_- L_n \left(2 \frac{\mathbf{k}_\perp^2}{eB} \right) - \mathcal{O}_+ L_{n-1} \left(2 \frac{\mathbf{k}_\perp^2}{eB} \right) \right\} - 2\mathbf{k}_\perp \cdot \gamma_\parallel L_{n-1}^{(1)} \left(2 \frac{\mathbf{k}_\perp^2}{eB} \right), \quad (\text{II.37})$$

where $\mathcal{O}_\pm \equiv \frac{1}{2} (1 \pm i\gamma_1 \gamma_2 \text{sign}(eB))$. In [19], the fermion propagator in a constant magnetic field (II.35)-(II.36) is used to determine $F_i^{\mu\nu}, i = 1, 2$ from (II.34). But, since we are interested only on the strong magnetic field

¹¹ See e.g. in [42] for more details.

¹² Note that here, $\sigma_0 = \text{const.}$ plays the role of the dynamical mass. It will be determined analytically by solving the corresponding gap equation in Sect. II B.

limit $eB \rightarrow \infty$, where the fermion dynamics is dominated by the lowest Landau level (LLL) pole of the fermion propagator, it is enough to use the fermion propagator in the LLL approximation

$$S(x) = p_{\perp}(\mathbf{x}_{\perp}) s_{\parallel}(\mathbf{x}_{\parallel}) \mathcal{O}_{-}, \quad (\text{II.38})$$

with

$$p_{\perp}(\mathbf{x}_{\perp}) \equiv \frac{ieB}{2\pi} e^{-\frac{eB}{4}\mathbf{x}_{\perp}^2}, \quad \text{and} \quad s_{\parallel}(\mathbf{x}_{\parallel}) \equiv \int \frac{d^2\mathbf{k}_{\parallel}}{(2\pi)^2} \frac{e^{-i\mathbf{k}_{\parallel} \cdot \mathbf{x}_{\parallel}}}{(\mathbf{k}_{\parallel} \cdot \boldsymbol{\gamma}_{\parallel} - \sigma_0)}. \quad (\text{II.39})$$

It arises from (II.35)-(II.37) by setting $n = 0$. In Sect. IV, a hydrodynamical description of the NJL model in the presence of a strong magnetic field will be presented, where the combination $G^{\mu\nu} \equiv F_1^{\mu\nu} + 2F_2^{\mu\nu}$ is shown to be relevant. Plugging therefore (II.38)-(II.39) in (II.34), the structure function $G^{\mu\nu}$ in the LLL approximation are given by

$$\begin{aligned} G^{11} &= G^{22} = -\frac{i}{4\pi} \int \frac{d^2k_{\parallel}}{(2\pi)^2} \text{tr}(\tilde{s}_{\parallel}(\mathbf{k}_{\parallel}) \mathcal{O}_{-} \tilde{s}_{\parallel}(\mathbf{k}_{\parallel}) \mathcal{O}_{-}), \\ G^{ab} &= \frac{ieB}{4\pi} \int \frac{d^2k_{\parallel}}{(2\pi)^2} \text{tr}\left(\tilde{s}_{\parallel}(\mathbf{k}_{\parallel}) \mathcal{O}_{-} \frac{\partial^2}{\partial k_a \partial k_b} \tilde{s}_{\parallel}(\mathbf{k}_{\parallel}) \mathcal{O}_{-}\right), \quad a, b \in \{0, 3\}, \end{aligned} \quad (\text{II.40})$$

where $\tilde{s}_{\parallel}(\mathbf{k}_{\parallel}) = (\mathbf{k}_{\parallel} \cdot \boldsymbol{\gamma}_{\parallel} - \sigma_0)^{-1}$ is the Fourier transform of $s_{\parallel}(\mathbf{x}_{\parallel})$. Plugging $\tilde{s}_{\parallel}(\mathbf{k}_{\parallel})$ in $G^{\mu\nu}$ and using the identities $\text{tr}(1) = 4$, $\text{tr}(\gamma^a \gamma^b) = 4g^{ab}$, $\mathcal{O}_{-}^2 = \mathcal{O}_{-}$, $\mathcal{O}_{-} \gamma_a = \gamma_a \mathcal{O}_{-}$, $\text{tr}(\mathcal{O}_{-} \gamma_a \mathcal{O}_{-} \gamma_b) = 2g_{ab}$, and $\text{tr}(\mathcal{O}_{-} \gamma_a) = 0$ for $a, b \in \{0, 3\}$, as well as $\text{tr}(\mathcal{O}_{-}) = 2$, we arrive first at

$$G^{11} = G^{22} = -\frac{i}{2\pi} \int \frac{d^2k_{\parallel}}{(2\pi)^2} \frac{(\mathbf{k}_{\parallel}^2 + \sigma_0^2)}{(\mathbf{k}_{\parallel}^2 - \sigma_0^2)^2}, \quad (\text{II.41})$$

and

$$G^{aa} = -\frac{ieB}{\pi} \int \frac{d^2k_{\parallel}}{(2\pi)^2} \frac{1}{(\mathbf{k}_{\parallel}^2 - \sigma_0^2)^3} \left(2k_a^2 + (\mathbf{k}_{\parallel}^2 + \sigma_0^2) - 4 \frac{k_a^2(\mathbf{k}_{\parallel}^2 + \sigma_0^2)}{(\mathbf{k}_{\parallel}^2 - \sigma_0^2)} \right), \quad (\text{II.42})$$

whereas the non-diagonal terms identically vanish, i.e.

$$G^{03} = G^{30} = -\frac{2ieB}{\pi} \int \frac{d^2k_{\parallel}}{(2\pi)^2} \frac{k_0 k_3}{(\mathbf{k}_{\parallel}^2 - \sigma_0^2)^3} \left(1 - 2 \frac{(\mathbf{k}_{\parallel} \cdot \boldsymbol{\gamma}_{\parallel} + \sigma_0^2)}{(\mathbf{k}_{\parallel}^2 - \sigma_0^2)} \right) = 0. \quad (\text{II.43})$$

To calculate $G^{\mu\nu}$ from (II.40) at finite temperature and density, we will first perform the following necessary replacements

$$k_0 \rightarrow i\tilde{k}_0 \quad \text{with} \quad \tilde{k}_0 = (\omega_{\ell} - i\mu), \quad \text{and} \quad \omega_{\ell} = \frac{(2\ell + 1)\pi}{\beta}, \quad (\text{II.44})$$

as well as

$$\int d^2k_{\parallel} \rightarrow iT \sum_{\ell=-\infty}^{\infty} \int dk_3, \quad (\text{II.45})$$

and arrive at

$$\begin{aligned} G^{11} = G^{22} &= -\frac{1}{4\pi^2\beta} \sum_{\ell=-\infty}^{\infty} \int \frac{dk_3}{2\pi} \frac{\tilde{k}_0^2 + k_3^2 - \sigma_0^2}{(\tilde{k}_0^2 + k_3^2 + \sigma_0^2)^2} \\ G^{00} &= \frac{eB}{2\pi^2\beta} \sum_{\ell=-\infty}^{\infty} \int \frac{dk_3}{2\pi} \frac{(k_3^4 - \tilde{k}_0^4 - \sigma_0^4 + 6\sigma_0^2 \tilde{k}_0^2)}{(\tilde{k}_0^2 + k_3^2 + \sigma_0^2)^4}, \\ G^{33} &= \frac{eB}{2\pi^2\beta} \sum_{\ell=-\infty}^{\infty} \int \frac{dk_3}{2\pi} \frac{(3k_3^4 - 6k_3^2 \sigma_0^2 - 4k_3^2 \tilde{k}_0^2 + \tilde{k}_0^4 - \sigma_0^4)}{(\tilde{k}_0^2 + k_3^2 + \sigma_0^2)^4}. \end{aligned} \quad (\text{II.46})$$

To evaluate the k_3 -integration as well as the sum over the Matsubara frequencies ℓ , we use the Mellin transformation technique. This technique, which is originally introduced in [41] for finite temperature and zero density, is generalized in Appendix B for finite temperature and nonzero chemical potential. Using in particular the main identity including an expansion in the orders of $(m\beta)$,

$$\begin{aligned} \frac{1}{\beta} \sum_{\ell=-\infty}^{\infty} \int \frac{d^d k}{(2\pi)^d} \frac{(\mathbf{k}^2)^a \tilde{k}_0^{2t}}{(\tilde{k}_0^2 + \mathbf{k}^2 + m^2)^\alpha} &= \frac{1}{2(4\pi)^{d/2} \Gamma(\alpha) \beta} \frac{\Gamma(\frac{d}{2} + a)}{\Gamma(\frac{d}{2})} \left(\frac{2\pi}{\beta}\right)^{-2\alpha + d + 2(t+a)} \\ &\times \sum_{k=0}^{\infty} \frac{(-1)^k}{k!} \Gamma\left(\alpha - a + k - \frac{d}{2}\right) \left[\zeta\left(2(\alpha + k - t - a) - d; \frac{1}{2} - \frac{i\mu\beta}{2\pi}\right) + (\mu \rightarrow -\mu) \right] \left(\frac{m\beta}{2\pi}\right)^{2k}, \end{aligned} \quad (\text{II.47})$$

and neglecting the temperature independent singularities, we arrive at

$$\begin{aligned} G^{11} = G^{22} &= \frac{1}{32\pi^3} \left[\psi\left(\frac{1}{2} - \frac{i\mu\beta}{2\pi}\right) + (\mu \rightarrow -\mu) \right] + \frac{3(\sigma_0\beta)^2}{256\pi^5} \left[\zeta\left(3; \frac{1}{2} - \frac{i\mu\beta}{2\pi}\right) + (\mu \rightarrow -\mu) \right] \\ &- \frac{15(\sigma_0\beta)^4}{4096\pi^7} \left[\zeta\left(5; \frac{1}{2} - \frac{i\mu\beta}{2\pi}\right) + (\mu \rightarrow -\mu) \right] + \mathcal{O}((\sigma_0\beta)^6), \end{aligned} \quad (\text{II.48})$$

and

$$\begin{aligned} G^{00} &= -\frac{eB\beta^2}{256\pi^5} \left\{ \left[\zeta\left(3; \frac{1}{2} - \frac{i\mu\beta}{2\pi}\right) + (\mu \rightarrow -\mu) \right] - \frac{23(\beta\sigma_0)^2}{8\pi^2} \left[\zeta\left(5; \frac{1}{2} - \frac{i\mu\beta}{2\pi}\right) + (\mu \rightarrow -\mu) \right] \right. \\ &\left. + \frac{295(\sigma_0\beta)^4}{128\pi^4} \left[\zeta\left(7; \frac{1}{2} - \frac{i\mu\beta}{2\pi}\right) + (\mu \rightarrow -\mu) \right] \right\} + \mathcal{O}((\sigma_0\beta)^6), \end{aligned} \quad (\text{II.49})$$

and

$$\begin{aligned} G^{33} &= \frac{5eB\beta^2}{512\pi^5} \left\{ \left[\zeta\left(3; \frac{1}{2} - \frac{i\mu\beta}{2\pi}\right) + (\mu \rightarrow -\mu) \right] - \frac{7(\beta\sigma_0)^2}{8\pi^2} \left[\zeta\left(5; \frac{1}{2} - \frac{i\mu\beta}{2\pi}\right) + (\mu \rightarrow -\mu) \right] \right. \\ &\left. + \frac{55(\sigma_0\beta)^4}{128\pi^4} \left[\zeta\left(7; \frac{1}{2} - \frac{i\mu\beta}{2\pi}\right) + (\mu \rightarrow -\mu) \right] \right\} + \mathcal{O}((\sigma_0\beta)^6). \end{aligned} \quad (\text{II.50})$$

In (II.47)-(II.50), $\zeta(s; a)$ is the generalized Riemann zeta function given by $\zeta(s; a) = \sum_{k=0}^{\infty} (k+a)^{-s}$, where any term with $(k+a) = 0$ is excluded. In (II.48), the digamma function $\psi(z) \equiv \frac{d}{dz} \ln \Gamma(z)$ arises by regularizing $\zeta(1; a)$,

$$\lim_{\epsilon \rightarrow 0} \zeta(1 + \epsilon; a) = \lim_{\epsilon \rightarrow 0} \frac{1}{\epsilon} - \psi(a). \quad (\text{II.51})$$

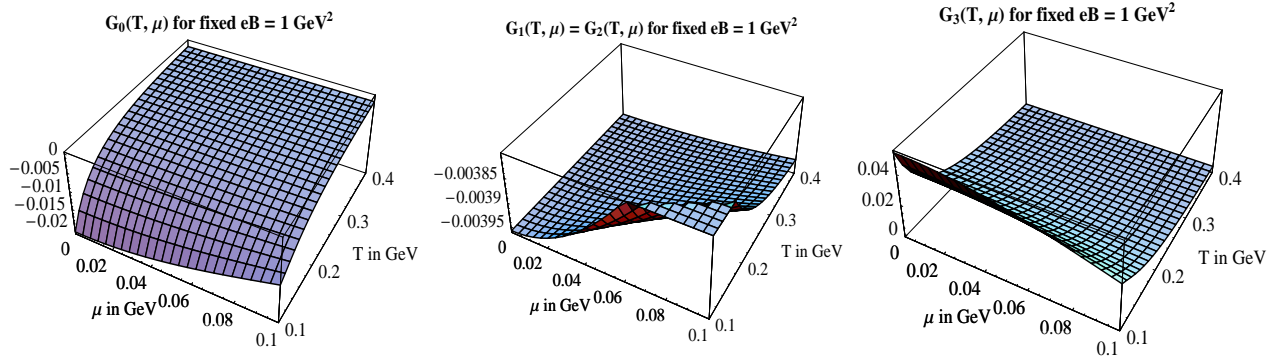


FIG. 3: Qualitative dependence of $G^i \equiv G^{ii}, i = 0, \dots, 3$ on (T, μ) for fixed $eB = 1 \text{ GeV}^2$ corresponding to $B = 10^{20} \text{ GauB}$. They exhibit a qualitative change in the transition region $T_c \sim 100 \text{ MeV}$ and small μ .

Fig. 3 shows $G^i \equiv G^{ii}$, $i = 0, \dots, 3$ in the (T, μ) phase space for $eB = 1 \text{ GeV}^2$ or equivalently $B \sim 10^{20} \text{ Gau\ss}$. To determine G^i , $i = 0, \dots, 3$, we have used the expression (II.29) for $\sigma_0(eB, T, \mu)$. The iteration is started as in the previous section with the value of the dynamical mass at zero temperature and density $\sigma_0(eB, T = \mu = 0)$ from (II.25). The sum in (II.29) is taken up to $n = k = 7$ and $G = 5.86 \text{ GeV}^{-2}$. To determine G^i , $i = 0, \dots, 3$ from (II.48)-(II.50), we have used (II.47). For the structure functions in Fig. 3, the high temperature approximation in (II.47) is up to order $(\sigma_0\beta)^6$. All three structure functions G^i , $i = 0, \dots, 3$ exhibit a qualitative change in the vicinity of the critical temperature T_c .

In the next section, we will use the effective kinetic term (II.30) and the effective potential (II.22) to determine the energy-momentum tensor of an effective NJL model described by the effective action (II.4).

III. THE EFFECTIVE NJL MODEL AT FINITE T, μ AND IN A STRONG MAGNETIC FIELD

The main goal of this paper is to present a hydrodynamical description of an expanding chiral *and* magnetized QGP at finite temperature T and baryon chemical potential μ . It will be described using the NJL model of QCD in the presence of a constant magnetic field, that exhibits, as we have shown in the previous section, a chiral symmetry breaking due to a dynamically generated fermion mass. The thermodynamics of the NJL model has been extensively studied in the past few decades [17, 18]. A systematic study concerning the existence, location and properties of the critical/tricritical point of various NJL type models is recently presented in [49]. In all previous treatments, the effective potential of the theory, Ω , was of fundamental interest. Within a mean field approximation, Ω can indeed be identified with the thermodynamical partition function of the theory, Z , through the relation $\Omega(\sigma_0, T, \mu) = -\frac{1}{\beta V} \ln Z$, where $\beta = T^{-1}$ is the inverse of the temperature and V is the volume. Using this partition function, it is then easy to derive all thermodynamic (static) quantities, like pressure, entropy, etc (see next section for more details on thermodynamics).

We, however, are interested in the dynamical properties of an expanding magnetized QGP near the chiral critical point. To study the time evolution of such a system, we shall go beyond the mean field approximation and to consider the full effective action of the NJL model (II.4) including the effective potential (II.22) as well as the kinetic term (II.30). The latter depends, in contrast to the linear σ model used in [12, 14], on (T, μ) and the external magnetic field. The linear σ model is in particular used in [12, 14] to describe an expanding QGP coupled to chiral fields.

In this section, using the full effective action of the NJL model, we will derive first the equation of motion (EoM) and eventually determine the energy-momentum tensor of the effective NJL model at finite (T, μ) and in the presence of constant magnetic field B . The energy-momentum tensor will be then used in Sect. IV to present a magnetohydrodynamical (MHD) description of an expanding perfect QGP near the chiral critical point.

Using the effective action (II.4), and in particular the general structure of the kinetic term (II.30), the EoM of the chiral fields $\vec{\rho} = (\sigma, \pi)$ of the strongly magnetized NJL effective model can be derived from the ordinary Euler-Lagrange equation

$$\frac{\partial \mathcal{L}_{\text{eff}}}{\partial \rho_k} - \partial_\lambda \frac{\partial \mathcal{L}_{\text{eff}}}{\partial (\partial_\lambda \rho_k)} = 0, \quad \text{with} \quad \vec{\rho} = (\sigma, \pi). \quad (\text{III.1})$$

It is given by

$$F_1^\mu \partial_\mu \partial^\mu \rho_k + \frac{2\rho_k}{\rho^2} F_2^\mu \left(\rho_i \partial_\mu \partial^\mu \rho_i + \partial_\mu \rho_i \partial^\mu \rho_i - \frac{1}{\rho^2} (\rho_i \partial_\mu \rho_i) (\rho_j \partial^\mu \rho_j) \right) = -R_k, \quad (\text{III.2})$$

where

$$R_k \equiv \frac{\partial \Omega}{\partial \rho_k}. \quad (\text{III.3})$$

Here, the effective potential $\Omega = V^{(0)} + V^{(1)}$ includes the tree level potential $V^{(0)}$ and the one loop effective potential $V^{(1)}$ presented in (II.22). In (III.2), we have used the property $F_i^{\mu\nu} = F_i^{\mu\nu} g^{\mu\nu}$ (no summation over μ, ν is considered) and denoted as in the previous section $F_i^{\mu\mu} \equiv F_i^\mu$, with $i = 1, 2$ and $\mu = 0, \dots, 3$. For $F_1^\mu = 1$ and $F_2^\mu = 0$, this result is indeed comparable with the results presented in [12, 14], where the equation of motion of a linear σ model at finite (T, μ) and with no magnetic field is given by $\square \rho_k = -R_k$.

Let us now look at the symmetric energy-momentum tensor corresponding to the effective action (II.4), that arises from the standard relation

$$T_{(tot)}^{\mu\nu} = g^{\mu\nu} \mathcal{L}_{\text{eff}} - \frac{\partial \mathcal{L}_{\text{eff}}}{\partial (\partial_\mu \xi_\ell)} \partial^\nu \xi_\ell, \quad (\text{III.4})$$

where the dynamical fields ξ are given by $\xi = \{\rho_k, A_\mu^{ext}\}$. The energy-momentum tensor will then consist of two parts: $T_{(tot)}^{\mu\nu} = T_{(\rho)}^{\mu\nu} + T_{(\mathcal{F})}^{\mu\nu}$. Here, the matter part $T_{(\rho)}^{\mu\nu}$, and the gauge part $T_{(\mathcal{F})}^{\mu\nu}$ are given by

$$T_{(\rho)}^{\mu\nu} = \frac{1}{2} \Theta_1^{\mu\nu\lambda\sigma} (\partial_\lambda \rho_k \partial_\sigma \rho_k) + \frac{1}{\rho^2} \Theta_2^{\mu\nu\lambda\sigma} (\rho_i \partial_\lambda \rho_i) (\rho_j \partial_\sigma \rho_j) - g^{\mu\nu} \Omega, \quad (\text{III.5})$$

with

$$\Theta_i^{\mu\nu\lambda\sigma} \equiv -2F_i^\mu g^{\mu\lambda} g^{\nu\sigma} + F_i^\lambda g^{\lambda\sigma} g^{\mu\nu}, \quad i = 1, 2, \quad (\text{III.6})$$

and

$$T_{(\mathcal{F})}^{\mu\nu} = -g^{\mu\nu} \mathcal{F} - 2F^\nu_\lambda \frac{\partial \mathcal{L}_{\text{eff}}}{\partial F_{\mu\lambda}} = -g^{\mu\nu} \mathcal{F} - F^\nu_\lambda F^{\mu\lambda} \frac{\partial \mathcal{L}_{\text{eff}}}{\partial \mathcal{F}}, \quad (\text{III.7})$$

with $\mathcal{F} \equiv \frac{1}{4}(F_{\mu\nu})^2$, respectively. The relation (III.7) can be brought in a more familiar form

$$T_{(\mathcal{F})}^{\mu\nu} = \left(F^\mu_\lambda F^{\lambda\nu} + g^{\mu\nu} \frac{1}{4} F_{\rho\sigma} F^{\sigma\rho} \right) \frac{\partial \mathcal{L}_{\text{eff}}}{\partial \mathcal{F}} + g^{\mu\nu} \left(-\mathcal{F} - \mathcal{F} \frac{\partial \mathcal{L}_{\text{eff}}}{\partial \mathcal{F}} \right), \quad (\text{III.8})$$

that appears also in [46] and reduces to the well-known Maxwell tensor

$$T_M^{\mu\nu} = -F^\mu_\lambda F^{\lambda\nu} - g^{\mu\nu} \frac{1}{4} F_{\rho\sigma} F^{\sigma\rho}, \quad (\text{III.9})$$

once $\mathcal{L}_{\text{eff}} = -\mathcal{F}$. For $F_1^\mu = 1$ and $F_2^\mu = 0$, (III.5) is comparable with the matter part of the energy-momentum tensor $T_{(\rho)}^{\mu\nu}$ of the linear σ model

$$T_{(\rho)}^{\mu\nu} = \frac{1}{2} (-2g^{\mu\lambda} g^{\nu\rho} + g^{\mu\nu} g^{\lambda\sigma}) (\partial_\lambda \rho_k \partial_\sigma \rho_k) - \Omega(\rho) g^{\mu\nu}. \quad (\text{III.10})$$

The energy-momentum tensor (III.10) is used in [12, 14] to present a hydrodynamical description of the linear σ model. To derive the energy-momentum conservation relation, we first identify the term $F^{\mu\lambda} \frac{\partial \mathcal{L}_{\text{eff}}}{\partial \mathcal{F}}$ in (III.7) with the *polarization tensor* $M^{\mu\lambda}$, that appears also in [44],¹³

$$M^{\mu\lambda} \equiv F^{\mu\lambda} \frac{\partial \mathcal{L}_{\text{eff}}}{\partial \mathcal{F}}. \quad (\text{III.11})$$

The total energy-momentum tensor can then be given as

$$T_{(tot)}^{\mu\nu} = T_k^{\mu\nu} - F^\nu_\lambda M^{\mu\lambda}, \quad (\text{III.12})$$

with

$$T_k^{\mu\nu} = T_{(\rho)}^{\mu\nu} - g^{\mu\nu} \mathcal{F}, \quad (\text{III.13})$$

where $T_{(\rho)}^{\mu\nu}$ is from (III.5) and $-g^{\mu\nu} \mathcal{F}$ is the first term on the r.h.s. of (III.7). Using the EoM of the effective NJL model (III.2) and the fact that for constant magnetic field $\partial_\mu \mathcal{F} = 0$, it is easy to show that

$$\partial_\mu T_k^{\mu\nu} = 0, \quad (\text{III.14})$$

¹³ See next section for more detail on the polarization tensor $M^{\mu\nu}$.

and that the energy-momentum conservation equation reduces to

$$\partial_\mu T_{(tot)}^{\mu\nu} = -F^\nu_\lambda \partial_\mu M^{\mu\lambda}. \quad (\text{III.15})$$

The same relation appears also in [44], where a magnetohydrodynamical description of the Nernst effect in condensed matter physics is presented. In the next section, we will identify the above energy-momentum tensor (III.12) arising from the effective NJL model in a strong magnetic field with the energy-momentum tensor of a perfect *chiral* and *magnetized* fluid. In contrast to the description in [44], the magnetohydrodynamical description of this theory will include a chiral symmetry breaking arising from the dynamical mass generation in the presence of a strong magnetic field.

IV. MAGNETOHYDRODYNAMIC DESCRIPTION OF THE EFFECTIVE NJL MODEL AT FINITE T, μ

In the first part of this section, we recall standard identities of thermodynamics *without matter fields* which are often used in hydrodynamical models with no background magnetic field. In the second part, generalizing the method introduced in [12], we will implement the chiral fields in a hydrodynamical description of an expanding magnetized QGP including a spontaneous chiral symmetry breaking in the presence of a strong magnetic field.

A. Thermodynamics in a constant magnetic field; General identities

Let us start with the identity

$$U(V, N, S, M) = -PV + TS + \mu N + \mathbf{B} \cdot \mathbf{M}, \quad (\text{IV.1})$$

that defines the internal energy, which is an extensive function of extensive variables; the volume V , the entropy S , the baryon number N , and the magnetization vector \mathbf{M} . Here, P is the pressure, μ is the chemical potential and \mathbf{B} is the constant induced magnetic field. Note that in nonrelativistic systems, N is generally the number of particles, which is conserved. In a relativistic system, the number of particles are not conserved: it is always possible to create a particle-antiparticle pair, provided the energy is available. In this case N no longer denotes a number of particles, but a conserved quantity, such as the baryon number (see [1] for a recent review on relativistic hydrodynamics). In what follows, we will assume that the magnetization vector is parallel to the external \mathbf{B} field, i.e. in our setup $\mathbf{B} = B\mathbf{e}_3$, we get $\mathbf{B} \cdot \mathbf{M} = BM$. The differential of internal energy is given by the thermodynamic identity

$$dU = -PdV + TdS + \mu dN + BdM. \quad (\text{IV.2})$$

The identity (IV.1) can be derived by differentiating the relation

$$U(\lambda V, \lambda N, \lambda S, \lambda M) = \lambda U(V, N, S, M), \quad (\text{IV.3})$$

with respect to λ , taking $\lambda = 1$, and using (IV.2). Differentiating (IV.1) and using again (IV.2), we obtain the Gibbs-Duhem relation

$$VdP = SdT + \mu dN + MdB, \quad (\text{IV.4})$$

that reduces to

$$dP = sdT + nd\mu + MdB, \quad (\text{IV.5})$$

where $s \equiv \frac{S}{V}$, $n \equiv \frac{N}{V}$, and $M \equiv \frac{M}{V}$, the entropy density, the baryon number density and the magnetization density are introduced. Defining further the energy density $\epsilon \equiv \frac{U}{V}$, (IV.1) and (IV.2) are given by

$$\epsilon + P = Ts + \mu n + BM, \quad (\text{IV.6})$$

and

$$d\epsilon = Tds + \mu dn + BdM. \quad (\text{IV.7})$$

Using the Gibbs-Duhem relation (IV.5), the thermodynamical variables are given by

$$s = \left(\frac{\partial P}{\partial T} \right)_{\mu, B}, \quad n = \left(\frac{\partial P}{\partial \mu} \right)_{T, B}, \quad M = \left(\frac{\partial P}{\partial B} \right)_{\mu, T}. \quad (\text{IV.8})$$

Similarly the temperature T , the chemical potential μ and the magnetic field B can be defined by (IV.7) using

$$T = \left(\frac{\partial \epsilon}{\partial s} \right)_{n, M}, \quad \mu = \left(\frac{\partial \epsilon}{\partial n} \right)_{s, M}, \quad B = \left(\frac{\partial \epsilon}{\partial M} \right)_{s, n}. \quad (\text{IV.9})$$

In the next section, we will generalize the above thermodynamic relations to the case where the energy density ϵ depends explicitly on the chiral fields $\vec{\rho} = (\sigma, \pi)$.

B. Chiral magnetohydrodynamics in and out of thermal equilibrium

Extended thermodynamic identities

Following the variational method presented in [12], we treat the gas of quarks for the chiral fields σ and π as a heat bath with temperature T and baryon chemical potential μ . In thermal equilibrium, this identification is justified by the relation

$$P_0 = -\Omega(\vec{\rho}; eB, T, \mu)|_{\sigma_0 \neq 0, \pi_0 = 0}, \quad (\text{IV.10})$$

which is often used in the standard thermal field theory. Here, P_0 is the thermodynamic pressure given by

$$P_0 = \frac{1}{\beta V} \ln Z, \quad (\text{IV.11})$$

where $\beta = T^{-1}$ is the inverse temperature, V the volume and Z the thermodynamic partition function. The effective potential Ω in (IV.10) arises by integrating out the fermions from the original theory. The configuration $(\sigma_0 \neq 0, \pi_0 = 0)$ builds the stationary point of the effective potential or equivalently describes the thermodynamic equilibrium. In Sect. V, where the sound velocity of a plane wave propagating in the magnetized QGP will be calculated, we will assume that the same relation between the pressure and the effective action as in (IV.10), i.e. $P = -\Omega(\vec{\rho}; eB, T, \mu)$, still holds in a system which is out of equilibrium. Here, $\vec{\rho} = (\sigma, \pi)$ is the out of equilibrium configuration of the chiral fields and depends in particular on the space-time point x .

As we have seen in the previous section, the thermodynamic pressure is related to the energy density ϵ through the relation (IV.6),¹⁴

$$P = -\epsilon + Ts + \mu n + BM.$$

In the above merging process of thermodynamics and quantum effective field theory, expressed by (IV.10) or more generally by $P = -\Omega(\vec{\rho}; eB, T, \mu)$, it is therefore natural that the energy density $\epsilon(\vec{\rho}; n, s, M)$ depends not only on (n, s, M) , as in the ordinary thermodynamics, but also on the chiral field $\vec{\rho} = (\sigma, \pi)$. For $\epsilon \equiv \epsilon(\vec{\rho}; n, s, M)$, (IV.7) is therefore generalized as [12]

$$d\epsilon = Tds + \mu dn + BdM + R_k d\rho_k, \quad (\text{IV.12})$$

with

$$T = \left(\frac{\partial \epsilon}{\partial s} \right)_{n, M, \rho_k}, \quad \mu = \left(\frac{\partial \epsilon}{\partial n} \right)_{s, M, \rho_k}, \quad B = \left(\frac{\partial \epsilon}{\partial M} \right)_{n, s, \rho_k}, \quad R_k \equiv \left(\frac{\partial \epsilon}{\partial \rho_k} \right)_{n, s, M}. \quad (\text{IV.13})$$

¹⁴ In the stability analysis, that will be performed in Sect. V, we will assume that B, T, μ and M are always constant. We will vary only $\rho_k = (\sigma, \pi), n$ and s and consequently P and ϵ around their equilibrium configurations σ_0, n_0, s_0 as well as P_0 and ϵ_0 .

In thermal equilibrium, where the only relevant configuration is $(\sigma_0 \neq 0, \pi_0 = 0)$, we have in particular, $\epsilon_0 \equiv \epsilon(\sigma_0; n_0, s_0, M)$. In this case, the last relation in (IV.13) is modified as

$$R_{\sigma_0} \equiv \left(\frac{\partial \epsilon_0}{\partial \sigma_0} \right)_{n_0, s_0, M}, \quad \text{and} \quad R_{\pi_0} \equiv \left(\frac{\partial \epsilon_0}{\partial \pi_0} \right)_{n_0, s_0, M}. \quad (\text{IV.14})$$

Using further (IV.6) and (IV.12), the corresponding Gibbs-Duhem relation (IV.5) becomes

$$dP = sdT + nd\mu + MdB - R_k d\rho_k. \quad (\text{IV.15})$$

This implies the definitions

$$s = \left(\frac{\partial P}{\partial T} \right)_{\mu, B, \rho_k}, \quad n = \left(\frac{\partial P}{\partial \mu} \right)_{T, B, \rho_k}, \quad M = \left(\frac{\partial P}{\partial B} \right)_{T, \mu, \rho_k}, \quad R_k \equiv - \left(\frac{\partial P}{\partial \rho_k} \right)_{T, \mu, B}. \quad (\text{IV.16})$$

In thermal equilibrium, $P_0 = P(\sigma_0; eB, T, \mu)$, the last relation in (IV.16) is modified, upon using (IV.10), as

$$R_{\sigma_0} \equiv \left(\frac{\partial \Omega(\sigma_0; eB, T, \mu)}{\partial \sigma_0} \right)_{T, \mu, B}, \quad R_{\pi_0} \equiv \left(\frac{\partial \Omega(\sigma_0; eB, T, \mu)}{\partial \pi_0} \right)_{T, \mu, B}. \quad (\text{IV.17})$$

Note that the definitions (IV.17) are indeed equivalent with (III.3) for $\sigma = \sigma_0$ and $\pi = \pi_0 = 0$. Using the EoM (III.2) for this constant field configuration, R_{σ_0} and R_{π_0} from (IV.17) as well as (IV.14) vanish, i.e. $R_{\sigma_0} = R_{\pi_0} = 0$.

MHD description of the magnetized QGP

Using the above generalized thermodynamic relations including the chiral matter fields in thermal equilibrium, it is indeed possible to derive all the thermodynamic (static) quantities of the effective NJL model in the presence of a strong magnetic field. It is, however, the goal of this paper to go beyond the thermal equilibrium to study dynamical properties of a magnetized QGP near the chiral critical point. To this purpose, we will use relativistic hydrodynamics which can be used as an effective description of the theory in the same footing as all the other effective descriptions including the time evolution of the fluid. There is only one assumption, which is associated with hydrodynamics: the local thermal equilibrium (LTE). No other assumption is made concerning the nature of the particles and fields included in the fluid. Their interactions and the classical/quantum nature of the phenomena involved are fully encoded in the thermodynamic properties, i.e. in the equation of state (see [1] for a recent review on relativistic hydrodynamics).

The fundamental ingredients of a hydrodynamic analysis at LTE are the conserved quantities and their equations of motion. Here, generalizing a similar treatment from [44], where a similar MHD theory in the vicinity of superfluid-insulator transition in two spatial dimensions is evaluated, we introduce the four velocity $u^\mu \equiv \frac{dx^\mu}{d\tau}$, that represents the velocity of the system in LTE with respect to the laboratory frame. In the rest frame $u^\mu = (1, 0, 0, 0)$. It satisfies the normalization $u_\mu u^\mu = 1$. Further, we will use the standard definition of the metric tensor $g^{\mu\nu} = \text{diag}(1, -1, -1, -1)$.

Let us start with the conservation laws of total energy-momentum tensor [44]

$$u_\nu \partial_\mu T_{(tot)}^{\mu\nu} = u_\mu F^{\mu\nu} J_\nu^{(tot)}, \quad (\text{IV.18})$$

where the hydrodynamic energy-momentum tensor in the presence of a background magnetic field is defined by

$$T_{(tot)}^{\mu\nu} \equiv (\epsilon + P)u^\mu u^\nu - Pg^{\mu\nu} + T_E^{\mu\nu} - F^\nu_\lambda M^{\mu\lambda}. \quad (\text{IV.19})$$

Here, $T_E^{\mu\nu}$ is the *energy magnetization current*. It appears also in [44], where the authors do not determine it explicitly, and use only its property $\partial_\mu T_E^{\mu\nu} = 0$. The latter will be shown to be only valid in the field free case and for $B = 0$. In our case, however, where, the perfect magnetized fluid is coupled to chiral fields σ and π , the combination $\mathcal{T}^{\mu\nu} \equiv (\epsilon + P)u^\mu u^\nu - Pg^{\mu\nu} + T_E^{\mu\nu}$ satisfies $\partial_\mu \mathcal{T}^{\mu\nu} = 0$.

On the r.h.s. of (IV.18), the total baryon current density $J_{(tot)}^\mu$ is defined by

$$J_{(tot)}^\mu \equiv nu^\mu + \partial_\nu M^{\mu\nu}, \quad (\text{IV.20})$$

and satisfies the total current conservation law

$$\partial_\mu J_{(tot)}^\mu = 0. \quad (\text{IV.21})$$

In (IV.20), n is the baryon number density, as is defined in the previous section,¹⁵ and $M^{\mu\nu}$ is the polarization tensor [43, 44]

$$M^{\mu\nu} \equiv \begin{pmatrix} 0 & 0 & 0 & 0 \\ 0 & 0 & M_s & 0 \\ 0 & -M_s & 0 & 0 \\ 0 & 0 & 0 & 0 \end{pmatrix}. \quad (\text{IV.22})$$

Note that due to the antisymmetry of $M^{\mu\nu}$, (IV.21) implies the third hydrodynamic relation

$$\partial_\mu (nu^\mu) = 0, \quad (\text{IV.23})$$

which is then completed with the fourth hydrodynamic relation

$$\partial_\mu (su^\mu) = 0. \quad (\text{IV.24})$$

The above entropy current density conservation (IV.24) is valid only in a perfect (non-dissipative) fluid. Next, we have to find a link between the hydrodynamic quantities defined in the above relations and the field theory identities derived in Sect. II, as well as the thermodynamics relations from Sect. IV B. In what follows, we will first define M_s in terms of magnetization density M that appears in the thermodynamic relations, (IV.5), (IV.12) and (IV.15). This will be done by identifying the polarization tensor $M^{\mu\nu}$ with the tensor defined in (III.11) using the standard field theoretical methods. We will then compare the hydrodynamic energy-momentum tensor (IV.19), with the total energy-momentum tensor of an effective NJL model in a strong magnetic field presented in (III.12), and determine $T_E^{\mu\nu}$ explicitly.

1. The polarization tensor $M^{\mu\nu}$

Let us start by understanding the relation between M_s appearing in (IV.22) with the magnetization density M appearing in the thermodynamic relations (IV.5), (IV.12) and (IV.15). To this purpose, we define a Gibbs free energy density \mathcal{G} in the presence of a constant magnetic field B [50]

$$\mathcal{G}(\vec{\rho}; eB, T, \mu) = \frac{B^2}{2} + \Omega(\vec{\rho}; eB, T, \mu) - HB, \quad (\text{IV.25})$$

where Ω is the free energy density, and H is the external magnetic field. Whereas in vacuum $H = B$, in a medium with finite magnetization density, the external magnetic field H is different from the induced magnetic field B [50]. Using thermodynamical argument, we will prove the relation $B = M + H$, that, apart from a normalization factor, appears also in [50]. To do this, let us evaluate \mathcal{G} at its stationary point with respect to $\vec{\rho} = (\sigma, \pi)$ and B . At this point, \mathcal{G} describes all the thermodynamic properties of the system at thermal equilibrium. The stationary point, which was in the previous sections characterized by the configuration $(\sigma, \pi) \rightarrow (\sigma_0, 0)$, corresponds to the solution of the gap equations

$$\begin{aligned} \left. \frac{\partial \mathcal{G}}{\partial \sigma} \right|_{\sigma_0 \neq 0, \pi_0 = 0} &= 0, & \text{or} & & \left. \frac{\partial \Omega}{\partial \sigma} \right|_{\sigma_0 \neq 0, \pi_0 = 0} &= 0, \\ \left. \frac{\partial \mathcal{G}}{\partial B} \right|_{\sigma_0 \neq 0, \pi_0 = 0} &= 0, & \text{or} & & \left. \frac{\partial \Omega}{\partial B} \right|_{\sigma_0 \neq 0, \pi_0 = 0} - H + B &= 0. \end{aligned} \quad (\text{IV.26})$$

The first equation in (IV.26) is the same as (II.26). In the second equation, we set, $P_0 = -\Omega|_{\sigma_0 \neq 0, \pi_0 = 0}$ from (IV.10). Using now $-\frac{\partial \Omega}{\partial B}|_{\sigma_0 \neq 0, \pi_0 = 0} = \frac{\partial P_0}{\partial B} = M$ from (IV.16), we arrive at

$$B = H + M, \quad (\text{IV.27})$$

¹⁵ This is in contrast to [44], where $J_{(tot)}^\mu$ is the electrical current and n is the charge density.

as was claimed. Comparing now the expression on the r.h.s. of (IV.25) with the definition of the effective action from (II.4), we get

$$\mathcal{G}(\vec{\rho}; eB, T, \mu) = -\mathcal{L}_{\text{eff}} + \mathcal{L}_k - HB. \quad (\text{IV.28})$$

At the stationary point, the effective kinetic term vanishes, i.e. $\mathcal{L}_k|_{\sigma_0 \neq 0, \pi_0=0} = 0$. The gap equation $\frac{\partial \mathcal{G}}{\partial B}|_{\sigma_0 \neq 0, \pi_0=0} = 0$ from (IV.26) leads therefore to

$$\left. \frac{\partial \mathcal{L}_{\text{eff}}}{\partial B} \right|_{\sigma_0 \neq 0, \pi_0=0} = -H = M - B. \quad (\text{IV.29})$$

Using the above relations, we will find in what follows the relation between M_s from (IV.22) and the magnetization density M from (IV.29). To do this, we will identify the polarization tensor $M^{\mu\nu}$ from (IV.22) with the polarization tensor defined in the field theory treatment of the effective NJL model (III.11), i.e. $M^{\mu\lambda} \equiv F^{\mu\lambda} \frac{\partial \mathcal{L}_{\text{eff}}}{\partial \mathcal{F}}$. For $\mathbf{B} = B\mathbf{e}_3$, we arrive at

$$M^{\mu\lambda} \equiv \begin{pmatrix} 0 & 0 & 0 & 0 \\ 0 & 0 & M_s & 0 \\ 0 & -M_s & 0 & 0 \\ 0 & 0 & 0 & 0 \end{pmatrix} = \begin{pmatrix} 0 & 0 & 0 & 0 \\ 0 & 0 & B & 0 \\ 0 & -B & 0 & 0 \\ 0 & 0 & 0 & 0 \end{pmatrix} \frac{\partial \mathcal{L}_{\text{eff}}}{\partial \mathcal{F}}, \quad (\text{IV.30})$$

that upon using $\mathcal{F} = \frac{1}{2}B^2$, leads to $M_s = \frac{\partial \mathcal{L}_{\text{eff}}}{\partial B}$. At the stationary point, this relation can be compared with (IV.29) and leads to the definition of M_s in terms of the magnetization M and the induced magnetic field B

$$M_s|_{\sigma_0 \neq 0, \pi_0=0} = M - B. \quad (\text{IV.31})$$

Note that without considering the gauge kinetic term $-\mathcal{F}$ in the effective action (II.4), $M_s|_{\sigma_0 \neq 0, \pi_0=0}$ would be the magnetization M at thermal equilibrium, as is also introduced in [44].

2. The total energy-momentum tensor $T_{(tot)}^{\mu\nu}$

Our next task will be to compare the energy-momentum tensor of the effective NJL model in the presence of a strong magnetic field (III.12) with the energy-momentum tensor of a magnetized fluid consisting of chiral fields (IV.19). First, let us show that the energy-momentum conservation law, (III.15), on the field theory side reduces to (IV.18) in the hydrodynamics side. To do this, we consider (III.12), that satisfies

$$\begin{aligned} u_\nu \partial_\mu T_{(tot)}^{\mu\nu} &= -u_\nu F^\nu_\lambda M^{\mu\lambda}, \\ &= -u_\nu F^\nu_\lambda \left(nu^\lambda - J_{(tot)}^\lambda \right), \\ &= u_\nu F^\nu_\lambda J_{(tot)}^\lambda, \end{aligned} \quad (\text{IV.32})$$

as expected. To derive (IV.32), we have used the facts from previous section, and replaced $M^{\mu\nu}$ from (III.11) appearing in the energy-momentum tensor in the field theory side, with $M^{\mu\nu}$ that appears in the definition of $J_{(tot)}^\mu$ from (IV.20) on the hydrodynamics side. Further, $\partial_\mu T_k^{\mu\nu} = 0$ with $T_k^{\mu\nu}$ from (III.13), and the antisymmetry of the field strength tensor $F^{\mu\nu}$ are used.

Next, we will determine $T_E^{\mu\nu}$, that appears in (IV.19). To do this, let us use the thermodynamic relations (IV.6), (IV.12) and (IV.15), and the hydrodynamic equations (IV.23) and (IV.24) to determine first $u_\nu \partial_\mu (wu^\mu u^\nu)$, where $w \equiv \epsilon + P$,

$$\begin{aligned} u_\nu \partial_\mu (wu^\mu u^\nu) &= (\partial_\mu w) u^\mu + w(\partial_\mu u^\mu) \\ &= \partial_\mu (\mu n + Ts + BM) u^\mu + (Ts + \mu n + BM) \partial_\mu u^\mu \\ &= u^\mu \partial_\mu P + u^\mu R_k \partial_\mu \rho_k + u_\nu \partial_\mu (BM u^\mu u^\nu). \end{aligned} \quad (\text{IV.33})$$

On the first line, we have used $u_\nu u^\nu = 1$, and set $u_\nu \partial_\mu u^\nu = 0$. The expression on the last line arises by making use of (IV.23), (IV.24), and (IV.15), as well as the fact that for constant magnetic field $\partial_\mu B = 0$. The relation

$$u_\nu \partial_\mu ((\epsilon + P - BM) u^\mu u^\nu) = u^\mu \partial_\mu P + u^\mu R_k \partial_\mu \rho_k, \quad (\text{IV.34})$$

with zero magnetic field appears also in [12]. It corresponds to the Euler's equation of energy-momentum conservation in the non-relativistic hydrodynamics, and will be used in Sect. V, to derive the dispersion relation and the sound velocity in the vicinity of chiral critical point. Plugging this relation back in (IV.19), and using the energy-momentum conservation (IV.18), we arrive first at

$$u_\nu \partial_\mu T_E^{\mu\nu} = -u^\mu R_k \partial_\mu \rho_k - u_\nu \partial_\mu (BM u^\mu u^\nu). \quad (\text{IV.35})$$

Using now the definition of $R_k = \frac{\partial \Omega}{\partial \rho_k}$ from (III.3) and assuming constant T, μ and B , we then get

$$T_E^{\mu\nu} = P g^{\mu\nu} - BM u^\mu u^\nu + C^{\mu\nu}, \quad (\text{IV.36})$$

where $P = -\Omega$ is used. Here, the constant tensor $C^{\mu\nu}$ satisfies $u_\nu \partial_\mu C^{\mu\nu} = 0$. Plugging (IV.36) back in (IV.19), the total energy-momentum tensor is given by

$$T_{(tot)}^{\mu\nu} = (\epsilon + P - BM) u^\mu u^\nu - F_\lambda^\nu M^{\mu\lambda} + C^{\mu\nu}. \quad (\text{IV.37})$$

where $C^{\mu\nu}$ can be determined by comparing $T_{(tot)}^{\mu\nu}$ from the effective field theory (IV.12) with the total energy-momentum tensor from the hydrodynamic side (IV.19). It turns out to be arbitrary. To show this, we will define, as in [12], an energy-momentum tensor of the fluid $T_{\text{fluid}}^{\mu\nu}$. This will done for the effective field theory, as well as for hydrodynamics. Only under the assumption that these two tensors are equal, it can be shown that $C^{\mu\nu}$ in (IV.37) vanishes.

Let us start by defining, as in [12], the energy-momentum tensor of the fluid $T_{\text{fluid}}^{(1)\mu\nu}$ using the notation of the hydrodynamics

$$T_{\text{fluid}}^{(1)\mu\nu} = w u^\mu u^\nu - P_{\text{fluid}} g^{\mu\nu} - BM u^\mu u^\nu, \quad (\text{IV.38})$$

where $P_{\text{fluid}} \equiv -V^{(1)} = P + V^{(0)}$, with $P = -\Omega = -(V^{(0)} + V^{(1)})$. Here, $V^{(0)}$ and $V^{(1)}$ are the tree level and one-loop effective potentials, respectively. They are defined in (II.7) generally and for our specific model in (II.22). In (IV.38), $T_{\text{fluid}}^{\mu\nu}$ satisfies

$$u_\nu \partial_\mu T_{\text{fluid}}^{(1)\mu\nu} = u_\mu R_k \partial^\mu \rho_k - u_\mu \partial^\mu V_0 = u_\mu \partial^\mu V_1, \quad (\text{IV.39})$$

where (IV.34) and the definition R_k from (III.3) are used. On the other hand, let us consider the energy-momentum tensor (IV.12) of the effective field theory, and define¹⁶

$$T_{\text{fluid}}^{(2)\mu\nu} \equiv T_k + V_1 g^{\mu\nu}, \quad (\text{IV.40})$$

where T_k is defined in (IV.13). Using the EoM, we have already shown that $\partial_\mu T_k^{\mu\nu} = 0$. We arrive therefore at

$$u_\nu \partial_\mu T_{\text{fluid}}^{(2)\mu\nu} = u_\mu \partial^\mu V_1. \quad (\text{IV.41})$$

Comparing (IV.41) with (IV.39) and assuming that $T_{\text{fluid}}^{(1)\mu\nu} = T_{\text{fluid}}^{(2)\mu\nu}$, we arrive at the relation

$$T_k = (\epsilon + P - BM) u^\mu u^\nu, \quad (\text{IV.42})$$

where $P_{\text{fluid}} \equiv -V^{(1)} = P + V^{(0)}$ and $P = -\Omega = -(V^{(0)} + V^{(1)})$ are used. Plugging finally (IV.42) back in (IV.12) and comparing the resulting expression with (IV.37), we get $C^{\mu\nu} = 0$, and

$$T_{(tot)}^{\mu\nu} = (\epsilon + P - BM) u^\mu u^\nu - F_\lambda^\nu M^{\mu\lambda}, \quad \text{with} \quad u_\nu \partial_\mu T_{(tot)}^{\mu\nu} = u_\nu F_\lambda^\nu J_{(tot)}^\lambda,$$

as expected. Note that the above assumption $T_{\text{fluid}}^{(1)\mu\nu} = T_{\text{fluid}}^{(2)\mu\nu}$ leading in particular to the relation (IV.42) is the link between effective field theory and hydrodynamics. Whereas T_k , on the effective field theory side of (IV.42), includes the detailed information concerning the matter content of the model and the interactions involved, the expression $(\epsilon + P - BM) u^\mu u^\nu$ on the hydrodynamic side describes effectively the state of a perfect

¹⁶ See [14] for a similar definition.

magnetized fluid through its energy density ϵ , its pressure P and its magnetization M . In contrast to [44], the present MHD description of a magnetized fluid consists of chiral field or equivalently quasiparticles σ and π in the language of condensed matter physics, and exhibits through the special construction of our model a spontaneous chiral symmetry breaking.

In the next section, using the above MHD description and performing a first order stability analysis, we will study the effect of the external magnetic field on the sound modes propagating in an expanding magnetized QGP including the chiral fields.

V. STABILITY ANALYSIS AND SOUND VELOCITY IN A STRONG MAGNETIC FIELD

In this section, we will first determine the dispersion relation of a perfect magnetized QGP at finite (T, μ) coupled to chiral fields. Using the dispersion relation, we will then determine the sound velocity of plane waves propagating in this hot and dense medium. Due to the broken rotational symmetry in the presence of a constant magnetic field, we expect the sound velocity to have an unisotropic distribution. In particular, for plane waves propagating in the transverse as well as longitudinal directions with respect to the external magnetic field, different dependence on the angle (θ, φ) of the spherical coordinate system will arise.

A. The dispersion relation in a perfect magnetized QGP coupled to chiral fields

To study the effect of the magnetic field on the magnetized plasma modeled in this paper via the effective NJL model in the presence of a strong magnetic field, we will study the onset of instabilities by performing a first order stability analysis. In Table I, a list of all the necessary relations from field theory, thermodynamics and hydrodynamics is presented. They are assumed to be valid in a state out of equilibrium.

Field theory	$F_1^\mu \partial_\mu \partial^\mu \rho_k + \frac{2\rho_k}{\rho^2} F_2^\mu \left(\rho_i \partial_\mu \partial^\mu \rho_i + \partial_\mu \rho_i \partial^\mu \rho_i - \frac{1}{\rho^2} (\rho_i \partial_\mu \rho_i) (\rho_j \partial^\mu \rho_j) \right) = -R_k,$	from (III.2)
Thermodynamics	$\epsilon + P = Ts + \mu n + BM,$	from (IV.6)
	$d\epsilon = Tds + \mu dn + BdM + R_k d\rho_k,$	from (IV.12)
	$dP = sdT + nd\mu + MdB - R_k d\rho_k,$	from (IV.15)
Hydrodynamics	$\partial_\mu (nu^\mu) = 0,$	from (IV.23)
	$\partial_\mu (su^\mu) = 0,$	from (IV.24)
	$u_\nu \partial_\mu ((\epsilon + P - BM)u^\mu u^\nu) = u^\mu \partial_\mu P + u^\mu R_k \partial_\mu \rho_k,$	from (IV.34)

TABLE I:

As was indicated in the previous section, we will assume that B, T, μ , and M remain constant (in the space-time x) and will expand $n, s, \vec{\rho} = (\sigma, \pi)$, and u_μ around their equilibrium configurations $n_0, s_0, \vec{\rho}_0$ and $v_0^\mu = (1, \mathbf{0})$ to first order

$$\begin{aligned}
n(x) &= n_0 + n_1(x), \\
s(x) &= s_0 + s_1(x), \\
\sigma(x) &= \sigma_0 + \sigma_1(x), \\
\pi(x) &= \pi_0 + \pi_1(x), \\
u^\mu(x) &= v_0^\mu + v_1^\mu(x).
\end{aligned} \tag{V.1}$$

Here, $\pi_0 = 0$, $v_0^\mu = (1, \mathbf{0})$ and $v_1^\mu = (0, \mathbf{v}_1)$. Further, according to the arguments in the paragraph following (IV.17), in the thermal equilibrium $R_{\sigma_0} = R_{\pi_0} = 0$. Perturbing first the EoM (III.2), we arrive at

$$F_1^\mu \partial_\mu \partial^\mu \rho_{1,k} + \frac{2\rho_{0,k}\rho_{0,j}}{\rho_0^2} F_2^\mu \partial_\mu \partial^\mu \rho_{1,j} = -n_1 \left(\frac{\partial R_k}{\partial n} \right)_{s_0, M, \vec{\rho}_0} - s_1 \left(\frac{\partial R_k}{\partial s} \right)_{n_0, M, \vec{\rho}_0} - m_{k\ell}^2 \rho_{1,\ell}, \tag{V.2}$$

with the mass matrix

$$m_{k\ell}^2 \equiv \left(\frac{\partial^2 \epsilon}{\partial \rho_k \partial \rho_\ell} \right)_{n_0, s_0, M}. \quad (\text{V.3})$$

Here, we have used the definition of $R_k = \frac{\partial \epsilon}{\partial \rho_k}$, which we assume to be also valid in a state out of equilibrium. Expanding $\epsilon(\vec{\rho}; n, s, M)$ up to second order in the thermodynamic quantities, we get

$$\epsilon = \epsilon_0 + n_1 \left(\frac{\partial \epsilon_0}{\partial n_0} \right)_{s_0, M, \rho_0} + s_1 \left(\frac{\partial \epsilon_0}{\partial s_0} \right)_{n_0, M, \rho_0} + \rho_{1,\ell} \left(\frac{\partial \epsilon_0}{\partial \rho_{0,\ell}} \right)_{n_0, s_0, M}, \quad (\text{V.4})$$

with $\epsilon_0 = \epsilon_0(\vec{\rho}_0, n_0, s_0, M)$. Differentiating (V.4) with respect to $\rho_{0,k}$ and using $R_{\sigma_0} = R_{\pi_0} = 0$, we arrive at (V.2). Note, that $F_i^\mu(\sigma_0; eB, T, \mu)$, $i = 1, 2$ are already defined at the vacuum configuration ($\sigma_0 \neq 0, \pi_0 = 0$) [see Sect. II C]. For $k = \sigma$, (V.2) reduces to

$$[G^\mu \partial_\mu \partial^\mu + m_\sigma^2] \sigma_1 = -n_1 \left(\frac{\partial R_\sigma}{\partial n} \right)_{s_0, M, \sigma_0} - s_1 \left(\frac{\partial R_\sigma}{\partial s} \right)_{n_0, M, \sigma_0}, \quad (\text{V.5})$$

with $m_{\sigma\sigma}^2 \equiv m_\sigma^2$ and $G^\mu(\sigma_0; eB, T, \mu) \equiv F_1^\mu + 2F_2^\mu$, whereas for $k = \pi$, we arrive at

$$F_1^\mu \partial_\mu \partial^\mu \pi_1 = 0. \quad (\text{V.6})$$

The conservation laws (IV.23) and (IV.24) lead to

$$\begin{aligned} \partial_0 n_1(x) + n_0 \nabla \cdot \mathbf{v}_1 &= 0, \\ \partial_0 s_1(x) + s_0 \nabla \cdot \mathbf{v}_1 &= 0. \end{aligned} \quad (\text{V.7})$$

Finally, perturbing the energy-momentum conservation law (IV.34), we get

$$W_0 \nabla \cdot \mathbf{v}_1 = -\partial_0 \epsilon_1, \quad (\text{V.8})$$

$$W_0 \partial_0 \mathbf{v}_1 = -\nabla P_1, \quad (\text{V.9})$$

where $W_0 \equiv \epsilon_0 + P_0 - BM = Ts + \mu n$. Using

$$\epsilon_1 = \mu n_1 + Ts_1, \quad (\text{V.10})$$

that arises from (V.4), and the conservation laws (V.7), the time component of the Euler's equation, (V.8), is automatically satisfied. As for (V.9), P_1 is given by

$$P_1 = n_1 \frac{\partial P_0}{\partial n_0} + s_1 \frac{\partial P_0}{\partial s_0} + \sigma_1 \frac{\partial P_0}{\partial \sigma_0}, \quad (\text{V.11})$$

where $P_0 \equiv P(\epsilon_0, n_0, s_0, \sigma_0, M)$. Using now $P_0 = -\epsilon_0 + Ts_0 + \mu n_0 + BM$, and the thermodynamic relations (V.14) in thermal equilibrium, we have

$$\begin{aligned} \frac{\partial P_0}{\partial n_0} &= n_0 \frac{\partial^2 \epsilon_0}{\partial n_0^2} + s_0 \frac{\partial^2 \epsilon_0}{\partial s_0 \partial n_0} + M \frac{\partial^2 \epsilon_0}{\partial M \partial n_0} \\ \frac{\partial P_0}{\partial s_0} &= n_0 \frac{\partial^2 \epsilon_0}{\partial n_0 \partial s_0} + s_0 \frac{\partial^2 \epsilon_0}{\partial s_0^2} + M \frac{\partial^2 \epsilon_0}{\partial M \partial s_0} \\ \frac{\partial P_0}{\partial \sigma_0} &= R_\sigma''(W_0 + BM) = R_\sigma''(\epsilon_0 + P_0), \end{aligned} \quad (\text{V.12})$$

with

$$R_\sigma'' \equiv \frac{1}{(W_0 + BM)} \left[n_0 \left(\frac{\partial R_\sigma}{\partial n} \right)_{s_0, M, \sigma_0} + s_0 \left(\frac{\partial R_\sigma}{\partial s} \right)_{n_0, M, \sigma_0} + M \left(\frac{\partial R_\sigma}{\partial M} \right)_{n_0, s_0, \sigma_0} \right]. \quad (\text{V.13})$$

To determine the dispersion law in the above magnetized QGP, we consider a plane wave of the form $\xi_1(x) = \tilde{\xi}_1 e^{-ikx}$, with $\xi_1 = \{n_1, s_1, \sigma_1, \pi_1, \mathbf{v}_1\}$ and $k^\mu = (\omega, \mathbf{k})$ in the medium and rewrite the relations (V.5)-(V.7), and (V.9) in the momentum space as

$$\begin{aligned} (F_1^0 \omega^2 - F_1^i k_i^2) \tilde{\pi}_1 &= 0, \\ (G^0 \omega^2 - G^i k_i^2 - m_\sigma^2) \tilde{\sigma}_1 &= \frac{W_0}{\omega} R'_\sigma \mathbf{k} \cdot \tilde{\mathbf{v}}_1, \\ (\omega^2 - \mathbf{k}^2 P') \mathbf{k} \cdot \tilde{\mathbf{v}}_1 &= \frac{\omega}{W_0} (W_0 + BM) \mathbf{k}^2 R''_\sigma \tilde{\sigma}_1, \end{aligned} \quad (\text{V.14})$$

where,

$$\begin{aligned} R'_\sigma &\equiv \frac{1}{W_0} \left[n_0 \left(\frac{\partial R_\sigma}{\partial n} \right)_{s_0, M, \sigma_0} + s_0 \left(\frac{\partial R_\sigma}{\partial s} \right)_{n_0, M, \sigma_0} \right], \\ P' &\equiv \frac{1}{W_0} \left[n_0 \left(\frac{\partial P}{\partial n} \right)_{s_0, M, \sigma_0} + s_0 \left(\frac{\partial P}{\partial s} \right)_{n_0, M, \sigma_0} \right]. \end{aligned} \quad (\text{V.15})$$

In Appendix C, we present a derivation of the last two equations in (V.14), using the relations

$$\frac{\tilde{n}_1}{n_0} = \frac{\tilde{s}_1}{s_0} = \frac{\mathbf{k} \cdot \tilde{\mathbf{v}}_1}{\omega}, \quad (\text{V.16})$$

that arise by plugging $n_1(x) = \tilde{n}_1 e^{-ikx}$ as well as $s_1(x) = \tilde{s}_1 e^{-ikx}$ in (V.7). Multiplying the last two equations in (V.14), we arrive at the dispersion relation

$$(G^0 \omega^2 - G^i k_i^2 - m_\sigma^2) (\omega^2 - \mathbf{k}^2 P') = \mathbf{k}^2 R'_\sigma R''_\sigma (W_0 + BM). \quad (\text{V.17})$$

In what follows, we will linearize the above dispersion relation in k and determine the sound velocity of a plane wave propagating in the magnetized QGP coupled to the chiral field σ . Note that, in the above first order perturbation, the pion field π is decoupled from the dynamics of the expanding magnetized QGP. Similar phenomenon is also observed in [12], where the effective action of the linear σ model is used to present a chiral hydrodynamic description of an expanding QGP.

B. Sound velocity in a perfect magnetized QGP coupled to chiral fields

Sound is defined as a small disturbance propagating in a uniform, field free fluid at rest. Perturbing the energy density $\epsilon(x)$ and the pressure $P(x)$ around their equilibrium values ϵ_0 and P_0 , up to small $\delta\epsilon$ and δP , and linearizing the energy-momentum conservation equation, we arrive at

$$\frac{\partial^2(\delta\epsilon)}{\partial t^2} - c_s^2 \Delta(\delta\epsilon) = 0, \quad (\text{V.18})$$

where $c_s^2 \equiv \frac{\partial P}{\partial \epsilon}$. For an ideal classical gas, consisting of independent and massless particles without interaction, $c_s^2 = 1/3$. This can be shown using the identity $P = \frac{\epsilon}{3}$, which is derived using the kinetic pressure and the energy density in terms of Maxwell-Boltzmann statistics, that replaces the Bose-Einstein and Fermi-Dirac statistics in a classical limit. Note that the relation $P = \frac{\epsilon}{3}$, leading to $c_s^2 = 1/3$, arises only by assuming the rotational symmetry. It holds approximately for a uniform QGP at high temperature, where interaction are small due to asymptotic freedom [1].

In [12], the sound velocity of a perfect chiral fluid is determined using the effective potential of a linear σ model in terms of chiral fields. The dispersion relation of this model is similar to (V.17), where $G^i = 1, i = 0, \dots, 3$ and $B = 0$. Assuming the rotational symmetry, the dispersion relation is then solved. For long wavelength fluctuations, the roots are approximately given by [12]

$$\begin{aligned} \omega_\sigma^2 &= m_\sigma^2 + \mathcal{O}(k^2), \\ \omega_p^2/k^2 &= \left(P' - \frac{w_0 R_\sigma'^2}{m_\sigma^2} \right) + \mathcal{O}(k^2), \end{aligned} \quad (\text{V.19})$$

where $w_0 \equiv \epsilon_0 + P_0$. Note, however, that in the presence of a constant magnetic field which is aligned e.g. in the third direction, the rotational symmetry is *a priori* broken, and the sound velocity will be therefore different from $c_s^2 = 1/3$ of an ideal non-interacting QGP. It will be also different from (V.19) for a perfect QGP coupled to chiral fields.

To determine the sound velocity in a perfect fluid in the presence of a constant magnetic field and consisting of chiral fields, we will use a method introduced in [16], where a linearized hydrodynamical theory of magnetic fluids¹⁷ in a strong magnetic field is presented. Solving the equations for a sound wave propagating at angle (θ, φ) with respect to the external magnetic field direction, the sound velocity is shown to be anisotropic. Here, (θ, φ) are the angle in spherical coordinate system. In the next paragraphs, we will consider two different cases separately: a) propagation in the $\mathbf{e}_1 - \mathbf{e}_2$ plane, and b) propagation in the $\mathbf{e}_1 - \mathbf{e}_3$ plane. We will show that whereas the the sound velocity for a propagation transverse to the external magnetic field $\mathbf{B} = B\mathbf{e}_3$ (case a) is independent of the angle φ , for the propagation longitudinal to \mathbf{B} (case b), it depends on the angle θ between the wave vector \mathbf{k} and the direction of the external magnetic field.

1. Propagation in $\mathbf{e}_1 - \mathbf{e}_2$ plane

Let us begin our derivation, by choosing a plane wave with the wave vector $\mathbf{k} = (k \sin \theta \cos \varphi, k \sin \theta \sin \varphi, k \cos \theta)$ in the $\mathbf{e}_1 - \mathbf{e}_2$ plane, transverse to the direction of the magnetic field $\mathbf{B} = B\mathbf{e}_3$. This corresponds to $\theta = \pi/2$ and $\varphi \neq 0$, where $0 \leq \theta \leq \pi$ and $0 \leq \varphi \leq 2\pi$ are angles in spherical coordinate system. The wave vector is therefore given by $\mathbf{k}_{12} = (k_{12} \sin \varphi, k_{12} \cos \varphi, 0)$, where the superscripts correspond to a propagation in the $\mathbf{e}_1 - \mathbf{e}_2$ plane. For a given frequency ω , equation (V.17) determines k . In a linearized hydrodynamics, we will evaluate k around $k_0 \equiv \frac{\omega}{c_s}$, where $c_s = 1/\sqrt{3}$ is the sound velocity in an ideal classical gas. Thus plugging, the relation

$$k_{12} = k_0 + k'_{12}, \quad (\text{V.20})$$

in the dispersion relation (V.17) and expanding the resulting expression in the order of k'_{12} up to $\mathcal{O}(k'_{12})$, we get

$$k'_{12} = \frac{\mathcal{N}_{12}}{\mathcal{D}_{12}}, \quad (\text{V.21})$$

with the numerator

$$\begin{aligned} \mathcal{N}_{12} = & -2c_s^2[m_\sigma^2(c_s^2 - P') + R'_\sigma R''_\sigma w_0] + \omega^2(2c_s^2 G^0 - G^1 - G^2)(c_s^2 - P') \\ & - \omega^2(G^1 - G^2)(c_s^2 - P') \cos(2\varphi), \end{aligned} \quad (\text{V.22})$$

with $w_0 \equiv W_0 + BM = \epsilon_0 + P_0$ and the denominator

$$\begin{aligned} \mathcal{D}_{12} = & 2c_s^2[m_\sigma^2(c_s^2 + P') - R'_\sigma R''_\sigma w_0] - \omega^2[2c_s^4 G^0 - 3(G^1 + G^2)P'] \\ & + c_s^2(G^1 + G^2 + 2G^0 P') - (G^1 - G^2)\omega^2 \cos(2\varphi). \end{aligned} \quad (\text{V.23})$$

Setting $G^i = 1, i = 0, 1, 2$, $P' = c_s^2$ and $B = 0$ as well as $R'_\sigma = R''_\sigma = 0$, we get $k'_{12} = 0$, as expected. To determine the frequency dependent anisotropy Δ , we use the identity $\omega \approx k_{12}v_{12}$ with $k_{12} = \frac{\omega}{c_s} + k'_{12}$ and $v_{12} \equiv c_s(1 + \Delta_{12})$. Using k'_{12} from (V.21)-(V.23), we arrive at

$$\Delta_{12}(G^0, G^1, G^2; \varphi, \omega) = -\frac{k'_{12}c_s}{k'_{12}c_s + \omega}, \quad (\text{V.24})$$

where $G^i, i = 0, 1, 2$ are functions of eB, T and μ . In our specific model with $G^1 = G^2$ [see Sect. II C], the φ -dependence in the anisotropy Δ_{12} vanishes. The anisotropy is then given by

$$\Delta_{12}(G^0, G^1; \omega) = \frac{-2c_s^2[m_\sigma^2(c_s^2 - P') + R'_\sigma R''_\sigma w_0] + \omega^2(2c_s^2 G^0 - 2G^1)(c_s^2 - P')}{2c_s^2[m_\sigma^2(c_s^2 + P') - R'_\sigma R''_\sigma w_0] - \omega^2[2c_s^4 G^0 - 6G^1 P' + c_s^2(2G^1 + 2G^0 P')]} \quad (\text{V.25})$$

Setting $G^i = 1, i = 0, 1$, $P' = c_s^2$ and $B = 0$ as well as $R'_\sigma = R''_\sigma = 0$, we get $\Delta_{12} = 0$, as expected.

¹⁷ In [16], a magnetic fluid is defined as a colloid of tiny (100 Å) magnetic particles or grains suspended in a carrier fluid as water.

2. Propagation in $\mathbf{e}_1 - \mathbf{e}_3$ plane

Setting $\theta \neq 0, \varphi = 0$, the wave vector in the $\mathbf{e}_1 - \mathbf{e}_3$ is given by $\mathbf{k}_{13} = (k_{13} \sin \theta, 0, k_{13} \cos \theta)$. Plugging now the approximation $k_{13} = k_0 + k'_{13}$, with $k_0 = \frac{\omega}{c_s}$ in the dispersion relation (V.17), and expanding the resulting expression in the orders of k'_{13} , we arrive at

$$k'_{13} = \frac{\mathcal{N}_{13}}{\mathcal{D}_{13}}, \quad (\text{V.26})$$

with the numerator

$$\begin{aligned} \mathcal{N}_{13} = & 2c_s^2 \omega [m_\sigma^2 (c_s^2 - P') + R'_\sigma R''_\sigma w_0] - \omega^3 (2c_s^2 G^0 - G^1 - G^3) (c_s^2 - P') \\ & - \omega^3 (G^1 - G^3) (c_s^2 - P') \cos(2\theta), \end{aligned} \quad (\text{V.27})$$

and the denominator

$$\begin{aligned} \mathcal{D}_{13} = & 4c_s \omega^2 (G^1 + G^3) P' + 2c_s^3 [2m_\sigma^2 P' - 2R'_\sigma R''_\sigma w_0 - \omega^2 (G^1 + G^3 + 2G^0 P')] \\ & + 2c_s \omega^2 (G^1 - G^3) (c_s^2 - 2P') \cos(2\theta). \end{aligned} \quad (\text{V.28})$$

Setting $G^i = 1, i = 0, 1, 2, P' = c_s^2$ and $B = 0$ as well as $R'_\sigma = R''_\sigma = 0$, we get $k'_{13} = 0$, as expected. The anisotropy Δ_{13} is then determined using the identity $\omega \approx k_{13} v_{13}$ with $k_{13} = k_0 + k'_{13}$ and $v_{13} = c_s (1 + \Delta_{13})$. Plugging k'_{13} from (V.26)-(V.28) in k_{13} , the anisotropy reads

$$\Delta_{13}(G^0, G^1, G^3; \theta, \omega) = \frac{\Delta_n}{\Delta_d}, \quad (\text{V.29})$$

with

$$\begin{aligned} \Delta_n = & -2c_s^2 [m_\sigma^2 (c_s^2 - P') + R'_\sigma R''_\sigma w_0] + \omega^2 (2c_s^2 G^0 - G^1 - G^3) (c_s^2 - P') \\ & + \omega^2 (G^1 - G^3) (c_s^2 - P') \cos(2\theta), \end{aligned} \quad (\text{V.30})$$

and

$$\begin{aligned} \Delta_d = & 2c_s^2 [m_\sigma^2 (c_s^2 + P') - R'_\sigma R''_\sigma w_0] - \omega^2 [2c_s^4 G^0 - 3(G^1 + G^3) P' + c_s^2 (G^1 + G^3 + 2G^0 P')] \\ & + \omega^2 (G^1 - G^3) (c_s^2 - 3P') \cos(2\theta). \end{aligned} \quad (\text{V.31})$$

Setting $G^i = 1, i = 0, 1, P' = c_s^2$ and $B = 0$ as well as $R'_\sigma = R''_\sigma = 0$, we get $\Delta_{13} = 0$, as expected. Here, in contrast to Δ_{12} , the θ -dependence remains in the anisotropy Δ_{13} . In the next section, we will determine numerically the anisotropy functions Δ_{12} and Δ_{13} for plane waves propagating in the transverse and longitudinal directions with respect to the external magnetic fields, respectively.

VI. NUMERICAL RESULTS AND DISCUSSION

A. Energy density and pressure of a magnetized QGP near the chiral phase transition point

In this section, we will use the results from previous sections to study the effect of a strong magnetic field on the sound velocity v_s of a plane wave propagating in an expanding *magnetized* QGP. The latter is modeled in this paper by the NJL effective action in the presence of a constant magnetic field. In previous section, using a linear approximation, we have defined an anisotropy function $\Delta \equiv \frac{v_s}{c_s} - 1$, where $c_s = 1/\sqrt{3}$ is the sound velocity in an ideal gas without matter fields. In [37], the temperature dependence of v_s in a hot QGP without magnetic field is studied. It is shown that the sound velocity shows a minimum at the chiral critical point. Whereas the results in [37] is found using purely hydrodynamical arguments, we intend to present in this paper a microscopic model which is merged carefully with hydrodynamics to study the (T, μ) dependence of sound velocity in a magnetized QGP. To this purpose, we have to know approximately at which critical temperature, T_c , the expected chiral phase transition may occur. The temperature dependence of the energy density of a system can give us a useful hint in this direction. As it is known from lattice QCD, we expect an increase in

pressure P and the energy density ϵ at the chiral critical point as a consequence of a first order phase transition. To determine P in our NJL model in a strong magnetic field, the relation (V.10) can be used between the thermodynamic pressure and the one-loop effective potential Ω which is determined in Sect. II A. The energy density ϵ can be determined using the equation of state (V.6), i.e. $\epsilon = -P + n\mu + TS + BM$. Here, the number and entropy densities n and s , as well as the magnetization density M are given by thermodynamic relations (V.16). To determine the thermodynamical quantities ϵ, P, n and s at thermal equilibrium, i.e. ϵ_0, P_0, n_0 and s_0 , we have to replace $\vec{\rho} = (\sigma, \pi)$ appearing in the thermodynamical potential (II.22) by the dynamical mass $\sigma_0(eB, T, \mu)$ which is determined in (II.29).¹⁸ As we have shown in Sect. II B, the dynamical mass can only be determined approximately. Using the same approximations as described in the last paragraph of Sects. II A and II B, we have determined the energy density ϵ_0/T^4 and pressure $3P_0/T^4$ as a function of T for a fixed value of the magnetic field $eB = 1 \text{ GeV}^2$ and two different values of the chemical potential $\mu = 0, 10^{-1} \text{ GeV}$ in Fig. 4. As it is expected, the energy density and pressure have a maximum at $T_c \sim 100 - 120 \text{ MeV}$.

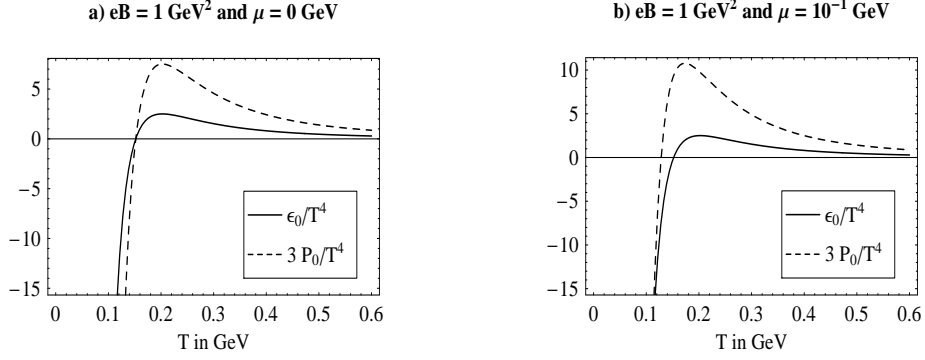


FIG. 4: The temperature dependence of the energy density ϵ_0 and pressure P_0 for $eB = 1 \text{ GeV}^2$ and $\mu = 0 \text{ GeV}$ (a) as well as $\mu = 10^{-1} \text{ GeV}$ (b) at thermal equilibrium. At $T_c \sim 100 - 120 \text{ MeV}$, there is an increase of the energy density as a consequence of a first order phase transition.

We will next study the effect of the strong magnetic field fixed at $eB = 1 \text{ GeV}^2$ on the sound velocity in the vicinity of the chiral critical point $T_c \sim 100 - 120 \text{ MeV}$. As we have seen in Sect. V B 1 and V B 2, the presence of an external magnetic field leads to an anisotropy in the sound velocity, so that the anisotropy function Δ for a plane wave propagating in the transverse (Δ_{12}) and longitudinal direction (Δ_{13}) with respect to the external magnetic fields have different dependence on the angles (θ, φ) of the spherical coordinate systems. In what follows, we will study the temperature dependence of Δ_{12} and Δ_{13} separately.

B. Anisotropy function and sound velocity for a propagation in $\mathbf{e}_1 - \mathbf{e}_2$ plane

As we have seen in Sect. V B 1, for a plane wave propagating in $\mathbf{e}_1 - \mathbf{e}_2$ plane, transverse to the magnetic field $\mathbf{B} = B\mathbf{e}_3$, the anisotropy Δ_{12} from (V.25) does not depend on the angle φ of the spherical coordinate system. On the other hand, Δ_{12} depends on the frequency of the incident plane wave ω . Fig. 5 shows Δ_{12} as a function of ω for fixed values of $eB = 1 \text{ GeV}^2$ and $\mu = 0 \text{ GeV}$ and for $T = 50 \text{ MeV}$ (below T_c), $T = 100 \text{ MeV}$ ($\sim T_c$) and $T = 150 \text{ MeV}$ (above T_c). The three curves show different slopes, but the maximum change of Δ_{12} for the frequency $\omega \in [0, 10] \text{ fm}^{-1}$ is small $\sim 0.2\%$.¹⁹ In what follows, we will fix the frequency to be $\omega = 0.1 \text{ fm}^{-1}$, where according to Fig. 5, Δ_{12} remains approximately constant for $T \gtrsim T_c$.

In Table II, the anisotropy function Δ_{12} and the velocity v_{12} are determined for fixed $eB = 1 \text{ GeV}^2$ and various $T \in [30, 450] \text{ MeV}$ and $\mu = 0, 10^{-3} \text{ GeV}$. Whereas for $\mu = 0$, the anisotropy Δ_{12} and the velocity v_{12} are real valued, they are imaginary for $\mu \neq 0$, e.g. $\mu = 10^{-3} \text{ GeV}$. Qualitatively, the real part of Δ_{12} as well as v_{12} for

¹⁸ Let us remind that the configuration $(\sigma_0 \neq 0, \pi_0 = 0)$ builds the stationary point of the effective potential or equivalently describes the thermodynamic equilibrium.

¹⁹ In [38] for the relevant frequency is taken in the interval $\omega \in [-0.1, +0.1] \text{ fm}^{-1}$.

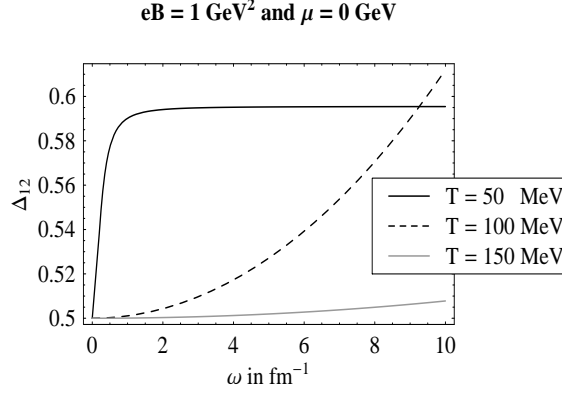


FIG. 5: The frequency dependence of $\Delta_{12} \equiv \frac{v_{12}}{c_s} - 1$ for three different temperature $T = 50 \text{ MeV}$ (below T_c), $T = 100 \text{ MeV}$ ($\sim T_c$) and $T = 150 \text{ MeV}$ (above T_c) for $eB = 1 \text{ GeV}^{-2}$ and zero chemical potential.

$\mu = 0$ and $\mu \neq 0$ has a maximum at $T \sim 40 - 45 \text{ MeV} \sim 0.4 - 0.45T_c$. In the transition regime $T_c \sim 100 - 150 \text{ MeV}$, they arrive at their local minimum and remain constant after phase transition $T > 150 \text{ MeV}$ (see Fig. 6). The constant values of v_{12} after the phase transition is $v_{12} = 1.5 c_s \sim 0.866$. The temperature dependence of the sound velocity is studied in [37] for $eB = 0$ and $\mu = 0$ using purely hydrodynamical methods: The authors use at high temperature $T > 1.15T_c$ the sound velocity function obtained from lattice QCD [52], whereas at low temperature $T < 0.15T_c$ the result of the hadron gas model is used. At moderate temperatures different interpolations between those two results are employed. It is shown that the interpolating functions have a local maximum at $T = 0.4T_c$ (corresponding to the maximal value of the sound velocity in the hadron gas) and a local minimum at $T = T_c$ (corresponding to the expected minimal value of the sound velocity at the phase transition). Comparing to the results from [37], our results show that for a wave propagating in the $\mathbf{e}_1 - \mathbf{e}_2$ plane, transverse to the direction of the magnetic field, the qualitative dependence of the sound velocity v_{12} on temperature does not change. As for the imaginary part of v_{12} for $\mu \neq 0$, as it can be seen in Table II, they are several orders of magnitude smaller than the real part of v_{12} . These kind of density fluctuations are studied in [38], and are interpreted as a possible origin for the suppression of Mach cone at the chiral critical point.

$eB = 1 \text{ GeV}^2, \mu = 0 \text{ GeV}, \omega = 0.1$			$eB = 1 \text{ GeV}^2, \mu = 10^{-3} \text{ GeV}, \omega = 0.1$	
T in MeV	Δ_{12}	v_{12}	Δ_{12}	v_{12}
30	0.518087	0.876468	$0.516894 + 2.87 \times 10^{-28}i$	$0.875779 - 1.66 \times 10^{-28}i$
40	0.54583	0.892486	$0.538411 - 6.81 \times 10^{-31}i$	$0.888202 - 3.93 \times 10^{-31}i$
45	0.569558	0.906184	$0.522862 + 1.17 \times 10^{-32}i$	$0.882020 - 3.93 \times 10^{-31}i$
50	0.513846	0.874019	$0.528016 - 1.69 \times 10^{-32}i$	$0.882200 - 9.73 \times 10^{-33}i$
100	0.500001	0.866032	$0.500005 - 3.31 \times 10^{-27}i$	$0.866029 - 1.91 \times 10^{-27}i$
150	0.500001	0.866026	$0.5 - 2.67 \times 10^{-28}i$	$0.866026 - 1.54 \times 10^{-28}i$
200	0.5	0.866025	$0.5 - 4.98 \times 10^{-34}i$	$0.866025 - 2.86 \times 10^{-34}i$
250	0.5	0.866025	$0.5 - 2.46 \times 10^{-33}i$	$0.866025 - 1.42 \times 10^{-33}i$
300	0.5	0.866025	$0.5 - 2.97 \times 10^{-30}i$	$0.866025 - 1.72 \times 10^{-30}i$
350	0.5	0.866025	$0.5 - 8.57 \times 10^{-31}i$	$0.866025 - 4.95 \times 10^{-31}i$
400	0.5	0.866025	$0.5 + 8.75 \times 10^{-35}i$	$0.866025 + 5.05 \times 10^{-35}i$
450	0.5	0.866025	$0.5 - 1.52 \times 10^{-34}i$	$0.866025 - 8.75 \times 10^{-32}i$

TABLE II: The anisotropy function Δ_{12} and the velocity v_{12} for $T \in [30, 450] \text{ MeV}$ and fixed $eB = 1 \text{ GeV}^2$. For nonzero baryon chemical potential Δ_{12} as well as v_{12} are imaginary. At the transition temperature Δ_{12} as well as v_{12} reach their minimum value and remain constant after the phase transition $T > T_c \approx 100 - 150 \text{ MeV}$.

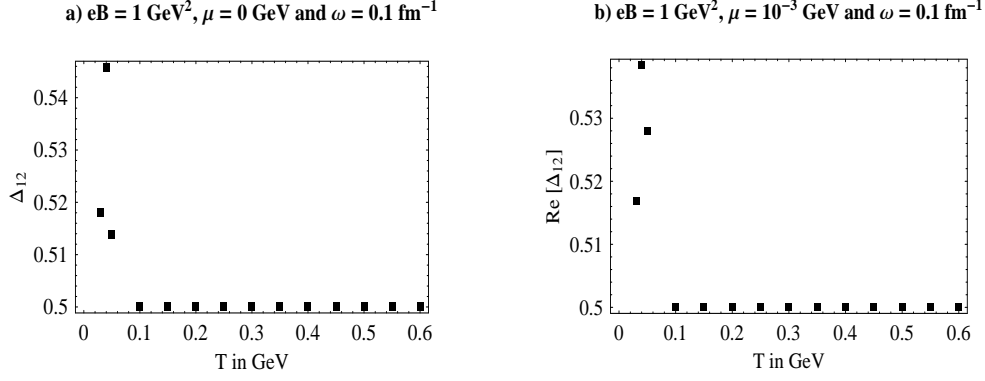


FIG. 6: The anisotropy $\Delta_{12} \equiv \frac{v_{12}}{c_s} - 1$ as a function of temperature T for fixed value of $eB = 1 \text{ GeV}^2$, $\omega = 0.1 \text{ fm}^{-1}$ as well as $\mu = 0 \text{ GeV}$ (a) and $\mu = 10^{-3} \text{ GeV}$ (b). The sound velocity has a maximum at $T \sim 0.4T_c - 0.45T_c$ and decreases at the critical temperature $T_c \sim 100 - 120 \text{ MeV}$. After the phase transition at $T > 150 \text{ MeV}$, it remains constant $v_{12} \approx 1.5c_s$.

C. Anisotropy function and sound velocity for a propagation in $\mathbf{e}_1 - \mathbf{e}_3$ plane

For a wave propagating in the $\mathbf{e}_1 - \mathbf{e}_3$ plane, parallel to the external magnetic field, the anisotropy function Δ_{13} from (V.29) as well as the velocity $v_{13} \equiv c_s(1 + \Delta_{13})$, depend on the angle θ of the spherical coordinate system. It depends also on the frequency ω , as for Δ_{12} . Fig. 7 shows the (ω, θ) dependence of Δ_{13} for fixed values of $eB = 1 \text{ GeV}^2$, $\mu = 0$ as well as $T = 50 \text{ MeV}$ (below T_c), $T = 100 \text{ MeV}$ ($\sim T_c$) and $T = 150 \text{ MeV}$ (above T_c). Qualitatively, whereas Δ_{12} increases with ω (see Fig. 5), $\Delta_{13}(\theta \neq \frac{\pi}{2})$ decreases with ω and depends at the same time on the angle θ between the wave vector \mathbf{k} and the external magnetic field \mathbf{B} . Note that primarily for $\theta = \frac{\pi}{2}$, the anisotropy is to be calculated from Δ_{12} (V.25). But, it turns out that

$$\Delta_{12}(G^0, G^1; \omega) = \Delta_{13}(G^0, G^1, G^3; \theta = \frac{\pi}{2}, \omega),$$

where Δ_{12} is given in (V.25) and Δ_{13} in (V.29). Thus, $\Delta_{13}(\theta = \frac{\pi}{2})$ has the same ω -dependence as Δ_{12} .

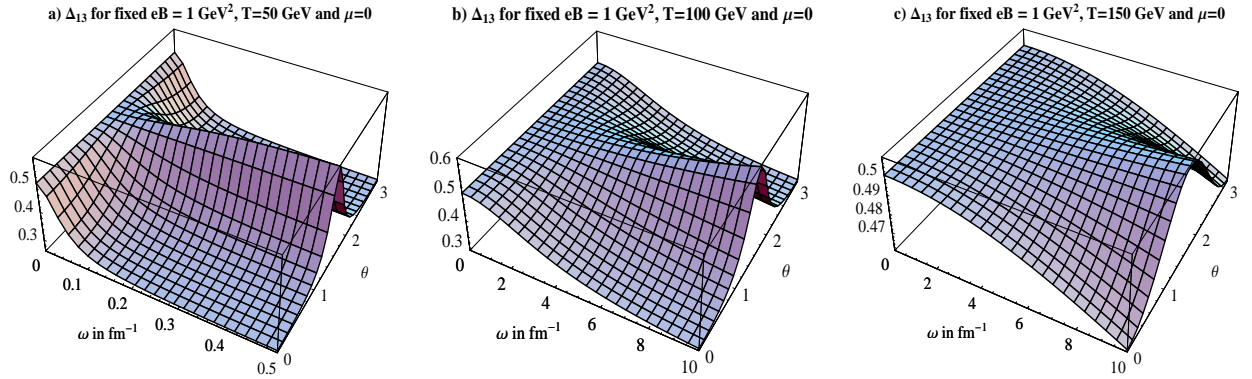


FIG. 7: Qualitative dependence of Δ_{13} on the frequency ω and the angle θ for fixed values of $eB = 1 \text{ GeV}^2$, $\mu = 0$ as well as (a) $T = 50 \text{ MeV}$ (below T_c), (b) $T = 100 \text{ MeV}$ ($\sim T_c$), and (c) $T = 150 \text{ MeV}$ (above T_c). In contrast to Δ_{12} , Δ_{13} as well as the sound velocity for $\theta \neq \frac{\pi}{2}$ decreases with ω . For $\theta = \frac{\pi}{2}$ Δ_{13} has the same behavior as Δ_{12} .

In what follows, we will work with a fixed value of $\omega = 0.1 \text{ fm}^{-1}$, where for $T \gtrsim T_c$, Δ_{13} is approximately constant (see Fig. 7). In Fig. 8 a) the temperature dependence of the sound velocity v_{13} is presented for fixed values of $\theta \in \{0, \frac{\pi}{6}, \frac{\pi}{4}, \frac{\pi}{6}\}$ and $eB = 1 \text{ GeV}^2$ as well as $\mu = 0 \text{ GeV}$ and $\omega = 0.1 \text{ fm}^{-1}$. In contrast to v_{12} , the sound velocity v_{13} increases with temperature. It has therefore a local minimum at $T < T_c$, reaches its local

maximum at $T \sim T_c$ and remains constant for $T > T_c$. Hence, the constant value $v_{13} = 1.5 c_s \approx 0.866$ of the sound velocity that arises in the above linear approximation, is a lower bound for v_{12} and an upper bound for v_{13} as the temperatures are higher than the critical temperature $T \gtrsim T_c$. For v_{13} this behavior is independent on the angle θ [see Fig. 8 b for a comparison between v_{12} and v_{13} at various angles].

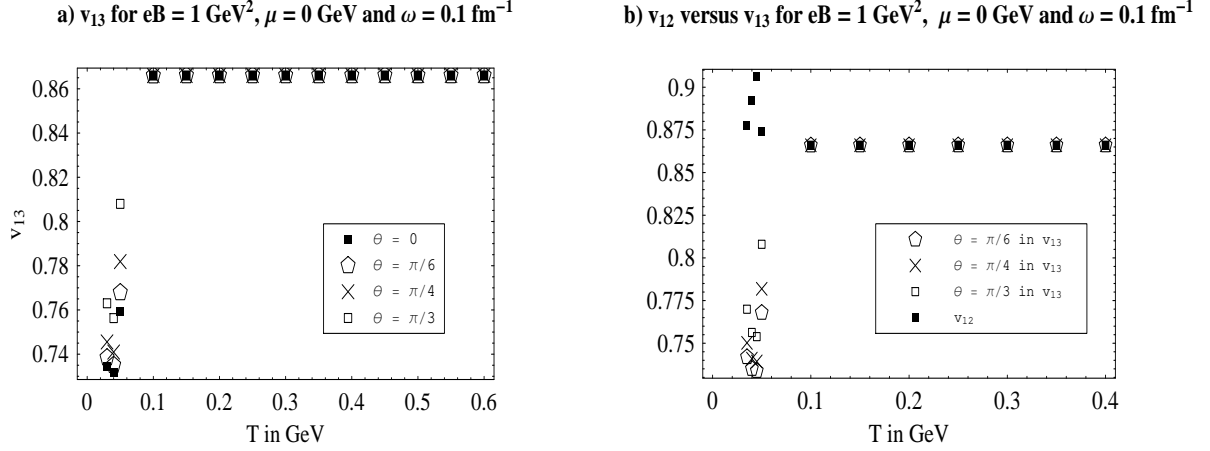


FIG. 8: a) Temperature dependence of the sound velocity v_{13} for fixed values of $\theta \in \{0, \frac{\pi}{6}, \frac{\pi}{4}, \frac{\pi}{6}\}$ and $eB = 1 \text{ GeV}^2$ as well as $\mu = 0 \text{ GeV}$ and $\omega = 0.1 \text{ fm}^{-1}$. b) Temperature dependence of v_{12} versus v_{13} for $\theta \in \{\frac{\pi}{6}, \frac{\pi}{4}, \frac{\pi}{6}\}$ and $eB = 1 \text{ GeV}^2$ as well as $\mu = 0 \text{ GeV}$ and $\omega = 0.1 \text{ fm}^{-1}$. The sound velocity v_{12} (v_{13}) has a local maximum (minimum) at $T < T_c$, reaches its local minimum (maximum) at $T \sim T_c$ and remains constant for $T > T_c$.

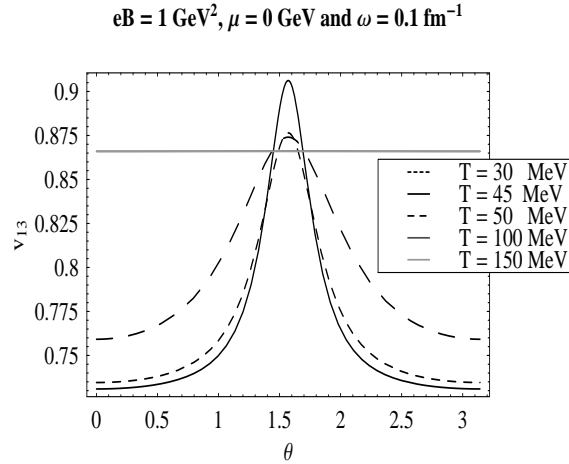


FIG. 9: The θ -dependence of v_{13} for $T = 30, 45, 50 \text{ MeV}$ ($< T_c$) $T = 100, 150$ ($\gtrsim T_c$) and for fixed values of $eB = 1 \text{ GeV}^2$, $\mu = 0 \text{ GeV}$ and $\omega = 0.1 \text{ fm}^{-1}$. Whereas for $T < T_c$, v_{13} is θ dependent and has its maximal value at $\theta = \frac{\pi}{2}$, for $T \geq T_c$ it is almost constant with $v_{13} = 1.5 c_s \approx 0.866$.

In Fig. 9, the θ dependence of v_{13} is plotted for $T = 30, 45, 50 \text{ MeV}$ ($< T_c$) $T = 100, 150$ ($\gtrsim T_c$) and for fixed values of $eB = 1 \text{ GeV}^2$, $\mu = 0 \text{ GeV}$ and $\omega = 0.1 \text{ fm}^{-1}$. As expected from Fig. 8, whereas for $T < T_c$, v_{13} is θ dependent and has its maximal value at $\theta = \frac{\pi}{2}$, for $T \geq T_c$ it is almost constant with $v_{13} = 0.5c_s \approx 0.866$.

VII. CONCLUSION

Strong magnetic fields play an important role in the physics of non-central heavy ion collisions. They provide a possible signature of the presence of CP-odd domains in the presumably formed QGP phase [22, 23, 24]. Apart

from other mechanisms, relativistic shock waves, that are believed to be built in the heavy ion collisions, can be made responsible for their generation. In astrophysics, the strong magnetic fields generated in collisionless relativistic shocks play an important role in the fire-ball model for Gamma-ray Bursts [29]. Recent studies on the effect of magnetic field in modifying the nature of the QCD chiral phase transition in a linear σ -model indicate that for high enough magnetic fields, comparable to the ones expected to be created in the non-central heavy ion collisions at RHIC, the original crossover is turned into a first order phase transition [33, 34, 35].

In the present paper, we have studied the possible effects of strong magnetic fields on the hydrodynamical signals of an expanding perfect magnetized QGP coupled to chiral fields. In particular, performing a first order stability analysis in a chiral magnetohydrodynamic framework, the sound velocity of a propagating plane wave in this medium is determined. To this purpose, we have extended the variational method applied in [12] on the effective potential of a linear σ -model at finite (T, μ) and zero magnetic field \mathbf{B} to the case of nonzero magnetic field. As for the effective action, we have used the NJL model of QCD at finite (T, μ) , and in the presence of a strong \mathbf{B} field. The magnetic field is assumed to be constant and aligned in the third direction, i.e. $\mathbf{B} = B\mathbf{e}_3$. This model is known to exhibit a dynamical chiral phase transition due to the phenomenon of magnetic catalysis arising from the dynamically generated fermion mass [19].

In the first part of this paper, we have explicitly determined the effective potential and effective kinetic term of the NJL model at finite (T, μ) and in the presence of a strong B field. In particular, the effective kinetic term is determined in a derivative expansion, where structure functions appear that depend on (T, μ) and the external magnetic field B . Using the effective Lagrangian density, we have derived the dynamical mass generated in the regime of LLL dominance. The dynamical mass, being the configuration that minimizes the effective potential of the model, is used, in the second part of the paper, as the equilibrium configuration once the instabilities in the strongly magnetized QGP are set on. It depends on (T, μ) and B and vanishes once the QCD matter has passed the chiral critical point (see Fig. 2 for its qualitative behavior for a fixed value of the magnetic field).

In the second part of the paper, a chiral magnetohydrodynamic description of the strongly magnetized QGP is presented. We have, in particular, compared the total energy-momentum $T^{\mu\nu}$ and the polarization tensor $M^{\mu\nu}$, that arise field theoretically from the Lagrangian density of the effective NJL model, with the corresponding quantities from hydrodynamics. The polarization tensor $M^{\mu\nu}$ appears in $T^{\mu\nu}$ and includes the magnetization density M of the medium. It is introduced in [44], where Nernst effect near the superfluid-insulator phase transition of condensed matter physics is studied using an appropriate MHD description. Note that in contrast to the work by Sachdev et al. [44], the magnetized fluid modeled in our paper is coupled to chiral fields and involves the effects of a possible chiral phase transition.

The dispersion relation of the hot and dense medium in the presence of a strong magnetic field is derived using a first order stability analysis. As for the sound velocity of a plane wave propagating in the magnetized QGP modeled in this paper, we have used a method presented in [16] and determined the anisotropy Δ in a linear approximation. Here, $\Delta \equiv \frac{v_s}{c_s} - 1$ with v_s the sound velocity in the medium, and $c_s = 1/\sqrt{3}$ the sound velocity in an ideal gas. In our model, Δ shows, as in the magnetic fluid considered in [16], a non-trivial frequency dependence. Moreover, for a plane wave propagating in the transverse $\mathbf{e}_1 - \mathbf{e}_2$ plane with respect to the external magnetic field $\mathbf{B} = B\mathbf{e}_3$, Δ_{12} does not depend on the angle φ between the wave vector \mathbf{k} and the external magnetic field \mathbf{B} . On the other hand, for a plane wave propagating parallel to the magnetic field in the $\mathbf{e}_1 - \mathbf{e}_3$ plane, Δ_{13} depends on the angle θ between \mathbf{k} and \mathbf{B} . Here, (θ, φ) are the angles in the spherical coordinate system. In Figs. 8 b we have compared the sound velocity v_{12} and v_{13} as a function of temperature for a fixed values of eB, μ, ω and various angles θ . In contrast to the sound velocity v_{13} of a plane wave propagating in the $\mathbf{e}_1 - \mathbf{e}_3$ plane, the sound velocity in the $\mathbf{e}_1 - \mathbf{e}_2$ plane, v_{12} , has a local maximum at $T < T_c$, reaches its local minimum at $T \sim T_c$ and remains constant for $T > T_c$. The constant value $v_s \sim 1.5 c_s \approx 0.866$ seems therefore to be, in this linear approximation, a *lower bound* for v_{12} and an *upper bound* for v_{13} as the temperatures are higher than the critical temperature $T > T_c$. For v_{13} this behavior is independent on the angle θ .

The universal properties of the equation of state $\epsilon(p)$, and in particular the temperature dependence of the speed of sound at $T \sim (2-3)T_c$, where the theory is close to being conformal, is recently investigated in [54, 55] using the holographic principle in the framework of gauge-gravity duality of string theory. It is shown, that for a general class of strongly interacting theories at high temperatures the speed of sound approaches the conformal value $c_s = 1/\sqrt{3}$ from *below*. It would be interesting to extend the method used in these papers to study the behavior of the sound velocity in a strongly magnetized QGP.

VIII. ACKNOWLEDGEMENTS

N.S. thanks F. Ardalan, Sh. Fayyazbakhsh, K. Sohrabi and Z. Davoudi for useful discussions. This work is supported by the research council of Sharif University of Technology and the Center of Excellence in Physics (CEP).

APPENDIX A: HIGH TEMPERATURE EXPANSION AND BESSEL FUNCTION IDENTITIES FOR FINITE T AND μ

As we have seen in Sect. II, the temperature dependent part of the effective potential as well as the gap equation of the NJL model of QCD consists of terms in the form

$$\sum_{\ell=1}^{\infty} (-1)^{\ell} \frac{1}{\ell^p} K_p(\ell z) \cosh(\mu\beta\ell). \quad (\text{A.1})$$

Here, $z = m\beta$, with m the dynamical mass,²⁰ and μ the finite chemical potential. This expression can be written in the generalized form

$$\sum_{\ell=1}^{\infty} \frac{1}{\ell^p} K_p(\ell z) \cos(\ell\phi), \quad (\text{A.2})$$

with $\phi = \pi + i\mu\beta$. This identity is determined for $\mu = 0$ in [40]. To derive the corresponding Bessel function identities for summations of the form of (A.2), the authors starts in particular with the identity

$$\sum_{\ell=1}^{\infty} K_0(\ell z) \cos(\ell\phi) = \frac{1}{2} \left[\gamma + \ln \left(\frac{z}{4\pi} \right) \right] + \frac{\pi}{2} \sum_{\ell}' \left[\frac{1}{\sqrt{z^2 + (\phi - 2\pi\ell)^2}} - \frac{1}{2\pi|\ell|} \right], \quad (\text{A.3})$$

where the notation \sum_{ℓ}' is used to indicate that singular terms in the summation over all values of $\ell \in (-\infty, +\infty)$, here $\ell = 0$ in $1/|\ell|$, are omitted [40]. In this appendix, we will first evaluate the sum over ℓ on the r.h.s. of (A.3) and present it in terms of a series expansion in $z = m\beta$. Then, using the result for $\phi = \pi + i\mu\beta$, as it appears in the effective potential and gap equation in Sect. II, we will determine (A.2) for $p = 0$ and $p = 1$. The method presented in this appendix can be used to give an expansion of (A.2) in terms of z for all p . This will be in particular useful if we are interested in a high temperature expansion of the effective potential, as well as the gap equation.

1. High temperature expansion of (A.2) for $p = 0$

To start let us consider (A.3) and denote the sum over ℓ on the r.h.s. by $C(\phi, z, z')$, where $z = m\beta$ and $z' = \mu\beta$

$$\sum_{\ell=1}^{\infty} K_0(\ell z) \cos(\ell\phi) = \frac{1}{2} \left[\gamma + \ln \left(\frac{z}{4\pi} \right) \right] + C(\phi, z, z'), \quad (\text{A.4})$$

where in particular

$$C(\pi, z, z') = \frac{\pi}{2} \sum_{\ell}' \left[\frac{1}{\sqrt{z^2 + (\pi + iz' - 2\pi\ell)^2}} - \frac{1}{2\pi|\ell|} \right]. \quad (\text{A.5})$$

Expanding $C(\pi, z, z')$ in the orders of z , we arrive first at

$$C(\pi, z, z') = \sum_{\ell=-\infty}^{\infty} \mathcal{A}_{\ell}(\pi, 0, z') + \sum_{\ell=-\infty}^{\infty} \mathcal{B}_{\ell}(\pi, z, z') + \sum_{\ell=1}^{\infty} \mathcal{C}_{\ell}, \quad (\text{A.6})$$

²⁰ In the case of the NJL model, m should be replaced by σ_0 .

where

$$\mathcal{A}_\ell(\pi, 0, z') \equiv \frac{1}{2|1 - 2\ell + \frac{iz'}{\pi}|}, \quad (\text{A.7})$$

is the zeroth order term in z , and

$$\mathcal{B}_\ell(\pi, z, z') = \left\{ -\frac{1}{4\pi^2} \frac{1}{|1 - 2\ell + \frac{iz'}{\pi}|^3} z^2 + \frac{3}{16\pi^4} \frac{1}{|1 - 2\ell + \frac{iz'}{\pi}|^5} z^4 - \frac{5}{32\pi^6} \frac{1}{|1 - 2\ell + \frac{iz'}{\pi}|^7} z^6 \pm \dots \right\}, \quad (\text{A.8})$$

denotes the higher order terms in z . Further, $\mathcal{C}_\ell \equiv -\frac{1}{2\ell}$. Let us first consider the sum over ℓ in \mathcal{A}_ℓ

$$\sum_{\ell=-\infty}^{\infty} \mathcal{A}_\ell(\pi, 0, z') = \frac{1}{2} \sum_{\ell=0}^{\infty} \left(\frac{1}{2\ell+1 + \frac{iz'}{\pi}} + \frac{1}{2\ell+1 - \frac{iz'}{\pi}} \right) = \sum_{\ell=0}^{\infty} \frac{(2\ell+1)}{(2\ell+1)^2 + \frac{z'^2}{\pi^2}}. \quad (\text{A.9})$$

Expanding \mathcal{A}_ℓ in the orders of $\frac{z'}{\pi} = \frac{\mu\beta}{\pi}$, we arrive at

$$\begin{aligned} \sum_{\ell=-\infty}^{\infty} \mathcal{A}_\ell(\pi, 0, z') &= \sum_{k=0}^{\infty} \sum_{\ell=0}^{\infty} \frac{(-1)^k}{(2\ell+1)^{2k+1}} \left(\frac{z'}{\pi} \right)^{2k} \\ &= \sum_{\ell=0}^{\infty} \frac{1}{(2\ell+1)} + \sum_{k=1}^{\infty} \frac{(-1)^k (2^{2k+1} - 1)}{2^{2k+1}} \left(\frac{z'}{\pi} \right)^{2k} \zeta(2k+1), \end{aligned} \quad (\text{A.10})$$

where the definition of the Riemann ζ -function

$$\zeta(z) \equiv \sum_{k=1}^{\infty} \frac{1}{k^z}, \quad z > 1,$$

is used. Using now the identity

$$\sum_{\ell=0}^{\infty} \frac{1}{2\ell+1} - \sum_{\ell=1}^{\infty} \frac{1}{2\ell} = \sum_{\ell=1}^{\infty} \frac{(-1)^{\ell+1}}{\ell} = \ln 2, \quad (\text{A.11})$$

we get

$$\sum_{\ell=-\infty}^{\infty} \mathcal{A}_\ell(\pi, 0, z') + \sum_{\ell=1}^{\infty} \mathcal{C}_\ell = \ln 2 + \sum_{k=1}^{\infty} \frac{(-1)^k (2^{2k+1} - 1)}{2^{2k+1}} \left(\frac{z'}{\pi} \right)^{2k} \zeta(2k+1). \quad (\text{A.12})$$

To evaluate $\sum_{\ell} \mathcal{B}_\ell$ on the r.h.s. of (A.6) with \mathcal{B}_ℓ given in (A.8), we split the sum over $\ell \in (-\infty, +\infty)$ in a sum over $\ell \in (-\infty, 0]$ and $\ell \in [1, \infty)$. We arrive at

$$\sum_{\ell=-\infty}^0 \mathcal{B}_\ell(\pi, z, z') = \sum_{n=1}^{\infty} \frac{(-1)^n}{4^{2n+1} (n!)^2} \left(\frac{z}{\pi} \right)^{2n} \left| \psi^{(2n)} \left(\frac{1}{2} + \frac{iz'}{2\pi} \right) \right|, \quad (\text{A.13})$$

as well as

$$\sum_{\ell=1}^{\infty} \mathcal{B}_\ell(\pi, z, z') = \sum_{n=1}^{\infty} \frac{(-1)^n}{4^{2n+1} (n!)^2} \left(\frac{z}{\pi} \right)^{2n} \left| \psi^{(2n)} \left(\frac{1}{2} - \frac{iz'}{2\pi} \right) \right|. \quad (\text{A.14})$$

Here, $\phi^{(p)}(z)$ is p -th derivative of the polygamma-function $\psi(z) \equiv \frac{d}{dz} \ln \Gamma(z)$ with respect to z . Plugging (A.12)-(A.14) in (A.6), $C(\pi, z, z')$ is given by

$$\begin{aligned} C(\pi, z, z') &= \ln 2 + \sum_{k=1}^{\infty} \frac{(-1)^k (2^{2k+1} - 1)}{2^{2k+1}} \left(\frac{z'}{\pi} \right)^{2k} \zeta(2k+1) \\ &\quad + \sum_{n=1}^{\infty} \frac{(-1)^n}{4^{2n+1} (n!)^2} \left(\frac{z}{\pi} \right)^{2n} \left\{ \left| \psi^{(2n)} \left(\frac{1}{2} + \frac{iz'}{2\pi} \right) \right| + \left| \psi^{(2n)} \left(\frac{1}{2} - \frac{iz'}{2\pi} \right) \right| \right\}. \end{aligned} \quad (\text{A.15})$$

This leads to the first Bessel-function identity

$$\begin{aligned} \sum_{\ell=1}^{\infty} K_0(\ell z) \cos(\ell(\pi + iz')) &= \frac{1}{2} \left[\gamma + \ln \left(\frac{z}{\pi} \right) \right] + \sum_{k=1}^{\infty} \frac{(-1)^k (2^{2k+1} - 1)}{2^{2k+1}} \left(\frac{z'}{\pi} \right)^{2k} \zeta(2k+1) \\ &+ \sum_{n=1}^{\infty} \frac{(-1)^n}{4^{2n+1} (n!)^2} \left(\frac{z}{\pi} \right)^{2n} \left\{ \left| \psi^{(2n)} \left(\frac{1}{2} + \frac{iz'}{2\pi} \right) \right| + \left| \psi^{(2n)} \left(\frac{1}{2} - \frac{iz'}{2\pi} \right) \right| \right\}, \end{aligned} \quad (\text{A.16})$$

where (A.4) is used.

2. High temperature expansion of (A.2) for $p = 1$

In what follows, we will determine (A.2) for $p = 1$, and $\phi = \pi + z'$ with $z' = \mu\beta$, by generalizing the method used in [40]. Using the relation

$$\frac{d}{dz} \sum_{\ell=1}^{\infty} \frac{z}{\ell} K_1(\ell z) \cos(\ell\phi) = -z \sum_{\ell=1}^{\infty} K_0(\ell z) \cos(\ell\phi), \quad (\text{A.17})$$

that follows from the recursion relation

$$\frac{d}{dz} K_{\nu}(z) = -K_{\nu-1}(z) - \frac{\nu}{z} K_{\nu}(z), \quad (\text{A.18})$$

we have

$$\sum_{\ell=1}^{\infty} \frac{1}{\ell} K_1(\ell z) \cos(\ell\phi) = -\frac{1}{z} \int dz \left(z \sum_{\ell=1}^{\infty} K_0(\ell z) \cos(\ell\phi) \right) + \frac{C(\phi)}{z}. \quad (\text{A.19})$$

Here, $C(\phi)$ is an unknown function of ϕ , that, in contrast to the derivation presented in [40], is a function of $z' = \mu\beta$. In particular, we will set $\phi = \pi + iz'$ to evaluate Bessel-function identities in the form (A.1). To determine $C(\phi)$, we multiply (A.19) with z and use the behavior (A.21) of the $K_{\nu}(z)$ in limit $z \rightarrow 0$,

$$K_{\nu}(z) \xrightarrow{z \rightarrow 0} \frac{1}{z} \Gamma(\nu) \left(\frac{2}{z} \right)^{\nu}, \quad (\text{A.20})$$

to arrive at

$$C(\phi) = \sum_{\ell=1}^{\infty} \frac{1}{\ell^2} \cos(\ell\phi) = \frac{1}{2} [\text{Li}_2(e^{+i\phi}) + \text{Li}_2(e^{-i\phi})], \quad (\text{A.21})$$

where the polylogarithm-function $\text{Li}_p(z)$ is defined, in general, as

$$\text{Li}_p(z) = \sum_{k=1}^{\infty} \frac{z^k}{k^p}. \quad (\text{A.22})$$

The second Bessel-function identity can therefore be derived from (A.19) in combination with (A.16) and (A.21) as

$$\begin{aligned} \sum_{\ell=1}^{\infty} \frac{1}{\ell} K_1(\ell z) \cos(\ell\phi) &= \frac{1}{8} z \left[1 - 2\gamma_E - 2 \ln \left(\frac{z}{\pi} \right) \right. \\ &- \sum_{n=1}^{\infty} \frac{(-1)^n (1+n)}{(\Gamma(2+n))^2} \left(\frac{z}{4\pi} \right)^{2n} \left\{ \left| \psi^{(2n)} \left(\frac{1}{2} - \frac{iz'}{2\pi} \right) \right| + \left| \psi^{(2n)} \left(\frac{1}{2} + \frac{iz'}{2\pi} \right) \right| \right\} \\ &- \frac{z^2}{3} \sum_{k=1}^{\infty} \frac{(-1)^k (2^{2k+1} - 1)}{2^{2k+1}} \left(\frac{z'}{\pi} \right)^{2k} \zeta(2k+1) + \frac{1}{2z} \left\{ \text{Li}_2 \left(e^{i(\pi+iz')} \right) + \text{Li}_2 \left(e^{-i(\pi+iz')} \right) \right\} \right]. \end{aligned} \quad (\text{A.23})$$

Same method can be used to determine (A.2) for arbitrary $p > 1$.

APPENDIX B: MELLIN TRANSFORMATION AND THE SUMMATION OVER MATSUBARA FREQUENCIES AT FINITE T AND μ

As we have shown in Sect. II C, the integrals arising in the expressions for the structure functions $G^\mu, \mu = 0, \dots, 4$ from (II.46), have the general form

$$I = \frac{1}{\beta} \sum_{\ell=-\infty}^{+\infty} f(\omega_\ell - i\mu) = \frac{1}{\beta} \sum_{\ell=-\infty}^{+\infty} \int \frac{d^d k}{(2\pi)^d} \frac{(\mathbf{k}^2)^a \tilde{k}_0^{2t}}{(\mathbf{k}^2 + \tilde{k}_0^2 + m^2)^\alpha}, \quad (\text{B.1})$$

where, $\tilde{k}_0 \equiv (\omega_\ell - i\mu)$ with $\omega_\ell \equiv \frac{2\pi}{\beta}(2\ell + 1)$ the Matsubara frequencies, and μ the chemical potential. In [41], a similar integral as in (B.1), with $a = 0, t = 0$ and $\mu = 0$ potential is evaluated using the Mellin transformation

$$f(x) = \frac{1}{2\pi i} \int_{c-i\infty}^{c+i\infty} x^{-s} \mathcal{M}[f; s] ds, \quad (\text{B.2})$$

and its inverse transformation

$$\mathcal{M}[f; s] = \int_0^\infty x^{s-1} f(x) dx. \quad (\text{B.3})$$

As it is denoted in [41], the above transformation normally exists only in a strip $\alpha < \Re[s] < \beta$, and the inversion contour must lie in this strip $\alpha < c < \beta$. In this appendix, we will present a generalization of the results in [41] for arbitrary a, t and nonzero chemical potential $\mu \neq 0$. To this purpose, let us start with $\sum_\ell f(\omega_\ell - i\mu)$ on the l.h.s. of (B.1). Using (B.2), we arrive first at

$$\begin{aligned} I &= \frac{1}{\beta} \sum_{\ell=-\infty}^{+\infty} f(\omega_\ell - i\mu) = \frac{1}{2\pi i \beta} \sum_{\ell=-\infty}^{+\infty} \int_{c-i\infty}^{c+i\infty} ds (\omega_\ell - i\mu)^{-s} \mathcal{M}[f; s] \\ &= \frac{1}{2\pi i \beta} \int_{c-i\infty}^{c+i\infty} ds \left(\frac{2\pi}{\beta} \right)^{-s} \sum_{\ell=-\infty}^{+\infty} \left(\ell + \frac{1}{2} - \frac{i\mu\beta}{2\pi} \right)^{-s} \mathcal{M}[f; s], \end{aligned} \quad (\text{B.4})$$

where the definition of ω_ℓ is used. Performing now the sum over ℓ , as

$$\sum_{\ell=-\infty}^{+\infty} \left(\ell + \frac{1}{2} - \frac{i\mu\beta}{2\pi} \right)^{-s} = \zeta \left(s; \frac{1}{2} - \frac{i\mu\beta}{2\pi} \right) + \zeta \left(s; \frac{1}{2} + \frac{i\mu\beta}{2\pi} \right), \quad (\text{B.5})$$

and plugging this expression on the r.h.s. of (B.4), the integral I is given by $I = I_{-\mu} + I_{+\mu}$, with

$$I_{\pm\mu} = \frac{1}{2\pi i \beta} \int_{c-i\infty}^{c+i\infty} ds \left(\frac{2\pi}{\beta} \right)^{-s} \zeta \left(s; \frac{1}{2} \pm \frac{i\mu\beta}{2\pi} \right) \mathcal{M}[f; s]. \quad (\text{B.6})$$

On the other hand, comparing (B.3) with (B.1), $\mathcal{M}[f; s]$ can be determined. It is given by

$$\mathcal{M}[f; s] = \int y^{s-1} dy \int \frac{d^d k}{(2\pi)^d} \frac{k^{2a} y^{2t}}{(\mathbf{k}^2 + \mathbf{y}^2 + m^2)^\alpha}. \quad (\text{B.7})$$

To evaluate this integral, we combine two vectors \mathbf{k} and \mathbf{y} to a $D \equiv s + d + 2(t + a)$ -dimensional Euclidean vector. Evaluating now the D -dimensional integral using standard identities from dimensional regularization [56], $\mathcal{M}[f; s]$ is given by

$$\begin{aligned} \mathcal{M}[f; s] &= \frac{(2\pi)^{s+2t}}{d\Omega_{s+2t}} \frac{d\Omega_d (2\pi)^{2a}}{d\Omega_{d+2a}} \int \frac{d^{d+2(a+t)+s} k}{(2\pi)^{d+2(a+t)+s}} \frac{1}{(\mathbf{k}^2 + m^2)^\alpha} \\ &= \frac{1}{2(4\pi)^{d/2}} \frac{\Gamma\left(\frac{d}{2} + a\right) \Gamma\left(\frac{s}{2} + t\right) \Gamma\left(\alpha - \frac{s}{2} - \frac{d}{2} - t - a\right)}{\Gamma\left(\frac{d}{2}\right) \Gamma(\alpha) m^{2(\alpha-t-a)-s-d}}, \end{aligned} \quad (\text{B.8})$$

where $d\Omega_d = \frac{2\pi^{d/2}}{\Gamma(d/2)}$ is used. Plugging now this expression in I_{\pm} from (B.6) and evaluating the contour integration over s using the residue theorem, we arrive at

$$I = \frac{1}{2(4\pi)^{d/2}\Gamma(\alpha)\beta} \frac{\Gamma\left(\frac{d}{2} + a\right)}{\Gamma\left(\frac{d}{2}\right)} \left(\frac{2\pi}{\beta}\right)^{-2\alpha+d+2(t+a)} \\ \times \sum_{k=0}^{\infty} \frac{(-1)^k}{k!} \Gamma\left(\alpha - a + k - \frac{d}{2}\right) \left[\zeta\left(2(\alpha + k - t - a) - d; \frac{1}{2} - \frac{i\mu\beta}{2\pi}\right) + (\mu \rightarrow -\mu) \right] \left(\frac{m\beta}{2\pi}\right)^{2k}. \quad (\text{B.9})$$

Here, $k = 0, 1, 2, \dots, \infty$ labels the pole of the Γ -function at $s = 2(\alpha - t - a + k) - d$. Being a power series in $(m\beta)$, the result from (B.9) can be easily used whenever a high temperature expansion of Feynman integrals at finite temperature and density is possible. Note that a similar result is also presented in [53], where the integral in (B.1) is evaluate for arbitrary a, t and zero chemical potential $\mu = 0$.

APPENDIX C: THE DERIVATION OF THE EQUATIONS IN (V.14)

1. Derivation of the second equation in (V.14)

The first equation in (V.14) is already derived in (V.6). To derive the second equation in (V.14), let us consider (V.5), that is derived from (V.2) by setting $k = \sigma$ and using the definition (V.3)

$$[G^0\partial_0^2 - G^i\partial_i^2 + m_\sigma^2]\sigma_1 = -n_1 \left(\frac{\partial R_\sigma}{\partial n}\right)_{s_0, M, \sigma_0} + s_1 \left(\frac{\partial R_\sigma}{\partial s}\right)_{n_0, M, \sigma_0}. \quad (\text{C.1})$$

Plugging $\xi_1 = \tilde{\xi}_1 e^{-ikx}$ with $\xi_1 = \{n_1, s_1, \sigma_1, \mathbf{v}_1\}$ and $k^\mu = (\omega, \mathbf{k})$, we get first

$$(G^0\omega^2 - G^i k_i^2 - m_\sigma^2) \tilde{\sigma}_1 = \frac{\mathbf{k} \cdot \tilde{\mathbf{v}}_1}{\omega} \left[n_0 \left(\frac{\partial R_\sigma}{\partial n}\right)_{s_0, M, \sigma_0} + s_0 \left(\frac{\partial R_\sigma}{\partial s}\right)_{n_0, M, \sigma_0} \right], \quad (\text{C.2})$$

where (V.16) is used. Defining now

$$R'_\sigma \equiv \frac{1}{W_0} \left[n_0 \left(\frac{\partial R_\sigma}{\partial n}\right)_{s_0, M, \sigma_0} + s_0 \left(\frac{\partial R_\sigma}{\partial s}\right)_{n_0, M, \sigma_0} \right], \quad (\text{C.3})$$

we arrive at the second equation in (V.14)

$$(G^0\omega^2 - G^i k_i^2 - m_\sigma^2) \tilde{\sigma}_1 = \frac{W_0}{\omega} R'_\sigma \mathbf{k} \cdot \tilde{\mathbf{v}}_1. \quad (\text{C.4})$$

Let us now consider (C.3) and write it as

$$R'_\sigma \equiv \frac{1}{W_0} \left\{ \frac{\partial(T, \mu, B, \sigma)}{\partial(n, s, M, \sigma)} \left[n \frac{\partial(R_\sigma, s, M, \sigma)}{\partial(T, \mu, B, \sigma)} - s \frac{\partial(R_\sigma, n, M, \sigma)}{\partial(T, \mu, B, \sigma)} \right] \right\}_0, \quad (\text{C.5})$$

where the notation $\left(\frac{\partial A}{\partial B}\right)_C \equiv \frac{\partial(A, C)}{\partial(B, C)}$ is used. Generalizing now the identity $\frac{\partial(A, C)}{\partial(M, N)} = \det \begin{pmatrix} \frac{\partial A}{\partial M} & \frac{\partial A}{\partial N} \\ \frac{\partial C}{\partial M} & \frac{\partial C}{\partial N} \end{pmatrix}$ from [57]

for a case with four variables, and replacing the Jacobian $\frac{\partial(T, \mu, B, \sigma)}{\partial(n, s, M, \sigma)}$ on the r.h.s. of (C.5) by $\left(\frac{\partial(n, s, M, \sigma)}{\partial(T, \mu, B, \sigma)}\right)^{-1}$, we get first

$$R'_\sigma = \frac{1}{W_0} \left\{ \left(\left(\begin{vmatrix} \frac{\partial n}{\partial T} & \frac{\partial n}{\partial \mu} & \frac{\partial n}{\partial B} & \frac{\partial n}{\partial \sigma} \\ \frac{\partial s}{\partial T} & \frac{\partial s}{\partial \mu} & \frac{\partial s}{\partial B} & \frac{\partial s}{\partial \sigma} \\ \frac{\partial M}{\partial T} & \frac{\partial M}{\partial \mu} & \frac{\partial M}{\partial B} & \frac{\partial M}{\partial \sigma} \\ \frac{\partial \sigma}{\partial T} & \frac{\partial \sigma}{\partial \mu} & \frac{\partial \sigma}{\partial B} & \frac{\partial \sigma}{\partial \sigma} \end{vmatrix} \right)^{-1} \left(n \begin{vmatrix} \frac{\partial R_\sigma}{\partial T} & \frac{\partial R_\sigma}{\partial \mu} & \frac{\partial R_\sigma}{\partial B} & \frac{\partial R_\sigma}{\partial \sigma} \\ \frac{\partial n}{\partial T} & \frac{\partial n}{\partial \mu} & \frac{\partial n}{\partial B} & \frac{\partial n}{\partial \sigma} \\ \frac{\partial s}{\partial T} & \frac{\partial s}{\partial \mu} & \frac{\partial s}{\partial B} & \frac{\partial s}{\partial \sigma} \\ \frac{\partial M}{\partial T} & \frac{\partial M}{\partial \mu} & \frac{\partial M}{\partial B} & \frac{\partial M}{\partial \sigma} \end{vmatrix} - s \begin{vmatrix} \frac{\partial R_\sigma}{\partial T} & \frac{\partial R_\sigma}{\partial \mu} & \frac{\partial R_\sigma}{\partial B} & \frac{\partial R_\sigma}{\partial \sigma} \\ \frac{\partial n}{\partial T} & \frac{\partial n}{\partial \mu} & \frac{\partial n}{\partial B} & \frac{\partial n}{\partial \sigma} \\ \frac{\partial s}{\partial T} & \frac{\partial s}{\partial \mu} & \frac{\partial s}{\partial B} & \frac{\partial s}{\partial \sigma} \\ \frac{\partial M}{\partial T} & \frac{\partial M}{\partial \mu} & \frac{\partial M}{\partial B} & \frac{\partial M}{\partial \sigma} \end{vmatrix} \right) \right\}_0, \quad (\text{C.6})$$

where the subscript 0 means that the (n, s, σ) in the final result of the determinants are to be replaced by (n_0, s_0, σ_0) from the thermal equilibrium. At this stage the thermodynamic relations from (IV.16) can be used to get the final expression for R'_σ

$$R'_\sigma = \frac{\mathcal{J}}{W_0} \left\{ \frac{\partial P_0}{\partial \mu} \begin{vmatrix} \frac{\partial^2 P_0}{\partial T \partial \sigma_0} & \frac{\partial^2 P_0}{\partial \mu \partial \sigma_0} & \frac{\partial^2 P_0}{\partial B \partial \sigma_0} & \frac{\partial^2 P_0}{\partial \sigma_0^2} \\ \frac{\partial^2 P_0}{\partial^2 T} & \frac{\partial^2 P_0}{\partial \mu \partial T} & \frac{\partial^2 P_0}{\partial B \partial T} & \frac{\partial^2 P_0}{\partial \sigma_0 \partial T} \\ \frac{\partial^2 P_0}{\partial T \partial B} & \frac{\partial^2 P_0}{\partial \mu \partial B} & \frac{\partial^2 P_0}{\partial^2 B} & \frac{\partial^2 P_0}{\partial \sigma_0 \partial B} \\ \frac{\partial \sigma_0}{\partial T} & \frac{\partial \sigma_0}{\partial \mu} & \frac{\partial \sigma_0}{\partial B} & 1 \end{vmatrix} - \frac{\partial P_0}{\partial T} \begin{vmatrix} \frac{\partial^2 P_0}{\partial T \partial \sigma_0} & \frac{\partial^2 P_0}{\partial \mu \partial \sigma_0} & \frac{\partial^2 P_0}{\partial B \partial \sigma_0} & \frac{\partial^2 P_0}{\partial \sigma_0^2} \\ \frac{\partial^2 P_0}{\partial T \partial \mu} & \frac{\partial^2 P_0}{\partial^2 \mu} & \frac{\partial^2 P_0}{\partial B \partial \mu} & \frac{\partial^2 P_0}{\partial \sigma_0 \partial \mu} \\ \frac{\partial^2 P_0}{\partial T \partial B} & \frac{\partial^2 P_0}{\partial \mu \partial B} & \frac{\partial^2 P_0}{\partial^2 B} & \frac{\partial^2 P_0}{\partial \sigma_0 \partial B} \\ \frac{\partial \sigma_0}{\partial T} & \frac{\partial \sigma_0}{\partial \mu} & \frac{\partial \sigma_0}{\partial B} & 1 \end{vmatrix} \right\}, \quad (\text{C.7})$$

where $P_0 \equiv P_0(T, \mu, B, \sigma_0)$, and the Jacobian \mathcal{J} is defined by

$$\mathcal{J} \equiv \begin{vmatrix} \frac{\partial^2 P_0}{\partial T \partial \mu} & \frac{\partial^2 P_0}{\partial^2 \mu} & \frac{\partial^2 P_0}{\partial B \partial \mu} & \frac{\partial^2 P_0}{\partial \sigma_0 \partial \mu} \\ \frac{\partial^2 P_0}{\partial^2 T} & \frac{\partial^2 P_0}{\partial \mu \partial T} & \frac{\partial^2 P_0}{\partial B \partial T} & \frac{\partial^2 P_0}{\partial \sigma_0 \partial T} \\ \frac{\partial^2 P_0}{\partial T \partial B} & \frac{\partial^2 P_0}{\partial \mu \partial B} & \frac{\partial^2 P_0}{\partial^2 B} & \frac{\partial^2 P_0}{\partial \sigma_0 \partial B} \\ \frac{\partial \sigma_0}{\partial T} & \frac{\partial \sigma_0}{\partial \mu} & \frac{\partial \sigma_0}{\partial B} & 1 \end{vmatrix}^{-1}. \quad (\text{C.8})$$

2. Derivation of the third equation in (V.14)

To derive the third equation in (V.14), let us start with (V.9), where P_1 is defined in (V.11). Plugging, as above, $\xi_1 = \tilde{\xi}_1 e^{-ikx}$ with $\xi_1 = \{n_1, s_1, \sigma_1, \mathbf{v}_1\}$, we get first

$$W_0 \omega \tilde{\mathbf{v}}_1 = \left[\tilde{n}_1 \left(\frac{\partial P}{\partial n} \right)_{s_0, M, \sigma_0} + \tilde{s}_1 \left(\frac{\partial P}{\partial s} \right)_{n_0, M, \sigma_0} + \tilde{\sigma}_1 \left(\frac{\partial P}{\partial \sigma} \right)_{n_0, s_0, M} \right]. \quad (\text{C.9})$$

Using now (V.16) and defining P' as in (V.15)

$$P' \equiv \frac{1}{W_0} \left[n_0 \left(\frac{\partial P}{\partial n} \right)_{s_0, M, \sigma_0} + s_0 \left(\frac{\partial P}{\partial s} \right)_{n_0, M, \sigma_0} \right], \quad (\text{C.10})$$

we get

$$(\omega^2 - \mathbf{k}^2 P') (\mathbf{k} \cdot \tilde{\mathbf{v}}_1) = \frac{\mathbf{k}^2 \omega}{W_0} \left(\frac{\partial P}{\partial \sigma} \right)_{n_0, s_0, M} \tilde{\sigma}_1. \quad (\text{C.11})$$

Defining $\left(\frac{\partial P}{\partial \sigma} \right)_{n_0, s_0, M} = R'_\sigma (W_0 + BM)$ with R'_σ given in (V.13), we arrive at

$$(\omega^2 - \mathbf{k}^2 P') (\mathbf{k} \cdot \tilde{\mathbf{v}}_1) = \frac{\mathbf{k}^2 \omega}{W_0} R'_\sigma (W_0 + BM) \tilde{\sigma}_1, \quad (\text{C.12})$$

as expected. In what follows, we present the final results for P' and R'_σ from (C.10) and (V.13), respectively. Using the same method leading from (C.5) to (C.7), P' from (C.10) can be first given as

$$P' = \frac{1}{W_0} \left\{ \left(\begin{vmatrix} \frac{\partial n}{\partial T} & \frac{\partial n}{\partial \mu} & \frac{\partial n}{\partial B} & \frac{\partial n}{\partial \sigma} \\ \frac{\partial s}{\partial T} & \frac{\partial s}{\partial \mu} & \frac{\partial s}{\partial B} & \frac{\partial s}{\partial \sigma} \\ \frac{\partial M}{\partial T} & \frac{\partial M}{\partial \mu} & \frac{\partial M}{\partial B} & \frac{\partial M}{\partial \sigma} \\ \frac{\partial \sigma}{\partial T} & \frac{\partial \sigma}{\partial \mu} & \frac{\partial \sigma}{\partial B} & \frac{\partial \sigma}{\partial \sigma} \end{vmatrix} \right)^{-1} \left(n \begin{vmatrix} \frac{\partial P}{\partial T} & \frac{\partial P}{\partial \mu} & \frac{\partial P}{\partial B} & \frac{\partial P}{\partial \sigma} \\ \frac{\partial s}{\partial T} & \frac{\partial s}{\partial \mu} & \frac{\partial s}{\partial B} & \frac{\partial s}{\partial \sigma} \\ \frac{\partial M}{\partial T} & \frac{\partial M}{\partial \mu} & \frac{\partial M}{\partial B} & \frac{\partial M}{\partial \sigma} \\ \frac{\partial \sigma}{\partial T} & \frac{\partial \sigma}{\partial \mu} & \frac{\partial \sigma}{\partial B} & \frac{\partial \sigma}{\partial \sigma} \end{vmatrix} - s \begin{vmatrix} \frac{\partial P}{\partial T} & \frac{\partial P}{\partial \mu} & \frac{\partial P}{\partial B} & \frac{\partial P}{\partial \sigma} \\ \frac{\partial n}{\partial T} & \frac{\partial n}{\partial \mu} & \frac{\partial n}{\partial B} & \frac{\partial n}{\partial \sigma} \\ \frac{\partial M}{\partial T} & \frac{\partial M}{\partial \mu} & \frac{\partial M}{\partial B} & \frac{\partial M}{\partial \sigma} \\ \frac{\partial \sigma}{\partial T} & \frac{\partial \sigma}{\partial \mu} & \frac{\partial \sigma}{\partial B} & \frac{\partial \sigma}{\partial \sigma} \end{vmatrix} \right) \right\}_0. \quad (\text{C.13})$$

Using now the thermodynamic relations from (IV.16) to replace n_0, s_0, M, σ_0 by the derivative of P_0 with respect to μ, T, B respectively, we get

$$P' = \frac{\mathcal{J}}{W_0} \left\{ \frac{\partial P_0}{\partial \mu} \begin{vmatrix} \frac{\partial P_0}{\partial T} & \frac{\partial P_0}{\partial \mu} & \frac{\partial P_0}{\partial B} & \frac{\partial P_0}{\partial \sigma_0} \\ \frac{\partial^2 P_0}{\partial^2 T} & \frac{\partial^2 P_0}{\partial \mu \partial T} & \frac{\partial^2 P_0}{\partial B \partial T} & \frac{\partial^2 P_0}{\partial \sigma_0 \partial T} \\ \frac{\partial^2 P_0}{\partial T \partial B} & \frac{\partial^2 P_0}{\partial \mu \partial B} & \frac{\partial^2 P_0}{\partial^2 B} & \frac{\partial^2 P_0}{\partial \sigma_0 \partial B} \\ \frac{\partial \sigma_0}{\partial T} & \frac{\partial \sigma_0}{\partial \mu} & \frac{\partial \sigma_0}{\partial B} & 1 \end{vmatrix} - \frac{\partial P_0}{\partial T} \begin{vmatrix} \frac{\partial P_0}{\partial T} & \frac{\partial P_0}{\partial \mu} & \frac{\partial P_0}{\partial B} & \frac{\partial P_0}{\partial \sigma_0} \\ \frac{\partial^2 P_0}{\partial T \partial \mu} & \frac{\partial^2 P_0}{\partial^2 \mu} & \frac{\partial^2 P_0}{\partial B \partial \mu} & \frac{\partial^2 P_0}{\partial \sigma_0 \partial \mu} \\ \frac{\partial^2 P_0}{\partial T \partial B} & \frac{\partial^2 P_0}{\partial \mu \partial B} & \frac{\partial^2 P_0}{\partial^2 B} & \frac{\partial^2 P_0}{\partial \sigma_0 \partial B} \\ \frac{\partial \sigma_0}{\partial T} & \frac{\partial \sigma_0}{\partial \mu} & \frac{\partial \sigma_0}{\partial B} & 1 \end{vmatrix} \right\}, \quad (\text{C.14})$$

with the Jacobian \mathcal{J} defined in (C.8). As next, using the definition of R''_σ from (V.13),

$$R''_\sigma \equiv \frac{1}{(W_0 + BM)} \left[n_0 \left(\frac{\partial R_\sigma}{\partial n} \right)_{s_0, M, \sigma_0} + s_0 \left(\frac{\partial R_\sigma}{\partial s} \right)_{n_0, M, \sigma_0} + M \left(\frac{\partial R_\sigma}{\partial M} \right)_{n_0, s_0, \sigma_0} \right], \quad (\text{C.15})$$

and following the same method as described above, we arrive at

$$R''_\sigma = \frac{\mathcal{J}}{(W_0 + BM)} \left\{ \frac{\partial P_0}{\partial \mu} \begin{vmatrix} \frac{\partial^2 P_0}{\partial T \partial \sigma_0} & \frac{\partial^2 P_0}{\partial \mu \partial \sigma_0} & \frac{\partial^2 P_0}{\partial B \partial \sigma_0} & \frac{\partial^2 P_0}{\partial \sigma_0^2} \\ \frac{\partial^2 P_0}{\partial^2 T} & \frac{\partial^2 P_0}{\partial \mu \partial T} & \frac{\partial^2 P_0}{\partial B \partial T} & \frac{\partial^2 P_0}{\partial \sigma_0 \partial T} \\ \frac{\partial^2 P_0}{\partial T \partial B} & \frac{\partial^2 P_0}{\partial \mu \partial B} & \frac{\partial^2 P_0}{\partial^2 B} & \frac{\partial^2 P_0}{\partial \sigma_0 \partial B} \\ \frac{\partial \sigma_0}{\partial T} & \frac{\partial \sigma_0}{\partial \mu} & \frac{\partial \sigma_0}{\partial B} & 1 \end{vmatrix} - \frac{\partial P_0}{\partial T} \begin{vmatrix} \frac{\partial^2 P_0}{\partial T \partial \sigma_0} & \frac{\partial^2 P_0}{\partial \mu \partial \sigma_0} & \frac{\partial^2 P_0}{\partial B \partial \sigma_0} & \frac{\partial^2 P_0}{\partial \sigma_0^2} \\ \frac{\partial^2 P_0}{\partial T \partial \mu} & \frac{\partial^2 P_0}{\partial^2 \mu} & \frac{\partial^2 P_0}{\partial B \partial \mu} & \frac{\partial^2 P_0}{\partial \sigma_0 \partial \mu} \\ \frac{\partial^2 P_0}{\partial T \partial B} & \frac{\partial^2 P_0}{\partial \mu \partial B} & \frac{\partial^2 P_0}{\partial^2 B} & \frac{\partial^2 P_0}{\partial \sigma_0 \partial B} \\ \frac{\partial \sigma_0}{\partial T} & \frac{\partial \sigma_0}{\partial \mu} & \frac{\partial \sigma_0}{\partial B} & 1 \end{vmatrix} \right. \\ \left. + \frac{\partial P_0}{\partial B} \begin{vmatrix} \frac{\partial^2 P_0}{\partial T \partial \sigma_0} & \frac{\partial^2 P_0}{\partial \mu \partial \sigma_0} & \frac{\partial^2 P_0}{\partial B \partial \sigma_0} & \frac{\partial^2 P_0}{\partial \sigma_0^2} \\ \frac{\partial^2 P_0}{\partial T \partial \mu} & \frac{\partial^2 P_0}{\partial^2 \mu} & \frac{\partial^2 P_0}{\partial B \partial \mu} & \frac{\partial^2 P_0}{\partial \sigma_0 \partial \mu} \\ \frac{\partial^2 P_0}{\partial^2 T} & \frac{\partial^2 P_0}{\partial \mu \partial T} & \frac{\partial^2 P_0}{\partial B \partial T} & \frac{\partial^2 P_0}{\partial \sigma_0 \partial T} \\ \frac{\partial \sigma_0}{\partial T} & \frac{\partial \sigma_0}{\partial \mu} & \frac{\partial \sigma_0}{\partial B} & 1 \end{vmatrix} \right\}, \quad (\text{C.16})$$

where the Jacobian \mathcal{J} defined in (C.8).

-
- [1] J. Y. Ollitrault, *Relativistic hydrodynamics*, Eur. J. Phys. **29**, 275 (2008), arXiv: 0708.2433 [nucl-th].
P. Romatschke, *New Developments in Relativistic Viscous Hydrodynamics*, arXiv: 0902.3663 [hep-ph].
 - [2] T. Hirano, N. van der Kolk and A. Bilandzic, *Hydrodynamics and flow*, arXiv: 0808.2684 [nucl-th].
 - [3] T. Schaefer and D. Teaney, *Nearly Perfect Fluidity: From cold atomic gases to hot quark gluon plasmas*, arXiv: 0904.3107 [hep-ph].
 - [4] E. V. Shuryak, *Quantum Chromodynamics and the theory of superdense matter*, Phys. Rept. **61** (1980) 71.
 - [5] e.g. C. M. Hung and E. V. Shuryak, *Hydrodynamics near The QCD phase transition: Looking for the longest lived fireball*, Phys. Rev. Lett. **75**, 4003 (1995), arXiv: hep-ph/9412360.
D. Teaney, J. Lauret and E. V. Shuryak, *Hydro+cascade, flow, the equation of state, predictions and data*, Nucl. Phys. A **698**, 479 (2002), arXiv: nucl-th/0104041.
D. Teaney, J. Lauret and E. V. Shuryak, *A hydrodynamic description of heavy ion collisions at the SPS and RHIC*, arXiv: nucl-th/0110037.
J. Casalderrey-Solana, E. V. Shuryak and D. Teaney, *Hydrodynamic flow from fast particles*, arXiv: hep-ph/0602183.
 - [6] e.g. F. Karsch, D. Kharzeev and K. Tuchin, *Universal properties of bulk viscosity near the QCD phase transition*, Phys. Lett. B **663**, 217 (2008), arXiv: 0711.0914 [hep-ph].
G. S. Denicol, T. Kodama, T. Koide and Ph. Mota, *Effect of bulk viscosity on elliptic flow near QCD phase transition*, arXiv: 0903.3595 [hep-ph].
B. C. Li and M. Huang, *Thermodynamic properties and bulk viscosity near phase transition in the Z(2) and O(4) models*, arXiv: 0903.3650 [hep-ph].
 - [7] H. Fujii, K. Itakura and A. Iwazaki, *Instabilities in non-expanding glasma*, arXiv: 0903.2930 [hep-ph].
 - [8] H. Nastase, *On high energy scattering inside gravitational backgrounds*, arXiv: hep-th/0410124.
H. Nastase, *The RHIC fireball as a dual black hole*, arXiv: hep-th/0501068.
E. Shuryak, S. J. Sin and I. Zahed, *A Gravity Dual of RHIC Collisions*, J. Korean Phys. Soc. **50**, 384 (2007), arXiv: hep-th/0511199.
A. J. Amsel, D. Marolf and A. Virmani, *Collisions with Black Holes and Deconfined Plasmas*, JHEP **0804**, 025 (2008), arXiv: 0712.2221 [hep-th].
D. Grumiller and P. Romatschke, *On the collision of two shock waves in AdS5*, JHEP **0808**, 027 (2008), arXiv: 0803.3226 [hep-th].
 - [9] S. S. Gubser, S. S. Pufu and A. Yarom, *Entropy production in collisions of gravitational shock waves and of heavy ions*, Phys. Rev. D **78**, 066014 (2008), arXiv: 0805.1551 [hep-th].
S. Lin and E. Shuryak, *Grazing collisions of gravitational shock waves and entropy production in heavy ion collision*, arXiv: 0902.1508 [hep-th].
J. L. Albacete, Y. V. Kovchegov and A. Taliotis, *Asymmetric collision of two shock waves in AdS5*, arXiv: 0902.3046 [hep-th].
S. S. Gubser, S. S. Pufu and A. Yarom, *Off-center collisions in AdS5 with applications to multiplicity estimates in heavy-ion collisions*, arXiv: 0902.4062 [hep-th].

- [10] A. Bazavov *et al.*, *Equation of state and QCD transition at finite temperature*, arXiv: 0903.4379 [hep-lat].
- [11] E. W. Kolb and M. S. Turner, *The Early Universe*, Redwood City, USA, Addison-Wesley (1988).
- [12] C. E. Aguiar, E. S. Fraga and T. Kodama, *Hydrodynamical instabilities beyond the chiral critical point*, J. Phys. G **32**, 179 (2006), arXiv: nucl-th/0306041.
- [13] J. Rafelski and J. Letessier, *Sudden hadronization in relativistic nuclear collisions*, Phys. Rev. Lett. **85**, 4695 (2000), arXiv: hep-ph/0006200.
O. Scavenius, A. Dumitru and A. D. Jackson, *Explosive decomposition in ultrarelativistic heavy ion collision*, Phys. Rev. Lett. **87**, 182302 (2001), arXiv: hep-ph/0103219.
A. Dumitru and R. D. Pisarski, *Explosive collisions at RHIC?*, Nucl. Phys. A **698**, 444 (2002), arXiv: hep-ph/0102020.
- [14] K. Paech, H. Stoecker and A. Dumitru, *Hydrodynamics near a chiral critical point*, Phys. Rev. C **68**, 044907 (2003), arXiv: nucl-th/0302013.
- [15] H. T. Elze, T. Kodama, Y. Hama, M. Makler and J. Rafelski, *Variational approach to hydrodynamics: From QGP to general relativity*, arXiv:hep-ph/9809570.
H. T. Elze, Y. Hama, T. Kodama, M. Makler and J. Rafelski, *Variational Principle for Relativistic Fluid Dynamics*, J. Phys. G **25**, 1935 (1999), arXiv: hep-ph/9910208.
- [16] J. D. Parsons, *Sound velocity in a magnetic field*, J. Phys. D **8**, 1219, (1975).
- [17] Y. Nambu and G. Jona-Lasinio, *Dynamical model of elementary particles based on an analogy with superconductivity. I*, Phys. Rev. **122**, 345 (1961).
Y. Nambu and G. Jona-Lasinio, *Dynamical model of elementary particles based on an analogy with superconductivity. II*, Phys. Rev. **124**, 246 (1961).
U. Vogl and W. Weise, *The Nambu and Jona-Lasinio model: Its implications for hadrons and nuclei*, Prog. Part. Nucl. Phys. **27**, 195 (1991).
S. P. Klevansky, *The Nambu-Jona-Lasinio model of quantum chromodynamics*, Rev. Mod. Phys. **64**, 649 (1992).
- [18] T. M. Schwarz, S. P. Klevansky and G. Papp, *The phase diagram and bulk thermodynamical quantities in the NJL model at finite temperature and density*, Phys. Rev. C **60**, 055205 (1999), arXiv: nucl-th/9903048.
- [19] V. P. Gusynin, V. A. Miransky and I. A. Shovkovy, *Dimensional reduction and catalysis of dynamical symmetry breaking by a magnetic field*, Nucl. Phys. B **462**, 249 (1996), arXiv: hep-ph/9509320.
- [20] E. Elizalde, E. J. Ferrer and V. de la Incera, *Neutrino propagation in a strongly magnetized medium*, Phys. Rev. D **70**, 043012 (2004).
E. J. Ferrer and V. de la Incera, *Neutrino propagation and oscillations in a strong magnetic field*, Int. J. Mod. Phys. A **19**, 5385 (2004).
- [21] K. Farakos, G. Koutsoumbas and N. E. Mavromatos, *Dynamical flavour symmetry breaking by a magnetic field in lattice QED(3)*, Phys. Lett. B **431**, 147 (1998).
K. Farakos and N. E. Mavromatos, *Hidden non-Abelian gauge symmetries in doped planar antiferromagnets*, Phys. Rev. B **57**, 3017 (1998).
G. W. Semenoff, I. A. Shovkovy and L. C. R. Wijewardhana, *Phase transition induced by a magnetic field*, Mod. Phys. Lett. A **13**, 1143 (1998).
E. J. Ferrer, V. P. Gusynin and V. de la Incera, *Magnetic field induced gap and kink behavior of thermal conductivity in cuprates*, Mod. Phys. Lett. B **16**, 107 (2002).
E. J. Ferrer, V. P. Gusynin and V. de la Incera, *Thermal conductivity in 3D NJL model under external magnetic field*, Eur. Phys. J. B **33**, 397 (2003).
E. V. Gorbar, V. P. Gusynin, V. A. Miransky and I. A. Shovkovy, *Dynamics in the quantum Hall effect and the phase diagram of graphene*, Phys. Rev. B **78**, 085437 (2008), arXiv: 0806.0846 [cond-mat.mes-hall].
- [22] D. E. Kharzeev, L. D. McLerran and H. J. Warringa, *The effects of topological charge change in heavy ion collisions: 'Event by event P and CP violation'*, Nucl. Phys. A **803**, 227 (2008), arXiv: 0711.0950 [hep-ph].
H. J. Warringa, *Implications of CP-violating transitions in hot quark matter on heavy ion collisions*, J. Phys. G **35**, 104012 (2008), arXiv: 0805.1384 [hep-ph].
A. J. Mizher and E. S. Fraga, *CP Violation in the Linear Sigma Model*, Nucl. Phys. A **820**, 247 (2009), arXiv: 0810.4115 [hep-ph].
A. J. Mizher and E. S. Fraga, *CP violation and chiral symmetry restoration in the hot linear sigma model in a strong magnetic background*, arXiv: 0810.5162 [hep-ph].
- [23] K. Fukushima, D. E. Kharzeev and H. J. Warringa, *The Chiral Magnetic Effect*, Phys. Rev. D **78**, 074033 (2008), arXiv: 0808.3382 [hep-ph].
- [24] D. E. Kharzeev, *Hot and dense matter: from RHIC to LHC: Theoretical overview*, arXiv: 0902.2749 [hep-ph].
- [25] S. A. Voloshin, *Parity violation in hot QCD: How to detect it*, Phys. Rev. C **70**, 057901 (2004), arXiv: hep-ph/0406311.
- [26] I. V. Selyuzhenkov [STAR Collaboration], *Global polarization and parity violation study in Au + Au collisions*, Rom. Rep. Phys. **58**, 049 (2006), arXiv: nucl-ex/0510069.

- [27] A. D. Sakharov, *Violation of CP invariance, C asymmetry, and baryon asymmetry of the universe*, Pisma Zh. Eksp. Teor. Fiz. **5**, 32 (1967) [JETP Lett. **5**, 24 (1967 SOPUA,34,392-393.1991 UFNAA,161,61-64.1991)].
- [28] M. Giovannini and M. E. Shaposhnikov, *Primordial magnetic fields, anomalous isocurvature fluctuations and big bang nucleosynthesis*, Phys. Rev. Lett. **80**, 22 (1998).
- [29] J. Wiersma and A. Achterberg, *Magnetic field generation in relativistic shocks - An early end of the exponential Weibel instability in electron-proton plasmas*, Astron. Astrophys. **428**, 365 (2004), arXiv: astro-ph/0408550.
- [30] E. S. Weibel, *Spontaneously growing transverse waves in a plasma due to anisotropic velocity distribution*, Phys. Rev. Lett. **2**, 83 (1959).
A. Rebhan, *Hard loop effective theory of the (anisotropic) quark gluon plasma*, arXiv: 0811.0457 [hep-ph].
- [31] H. Fujii, K. Itakura and A. Iwazaki, *Instabilities in non-expanding glasma*, arXiv:0903.2930 [hep-ph].
- [32] N. K. Nielsen and P. Olesen, *An Unstable Yang-Mills Field Mode*, Nucl. Phys. B **144**, 376 (1978).
N. K. Nielsen and P. Olesen, *Electric Vortex Lines From The Yang-Mills Theory*, Phys. Lett. B **79**, 304 (1978).
- [33] N. O. Agasian and S. M. Fedorov, *Quark-hadron phase transition in a magnetic field*, Phys. Lett. B **663**, 445 (2008), arXiv: 0803.3156 [hep-ph].
E. S. Fraga and A. J. Mizher, *Chiral transition in a strong magnetic background*, Phys. Rev. D **78**, 025016 (2008), arXiv: 0804.1452 [hep-ph].
E. S. Fraga and A. J. Mizher, *Can a strong magnetic background modify the nature of the chiral transition in QCD?*, Nucl. Phys. A **820**, 103C (2009), arXiv: 0810.3693 [hep-ph].
- [34] A. Ayala, A. Bashir, A. Raya and A. Sanchez, *Chiral phase transition in relativistic heavy-ion collisions with weak magnetic fields: ring diagrams in the linear sigma model*, arXiv: 0904.4533 [hep-ph].
- [35] L. Campanelli and M. Ruggieri, *Probing the QCD vacuum with an abelian chromomagnetic field: A study within an effective model*, arXiv: 0905.0853 [hep-ph].
- [36] N. Sadooghi and K. Sohrabi Anaraki, *Improved ring potential of QED at finite temperature and in the presence of weak and strong magnetic fields*, Phys. Rev. D **78**, 125019 (2008), arXiv: 0805.0078 [hep-ph].
- [37] M. Chojnacki and W. Florkowski, *Temperature dependence of sound velocity and hydrodynamics of ultra-relativistic heavy-ion collisions*, Acta Phys. Polon. B **38**, 3249 (2007), arXiv: nucl-th/0702030.
- [38] C. Sasaki, B. Friman and K. Redlich, *Density fluctuations as signature of a non-equilibrium first order phase transition*, J. Phys. G **35**, 104095 (2008), arXiv: 0804.3990 [hep-ph].
Y. Minami and T. Kunihiro, *Dynamical Density Fluctuations around QCD Critical Point Based on Dissipative Relativistic Fluid Dynamics*, arXiv:0904.2270 [hep-th].
- [39] D. Ebert and V. C. Zhukovsky, *Chiral phase transitions in strong chromomagnetic fields at finite temperature and dimensional reduction*, Mod. Phys. Lett. A **12**, 2567 (1997).
- [40] P. N. Meisinger and M. C. Ogilvie, *Complete high temperature expansions for one-loop finite temperature effects*, Phys. Rev. D **65**, 056013 (2002).
- [41] D. J. Bedingham, *Dimensional regularization and Mellin summation in high-temperature calculations*, arXiv: hep-ph/0011012.
- [42] V. A. Miransky, *On the generating functional for proper vertices of local composite operators in theories with dynamical symmetry breaking*, Int. J. Mod. Phys. A **8**, 135 (1993).
- [43] S. R. de Groot, *The Maxwell equations: Non-relativistic and relativistic derivations from electron theory*, North-Holland Pub. Co., Amsterdam (1969).
- [44] S. A. Hartnoll, P. K. Kovtun, M. Muller and S. Sachdev, *Theory of the Nernst effect near quantum phase transitions in condensed matter, and in dyonic black holes*, Phys. Rev. B **76**, 144502 (2007), arXiv:0706.3215 [cond-mat.str-el].
- [45] E. I. Buchbinder, A. Buchel and S. E. Vazquez, *Sound Waves in (2+1) Dimensional Holographic Magnetic Fluids*, JHEP **0812**, 090 (2008), arXiv: 0810.4094 [hep-th].
E. I. Buchbinder and A. Buchel, *The Fate of the Sound and Diffusion in Holographic Magnetic Field*, arXiv: 0811.4325 [hep-th].
E. I. Buchbinder and A. Buchel, *Relativistic Conformal Magneto-Hydrodynamics from Holography*, arXiv:0902.3170 [hep-th].
- [46] J. S. Schwinger, *On gauge invariance and vacuum polarization*, Phys. Rev. **82**, 664 (1951).
- [47] V. P. Gusynin, V. A. Miransky and I. A. Shovkovy, *Dynamical flavor symmetry breaking by a magnetic field in (2+1)-dimensions*, Phys. Rev. D **52**, 4718 (1995).
- [48] S. Kanemura, H. T. Sato and H. Tochimura, *Thermodynamic Gross-Neveu model under constant electromagnetic field*, Nucl. Phys. B **517**, 567 (1998).
- [49] P. Costa, M. C. Ruivo and C. A. de Sousa, *Thermodynamics and critical behavior in the Nambu-Jona-Lasinio model of QCD*, Phys. Rev. D **77**, 096001 (2008), arXiv:0801.3417 [hep-ph].
- [50] J. L. Noronha and I. A. Shovkovy, *Color-flavor locked superconductor in a magnetic field*, Phys. Rev. D **76**, 105030 (2007), arXiv:0708.0307 [hep-ph].
- [51] C. P. Herzog, P. K. Kovtun and D. T. Son, *Holographic model of superfluidity*, arXiv:0809.4870 [hep-th].
- [52] Y. Aoki, Z. Fodor, S. D. Katz and K. K. Szabo, *The equation of state in lattice QCD: With physical quark masses*

- towards the continuum limit, JHEP **0601**, 089 (2006), arXiv:hep-lat/0510084.
- [53] A. Sanchez, A. Ayala and G. Piccinelli, *Effective potential at finite temperature in a constant hypermagnetic field: Ring diagrams in the standard model*, Phys. Rev. D **75**, 043004 (2007), arXiv: hep-th/0611337.
A. Ayala, G. Piccinelli, A. Sanchez and M. E. Tejeda-Yeomans, *Feynman parametrization and Mellin summation at finite temperature*, Phys. Rev. D **78**, 096001 (2008), arXiv: 0804.3414 [hep-ph].
- [54] P. M. Hohler and M. A. Stephanov, *Holography and the speed of sound at high temperatures*, arXiv: 0905.0900 [hep-th].
- [55] A. Cherman, T. D. Cohen and A. Nellore, *A bound on the speed of sound from holography*, arXiv: 0905.0903 [hep-th].
- [56] M. E. Peskin and D. V. Schroeder, *An Introduction To Quantum Field Theory*, Reading, USA: Addison-Wesley (1995).
- [57] F. Schwabl, *Statistical Mechanics*, Second Edition, Springer Verlag, Berlin, Heidelberg, New York (2006).